Examining parameters that control spreading of a concentrated nourishment

Jianbiao Lyu

TU Delft

Examining parameters that control spreading of a concentrated nourishment

by

Jianbiao Lyu

to obtain the degree of Master of Science

at the Delft University of Technology,

to be defended publicly on Thursday November 28, 2019 at 15:00 AM.

Student number:	4714873	
Project duration:	February 1, 2019 – November 1, 2019	
Thesis committee:	Prof. dr. ir. Aarninkhof. S. G. J. (Stefan),	TU Delft
	Dr. ir. M. A. de Schipper,	TU Delft
	Dr. ir. J. J. van der Werf,	Deltares
	Ir. W. P. de Boer,	Deltares, TU Delft

An electronic version of this thesis is available at `http://repository.tudelft.nl/`.

Preface

This thesis report concludes the Master of Science program in Civil Engineering at Delft University of Technology, the Netherlands. This thesis concerns a study to test the impact of different parameters on the erosion rate of submerged nourishments.

I would like to thank all my supervising committees for their support during this graduation topic. Stefan Aarninkhof, thank you for your encouragement and positive attitudes during the meetings, and providing valuable information to guide me in the right way. Matthieu de Schipper, as my daily supervisor you helped me patiently when I encountered difficulties in my project and gave me valuable advice and great feedback to let me carry on my project. Moreover, I really appreciate that you read my report carefully and checked it word by word to bring my writing to a higher level, I highly valued your guidance during the whole process. I would like to thank Wiebe de Boer and Jebbe van der Werf for sharing your knowledge and experience to help me find the right direction.

Moreover, I would like to thank my friends for their support and encouragement. We had a great conversation about our lives and studies during the lunch and coffee break which let me have a wonderful time during the years I spent in Delft. Finally, I would like to thank my parents for their financial support and endless encouragement to help me finish my study successfully.

Jianbiao Lyu
Delft, November 2019

Summary

Due to sea level rise and subsidence of land, coastal erosion is a serious problem in the Netherlands. And nourishments are common solutions to mitigate coastal erosion. Over the last decades, many studies have been focusing on individual nourishment performance to help us increase understanding of it. However, it is still not clear for us how the nourishments behave under different parameters (such as water depth of the nourishment crest, wave heights or nourishment size etc). This thesis tests the impact of different parameters on the erosion rate of the nourishments through measured data and numerical model simulations.

Data is collected from the Dutch and international nourishment projects. These data are combined with dump site/ pits further offshore to extend the range of water depths. Further analysis has been done for the Dutch shoreface nourishments. The Dutch and international cases were combined to test for generic relationships. The measured data show that the erosion rate of the nourishments is dependent on the length/ volume, but the effect of the water depth or dimensionless wave height (H/d) can not be confirmed from the data. The larger volume/ length of the shoreface nourishments coincide with larger erosion rates, while the relation between the volume/ length of the shoreface nourishments and erosion rate per meter is opposite. And the dimensionless wave heights of all Dutch and internation shoreface nourishment cases are between 0.1-0.22.

A numerical model has been constructed using the XBeach model to explore the isolated effect of parameters on the erosion rate of the nourishments. The erosion rate of different scenarios has been compared. The numerical data show that the strong dependency on the hydrodynamic (water depth, dimensionless wave height) and geometric (length, volume per meter) aspects of the nourishments. For a specific wave condition (H_s=2.25m, T_p=7.8s at the offshore boundary), the erosion rate is 8 times smaller if the water depth is 7m compared to the water depth is 3m. Most erosion of the nourishment occurs when the dimensionless wave height is larger than 0.33. When the length is smaller than 2000m, the nourishment tends to have a faster erosion. The numerical data show that the volume per meter of the nourishment also affects the evolution of the nourishment. With a constant wave height ($H_s = 2.25m$) at the offshore boundary, changing the volume per meter of the nourishment from 200 m^3/m to 500 m^3/m impacts the erosion rate by factor 3.

Finally, the results of the measured data and modelling test are compared. In the measured

data, a multitude of parameters varies between cases, obscuring the view on relationships. In the numerical model, parameters are varied one at the time. That could be the main reason why depth dependency is more apparent in numerical results than the observed data.

For further analysis, it is recommended to apply existing topography and boundary conditions in the numerical model. In this way, the sediment transport processes can be described more accurately. It is also valuable to detect how the coastline varies in different hydrodynamic (depth of the nourishment crest, dimensionless wave height) and geometric conditions (length, volume or volume per meter etc) of the nourishments.

Contents

Chapter 1

Introduction

1.1. Background

Nowadays, due to sea level rise and shortage of sediment supply in coastal areas, the coastal erosion is becoming a severe problem for coastal zone management. Protection of the coastal zone is quite crucial, preventing the destruction of coastal structures, flood risk and loss of lives in coastal areas.
As for preventing coastal erosion, nourishment projects have become the most common solution in the Netherlands (Spanhoff and van de Graaff, 2007). In general there are two types of nourishments—beach nourishments and shoreface nourishments (Figure 1.1). Beach nourishments are the supply of sand to the shore to protect the coastline by placing sand on the beach. Shoreface nourishments supply sand to the outer part of coastal profile, typically on the seaside of the bar.

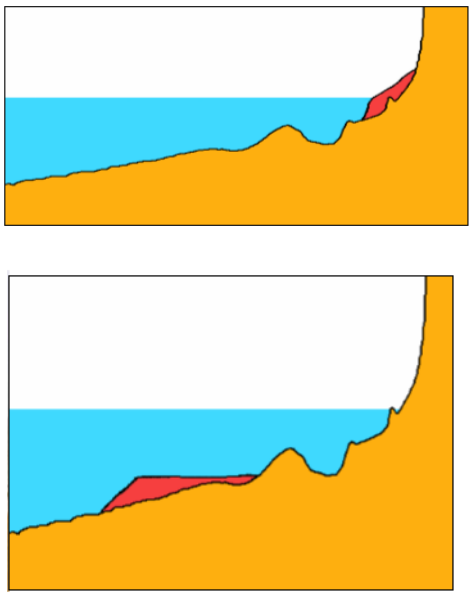

Figure 1.1: Cross-shore schematic of a beach nourishment (top) and a shoreface nourishment (bottom). The added volume is highlighted in red. (Source: Bougdanou, 2007)

Recently, shoreface nourishments are used more and more due to their lower implementation costs. The shoreface nourishment is about 2 to 5 times cheaper per m^3 than beach

nourishments (Huisman et al., 2019). This study is mainly focusing on examining the factors that influence the erosion rate of the shoreface nourishments. The shoreface nourishments can spread from the original area both in the alongshore and cross shore direction. It also can be regarded as a submerged breakwater so waves and hydraulic conditions will have a large influence on its migration speed, direction and coastline. Except the hydrodynamic conditions, the geometry of the shoreface nourishment influences the erosion rate as well.
The Netherlands have suffered from structural coastal erosion for a long time. The nourishments are applied in the Netherlands since 1950's and are implemented regularly at erosive stretches. Due to sea level rise and land subsidence in the Netherlands, nourishments may be needed more frequently.
For a good sandy strategy it is important for us to know better how nourishments behave. In this research, different parameters of submerged nourishments are tested to increase our understand of the nourishment.

1.2. Objective

The aim of this study is to examine how does the depth of the nourishment crest/ dimensionless wave height and nourishment size (length, volume, volume per meter etc) influence the erosion rate of the submerged nourishments. With this knowledge, we can have a better understanding of how the submerged nourishments behave and improve the efficiency of submerged nourishments, and to some extent also reduce the risk of coastal erosion.

1.3. Research questions

To achieve this objective, the project is separated into the following research questions:

Question 1: How does the depth of the nourishment crest/ dimensionless wave height influence the erosion rate of the submerged nourishments?

Question 2: How does the nourishment size (length, volume, volume per meter etc) influence the erosion rate of the submerged nourishments?

Both questions will be examined through the measured data and modelling test.

1.4. Approach

To examine the effect of parameters on the erosion rate of submerged nourishments, this thesis uses measured data of the Dutch and international nourishment projects in combination with the XBeach model. The parameters of wave conditions, geometries of the submerged nourishments are investigated. These can be used to examine how these factors influence the erosion rate of the submerged nourishments.

1.5. Scope

The scope of this thesis is focusing on the evolution of the submerged nourishment itself. The response of the landward area of the submerged nourishments is not included. This thesis includes the Dutch and international nourishment projects, the dump/ pits which are implemented in deep water are also involved.

1.6. Outline

This study is divided as follows:
Chapter 2: Theoretical introduction to the topic and presentation of hypothesis, knowledge gap.
Chapter 3: Methodology of data analysis and modelling test.
Chapter 4: Results and analysis of measured data.
Chapter 5: Results and analysis of modelling results.
Chapter 6: Discussion.
Chapter 7: Conclusions and recommendations.

Chapter 2

Literature review

2.1. Literature introduction

In general, shoreface nourishments can be regarded as a submerged hydraulic structure such as a soft reef berm or a submerged breakwater (Figure 2.1). Reef berms can be subdivided into (Van Rijn and Walstra, 2004):

• Stable breaker berms, (deep water) the reef or berm is functioning as a wave filter dissipating the energy of the larger breaking waves and creating a sheltered area in the lee of the reef. Most of the original volume of a stable reef is retained and the reef may remain at the placement site in deeper water (water depth: 10-15 m) for years;

• Active feeder berm, (shallow water) the berm is placed at a nearshore site in relatively shallow water (water depth is smaller than 8 m), where it will show significant dispersal of sediment during the initial period. It is supposed to act as a feeder berm for the adjacent and landward beaches resulting in widening of the beaches. The effectiveness increases with decreasing distance to the shoreline. Regular maintenance of the feeder berm is required to ensure a continuous flow of sediment to the beaches and for the berm to be fully effective.

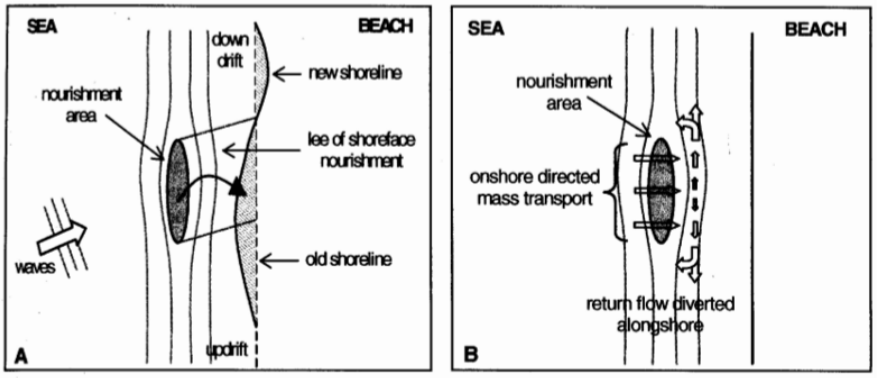

Figure 2.1: Effects as a consequence of shoreface nourishment (Source: Van Duin et al., 2004)

The presence of the submerged nourishment will have a high impact on the hydrodynamic and morphodynamic processes both in the longshore and cross shore direction. The detail description will be presented in the following sections.

In this research, several terms are used to describe the parameters of the nourishments. The terms that are used most in this research are explained as follows:
• Depth of the nourishment crest is the water depth on the nourishment crest just after placing the nourishment.
• Length of the nourishment is the distance between the edge of the nourishment in alongshore direction.
• Height of the nourishment is the crest level of the nourishment above the surrounding seabed.
• Volume per meter of the nourishment is the average cross section area of the nourishment.

2.2. Shoreface nourishment stability

According to Hamm et al. (2002), during a long time scale and large spatial scale, the implemented shoreface nourishment will be diffused in the cross-shore and longshore directions and tend to find a new equilibrium. The 'amplitude and wavelength' of the perturbation relative to the natural conditions and hydrodynamic climate affect the extent of the diffusion. In general, the larger the amplitude and the shorter the wavelength and the more energetic the hydrodynamic climate, the stronger the diffusion will be.
Most of the nourishments were executed shoreward of the outer bar and all in the form of a feeder berm (Koster, 2006). Observations show that most active feeder berms are relatively successful and most of them move onshore. Some berms remain stable, none of them move seaward (Ahrens and Hands, 1999; Bruins, 2016).

2.2.1. Depth of Closure

Beck et al. (2012) illustrates the stability of berm projects is related to the implemented depth and whether this depth is shallower or deeper as compared to the Inner and Outer Depth of Closure (Figure 2.2). The Inner depth of Closure is at the seaward limit of the littoral zone and the Outer depth of Closure is at the seaward limit of the shoal/ buffer zone. The stable berms were placed between 0 % and 50 % shallower than the Outer DOC Limit, but still were deeper than the Inner DOC Limit, and the berms which were placed less than half of water depth of the Outer DOC tend to be active (Beck et al., 2012).

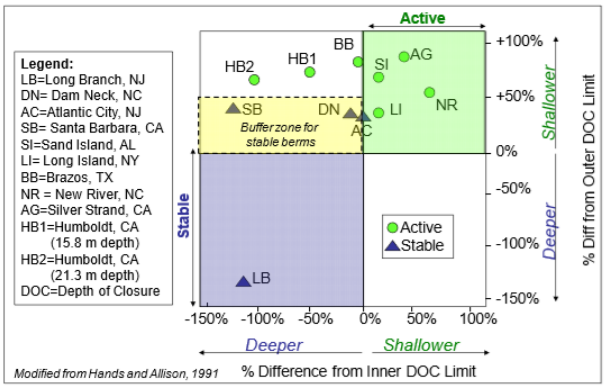

Figure 2.2: Nearshore berm stability graph illustrating the difference between active and stable berms in deep or shallow water (Source: Beck et al., 2012)

And the inner and outer depth of closure is calculated from the sand characteristics and the annual wave climate:

$$DOC_{inner} = 2H_s + 11\sigma_{H_s} \tag{2.1}$$

$$DOC_{outer} = (H_s - 0.3\sigma_{Hs})T_s\sqrt{g/(5000D)} \tag{2.2}$$

Where Hs is the meam annual significant wave height, σ_{H_s} is the associated standard deviation, T_s is the mean significant wave period, D is the typical median sand diameter near the project site.

2.2.2. Surf zone

The surf zone is defined by the region that waves start breaking when approaching the coastline. The outer limit of the surf zone is called the breaker line. In general, waves start breaking when the water depth is smaller than 3 three times of wave heights. Hoekstra et al. (1997) found that the suspended sediment transport is related to the wave breaking condition ($Hm0/h > 0.33$), which is inside the surf zone. It also indicates that the rapid evolution of the Terschelling nourishment is frequently occurring in the storm period.

2.3. Lifetime prediction of nourishments

The lifetime of the nourishments differs a lot. The estimated halftime of the nourishment varies from 3 years for the Katwijk' 98 to 30 years for the Terschelling '93 which was based

on a linear extrapolation (Huisman et al. (2019)).
de Sonneville and Van der Spek (2012) conclude that the small and isolated Egmond 1999 and Bergen 2000 nourishments disappeared about two to three years. The Camperduin 2002 fully merged with the outer bar and remained stable. The Egmond 2004 and Bergen 2005 which were larger than the earlier ones and remained much more stable, interrupting the autonomous behaviour for over six years.

2.4. Hydrodynamic processes around nourishments

Due to the presence of the nourishment, complex of hydrodynamic patterns may be induced. As waves enter the coastal zone, large waves tend to break more offshore after implementing the shoreface nourishment then a calmer wave climate will be created in the landward area of the shoreface nourishment, the longshore current and the transport capacity will decrease as well. And the remaining shoaling waves lead to onshore transport due to wave asymmetry over the nourishment area, the smaller waves in the lee side generate less stirring of the sediment and the wave-induced return flow reduces (Van Duin et al., 2004).
Rip current is a significant effect caused by the nourishment. In general rip currents towards the offshore in the nearshore zone and have an erosive character (Koster, 2006). The presence of the nourishment causes the alongshore variation of wave condition which generates rip currents. As the wave breaks over the nourishment alongshore pressure gradient appear due to the difference of breaking intensity which leads to the variation of radiation stresses and hence the set-up over the nourishment (Drønen et al., 2002). The pressure gradient drive alongshore currents toward the rip channel where the concentrated water mass is in the seaward direction.

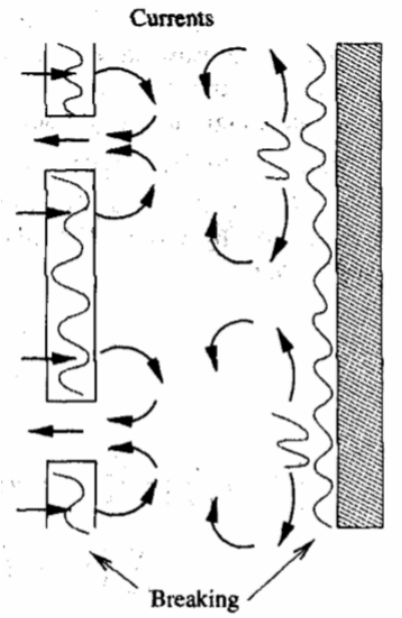

Figure 2.3: Horizontal circulation cells, the rectangles with wave line on the left hand side are the bar, the gray rectangles on the right hand side are the beach (Source: Haas et al., 1999)

Figure 2.3 (Haas et al., 1999) shows that the waves firstly break on the crest of the bar and cause the first horizontal circulation. In the mean time, the waves in the channel are still propagating and breaking much more shoreward which results in the second horizontal circulation. Onshore currents are present at the bar crest as a result of mass transport by the waves, wave skewness induced velocity asymmetry, while currents are in the offshore direction at both lateral sides of the bar.

Koster (2006) presents the hydrodynamic patterns around a nourishment area using a numerical model Delft 3D. Figure 2.4 shows that the onshore velocities can be found on the crest of the bar and the offshore velocities are presented in the deeper area just next to the nourishment. And for the larger water depth results in the smaller cross shore velocity. The wave dissipation energy around the nourishment area is the main cause of onshore transport. In deeper water waves break more offshore then the water level variation over the nourishment is significant less and also have less impact on the bottom, while in shallow water conditions the wave energy dissipation is much higher and also the water level variation above the nourishment is larger then results in larger onshore currents. Placing the shoreface nourishment in a relative shallow water depth will increase its potential to break waves and promote transport of sediment in onshore direction.

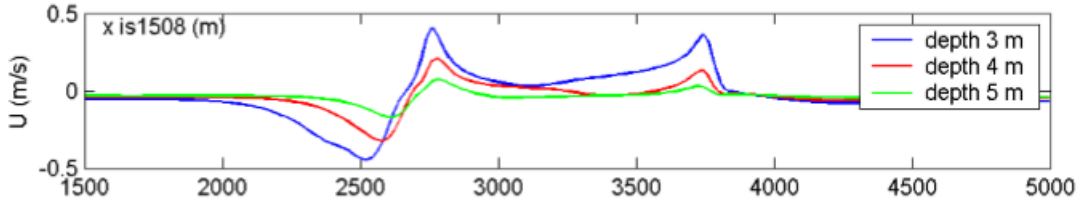

Figure 2.4: cross shore velocity on the crest of the bar nourishment, the depth is defined as the water depth above the crest of the nourishment, the positive sign is in the onshore direction (Source: Koster, 2006)

Koster (2006) also presents the longshore velocity and the largest influence can be found just onshore of the bar nourishment crest. The currents split into two symmetrical parts and flow through into opposite directions (Figure 2.5).

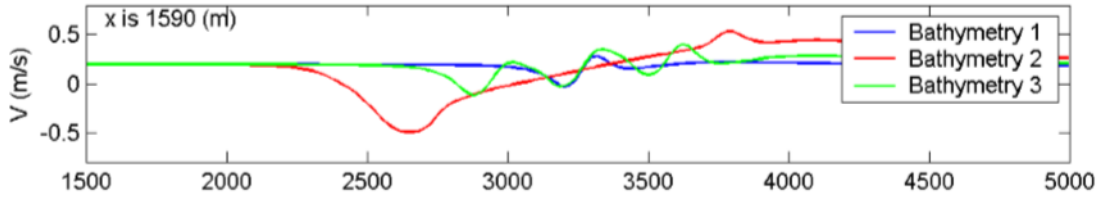

Figure 2.5: longshore velocities in the longshore direction, just onshore of the crest, bathymetry 1: one hump nourishment with the length of 50m; bathymetry 2: one bar nourishment with the length of 1000m; bathymetry 3: 3 hump nourishments with the length of 200m and the mutual distance is 200m (Source: Koster, 2006)

2.5. Morphodynamic processes around nourishments

The feedback between hydrodynamic and the changes in morphology is called morphodynamics. The implemented nourishment projects will highly influence the local morphodynamic process. In this section, the sediment transport in cross shore and longshore direction around the nourishment area will be discussed.

2.5.1. Cross shore sediment transport process

In the coastal zone, the wave asymmetry results in the onshore directed movement of sediments during calm periods. The offshore movement of sediments can be found during storms due to the high intensity of wave breaking. The net migration of the nourishment is the result of the onshore movement during calm periods and the offshore movement during storms (Walstra, 2016).
The net cross shore suspended sediment transport is given in Equation 2.3

$$< uc >=< \bar{u}\bar{c} > + < u'c' > \tag{2.3}$$

Where u is the net cross shore velocity, c is the sediment concentration, u' is the oscillatory velocity, $\bar{u}$ is the mean current velocity, $< uc >$ is the net suspended sediment transport, $< \bar{u}\bar{c} >$ is the sediment transport of mean currents, $< u'c' >$ is the oscillating transport (e.g. wave asymmetry). The oscillating term can be divided into a high and low-frequency part and the separation frequency is set up to 0.04 Hz (Houwman and Ruessink, 1997).
Hoekstra et al. (1997) presents the relation between cross shore sediment fluxes and the factor of Hm0/h (where $Hm0$ is l the ocal significant wave height and h is water depth) just offshore of the nourishment in Terschelling case Figure 2.6. Non-zero fluxes only occurred for Hm0/h is larger than 0.3-0.35. High frequency fluxes were in the onshore direction and were associated with the horizontal asymmetry of the incident short waves. While low frequency fluxes were in the offshore direction and were caused by bound long waves. The mean fluxes were in the seaward direction which were larger than the oscillating flux (i.e the sum of high frequency and low frequency flux). As a result, the net flux was in the offshore direction.

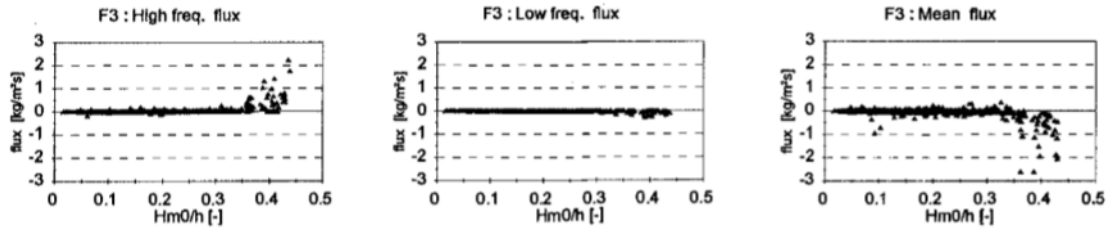

Figure 2.6: Cross shore sediment fluxes measured just offshore of the shoreface nourishment in Tershelling case (the measurement is at 0.15 m above the bed): high, low-frequency (f<0.04 Hz) fluxes and mean fluxes, positive flux is onshore and negative flux is offshore (Source: Hoekstra et al., 1997)

2.5.2. Longshore sediment transport process

For the Dutch coast, most of the times, the waves come from two dominant directions (Bougdanou, 2007). As the wave enter into the coastal zone, these incident oblique waves will result in longshore currents. The waves break and energy lose at the nourishment which leads to the increased shear stress. The sediment particles are stired up and transported by longshore currents. The influence of the wave-driven alongshore transport (contributing about 15% to 40% to the erosion) is much smaller at the shoreface nourishments compared to the cross shore transport (contributing about 15 % to 40 % to the erosion) (Huisman et al., 2019). Landward of the nourishment the wave condition is reduced, hence

the littoral drift and sand is trapped behind the nourishment which leads to the salient effect occurs (Figure 2.7).

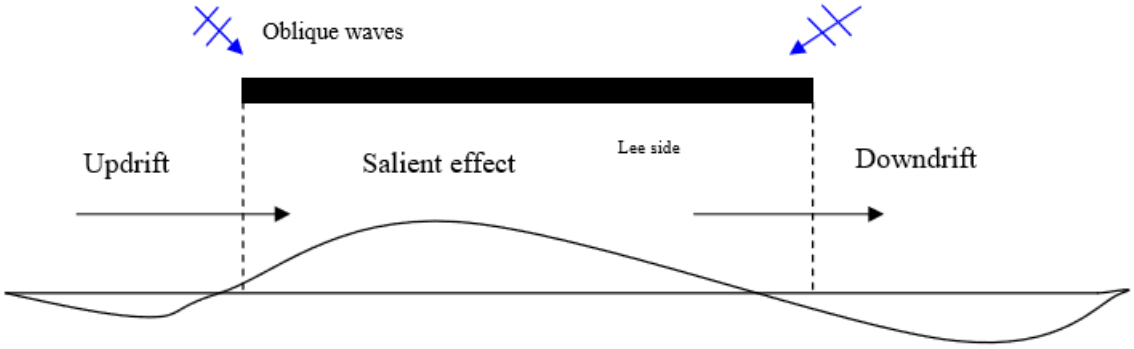

Figure 2.7: salient effect, the black box is the nourishment (Source: Bougdanou, 2007)

2.6. Erosion/ sedimentation pattern of nourishments

The erosion rate is relatively large in the initial phase after the placement of the nourishment. Koster (2006) presents the initial erosion/ sedimentation of a nourishment. It shows that the largest initial change is at the nourished area itself and just onshore of it. Both erosion and sedimentation pattern is found on the nourishment area, the tips have much more stronger erosion pattern than the middle section (Figure 2.8).

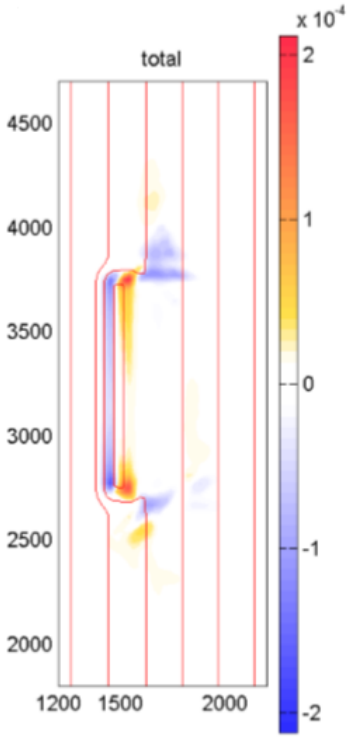

Figure 2.8: erosion/ sedimentation pattern of the nourishment, x=2300m is the location of the beach (Source: Koster, 2006)

2.7. Mobility parameter

The mobility parameter describes the tendency of sediment erosion (Equation 2.4). The larger mobility parameter, the more erosion of sediments will be.

$$\psi = \frac{U_0^2}{(S-1)gD_{50}} \tag{2.4}$$

Where U_0 is the amplitude velocity, S is the sediment specific gravity which is equal to 2.65 in this research, g is the gravity acceleration, D_50 is the median sand size.

$$U_0 = \frac{\pi H_{m0}}{Tsinh(\frac{2\pi h}{L})} \tag{2.5}$$

$$L = \frac{gT^2}{2\pi} tanh(\frac{2\pi h}{L}) \tag{2.6}$$

H_{m0} is the significant wave height, T is the wave period (in this research, the peak wave pe-

riod is used), L is the wave length in arbitrary depth can be calculated through the iterative method.

2.8. Sediment transport formula

The Van Thiel-Van Rijn transport equations describe the detail information of the sediment transport. It includes the important processes (orbital motion, current flow) of the sediment transport, the formulation is presented in Equation 2.7 and Equation 2.8 which calculate the equilibrium sediment concentration (Van Rijn, 2007):

$$C_{eq,b} = \frac{A_{sb}}{h}(\sqrt{v_{mg}^2 + 0.64u_{rms,2}^2} - U_{cr})^{1.5} \tag{2.7}$$

$$C_{eq,s} = \frac{A_{ss}}{h}(\sqrt{v_{mg}^2 + 0.64u_{rms,2}^2} - U_{cr})^{2.4} \tag{2.8}$$

Equation 2.7 and Equation 2.8 indicate that the sediment is stirred by the Eulerian mean velocity and wave orbital velocity. Where A_{sb} and A_{ss} is the bed-load and suspended load coefficient, v_{mg} is the velocity magnitude which is equal to the magnitude of the Eulerian velocity (Equation 2.9), $u_{rms,2}$ is the adjusted orbital velocity that includes turbulence effects (Equation 2.13).

$$v_{mg} = \sqrt{(u^E)^2 + (v^E)^2} \tag{2.9}$$

$$u^E = u^L - u^S, v^E = v^L - v^S \tag{2.10}$$

$$u^S = \frac{E_w sin\theta}{\rho hc}, v^S = \frac{E_w sin\theta}{\rho hc} \tag{2.11}$$

Where u^E and v^E are the cross shore Eulerian velocity and longshore Eulerian velocity, respectively. u^L and v^L are the cross shore Lagrangian velocity and longshore Lagrangian velocity, respectively. u^S and v^S are the cross shore Stokes and longshore Strokes drift, respectively. E_w is wave-group varying short wave energy, c is the wave velocity, ρ is the water density.

Assume the vertical wave mass transport is balanced between the Stokes drift and Eulerian

flow: $Q_{stokes} = Q_E$, then $u_E = u_S$. Wave energy transports in the nearshore can be regarded as a wave energy balance: wave energy flux is constant. If assume a shallow water condition, then the wave energy is dependent on the square root of water depth (Equation 2.12).

$$\frac{\partial E c_g}{\partial x} \approx \frac{\partial E\sqrt{gh}}{\partial x} = 0 \rightarrow E \sim h^{-1/2} \tag{2.12}$$

Then the relation between the Eulerian velocity and water depth can be derived based on Equation 2.11: $u_E \sim h^{-2}$. Additionally, the wave group energy (E) is also proportional to H^2. The numerator and denominator both multiply with $h^{0.5}$. Assume the shallow water condition and constant water depth, the relation between the Eulerian velocity and dimensionless wave height can be derived: $u_E \sim (\frac{H}{h})^2$.

$$u_{rms,2}^2 = u_{rms}^2 + 1.45 k_b \tag{2.13}$$

Where u_{rms} is the orbital velocity which is calculated in Equation 2.14 and k_b is the wave breaking induced turbulence due to short waves (Equation 2.15).

$$u_{rms} = \frac{\pi H_{rms}}{T_{rep}\sqrt{2} sinh(k(h + \delta H_{rms}))} \tag{2.14}$$

Where H_{rms} is the root-mean-square wave height, T_{rep} is the representative wave period, h is the water depth and in this equation the water depth is increased with a certain factor of the root- mean-square wave height (δ). In Equation 2.14, numerator and denominator both divide the water depth. Then the simplified relation between orbital motion and dimensionless wave height can be derived from Equation 2.14 with neglecting the effect of water depths: $u_{rms} \sim \frac{H/h}{sinh(1+H/h)}$.

$$k_b = \frac{\bar{k_s} \cdot T_{rep}/T_{bore}}{exp(h/L_{mix}) - 1} \tag{2.15}$$

Where L_{mix} is the mixing length which is proportional to the root-mean-square wave height. $\bar{k_s}$ is the time averaged turbulence variation at the water suirface, which is proportional to roller dissipation. T_{bore} is the wave period interval associated with breaking induced turbulence. The simplified relation between the turbulence intensity and dimensionless wave height can be derived through Equation 2.15: $k_b \sim (exp(H/h)^{-1})^{-1} = exp(H/h)$. The exponential relation is expected between the turbulence intensity and dimensionless wave

height.

2.9. Knowledge gap and Hypothesis

The objective of this thesis is to examine the parameters that influence the erosion rate of the nourishments. Previous literature has shown that the erosion rate or lifetime of the shoreface nourishment differ a lot between each other and the reason behind it is still unclear. The important still existing knowledge gaps are the following:

• According to Huisman et al. (2019) and Bruins (2016), there is no relation between the depth of the nourishment crest and erosion rate/ migration speed of the shoreface nourishments. But the relation can be expected based on the previous analysis. The Dutch nourishments were implemented on nearly similar water depths. Then it would be better to have a wider range of nourishments (such as dump sites/ pits and other international cases) and also test through the XBeach model.

• The relation between wave conditions and erosion rate of shoreface nourishments has not been investigated in the previous literature. These factors can be related to the ratio between wave heights and the depth of the nourishment crest, i.e the dimensionless wave height. So how the relation between the dimensionless wave heights and erosion rates of nourishments will be from the measured data and modelling test.

• Except the hydrodynamic condition, how the nourishment size (length, volume, volume per meter etc) influences the erosion rate of shoreface nourishments based on the measured data and modelling test.

Then the simple hypothesis is proposed as following:

(1) The evolution of the shoreface nourishment is highly dependent on the wave condition. It can be related to the generic term called dimensionless wave height (H/h). The erosion rate of the shoreface nourishments is sensitive when the dimensionless wave height is larger than 0.33. As the dimensionless wave height gets lower, the erosion rate of the nourishment is almost the same.

(2) The placement depth of the shoreface nourishment also affects the evolution of the shoreface nourishment. The deeper placement depth of the shoreface nourishment, the lower erosion rate will be. When the placement depth is relatively deep, the nourishment tends to be stable. It results in a nearly same erosion rate in deep water.

(3) The smaller length of the shoreface nourishment has a faster erosion process. The erosion rate is sensitive for a relatively small length. As the length of the shoreface nourishment gets longer, the erosion rate tends to be stable.

Chapter 3

Methods

3.1. Introduction

In this chapter the method is presented. The research steps are shortly listed below.
Examination of observations at nourishment case studies:
The erosion rate and the parameters (such as length, volume per meter, volume) of the Dutch nourishments are collected from the relevant Dutch reports. Depth of the nourishment crest and nourishment height are collected from the Jarkus survey. For the international nourishments, both the erosion rate and relevant parameters (wave heights,length, volume per meter, volume, depth of the crest and nourishment height) are collected from the international reports.
The Dutch hydrodynamic conditions (wave heights) are collected from offshore wave stations (IJmuiden, Europlatform and Eierlandse gat) and transferred into the specific nearshore location through the SWAN model. Then the relation between the dimensionless wave height and erosion rate of the nourishments is plotted for the Dutch cases.
The Dutch nourishments are divided into several subsets. For every subset, the related graphs are plotted and examine the potential relation. For the international case, the parameters and hydrodynamic conditions of the nourishments are collected from the corresponding reports. Then the international and Dutch cases are combined together to examine the further relation.
Numerical experiment:
The numerical model is constructed using the XBeach model and then the hydrodynamic and morphological conditions are validated.
Then different hydrodynamic conditions (depth of the nourishment crest, dimensionless wave height) and nourishment sizes (length, volume, volume per meter etc) are tested through the constructed model to examine the relation between these parameters and the erosion rate of the nourishments.

3.2. Nourishment data

3.2.1. Dutch nourishments

17 shoreface nourishments with a depth range of the crest is around 4-6m are collected from Huisman et al. (2019). Data on erosion rates of these 17 shoreface nourishments are collected from this report. The variation of the crest depth is quite narrow and therefore dump sites and sand pits at deeper water are included as well.
Data about the dump sites and pits are collected from Boers (2005), the filling rate of pits is taken as a representative morphological parameter to compare to the nourishment and dump cases.
Detailed information on the Dutch projects used is given in Table 3.1.

Table 3.1: overview of the Dutch shoreface nourishment and dump sites/ pits

ID	location	year	water depth (m)	volume (m^3)	length (m)	volume per meter (m^3/m)	height (m)	erosion/ filling rate (m^3/yr)	rate of volume change per length ($m^3/m/yr$)
1	Delfland-Scheveningen	1999	4.5	1425780	2774	514	2.73	56000	20
2	Delfland-Terheijde	1997	4.75	882605	1701	519	3	105000	62
3	Delfland-Terheijde	2001	5	2970879	5105	582	3.45	131000	26
4	Delfland-Monster	2005	5	882055	4410	200	1.15	143000	32
5	Rijnland-Katwijk	1998	5.7	753338	2004	376	-	150000	75
6	Rijnland-Noordwijk	1998	5	1266028	3000	422	1.29	159000	53
7	Rijnland-Noordwijkhout	2002	5.48	2645601	7018	377	-	217000	31
8	Rijnland-Wassenaar	2002	5.49	2508887	6002	418	1.27	177000	29
9	Rijnland-Zandvoort	2004	4.98	2203427	4897	450	1.65	221000	45
10	Rijnland-ZandvoortZuid	2008	4.74	509913	2512	203	-	56000	22
11	Rijnland-Bloemendaal	2008	4.85	1002956	2002	501	2.04	89000	44
12	Noord-Holland-julianadorp	2009	4.5	1301565	3006	433	1.95	83000	28
13	Noord-Holland-camperduin	2002	5.17	1972272	3503	563	2.45	64000	18
14	Noord-Holland-callantsoog	2003	5.5	2315360	6014	385	3.35	210000	35
15	Noord-Holland-Egmond	1999	5.3	880100	2200	400	1.39	126000	57
16	Noord-Holland-Bergen	2000	5	994000	2000	497	1	102000	51
17	Noord-Holland-Bergen Egmond	2005	5.5	3106812	8559	363	1.95	247000	52
18	Wijk aan Zee	1982	13	950000	-	-	-	31000	-
19	Simon Stevin pit	1981	15.5	60000	-	-	-	62000	-
20	PUTMOR pit	1999	23	4500000	-	-	-	12400	-
21	Ameland I pit	1990	9.5	140000	-	-	-	67000	-
22	Wiersma Ridge	1982	19	3500000	-	-	-	27300	-

* The water depth of shoreface nourishments (ID: 1-17) is the depth of the shoreface nourishment crest. The water depth of dump sites/ pits (ID: 18-22) is the initial water depth before dumping or dredging. The volume and volume per meter of the shoreface nourishments (ID: 1-17) is collected from the official data (https://publicwiki.deltares.nl/display/OET/Dataset+documentation+Nourishments). The length of the shoreface nourishments is determined by the ratio of the volume and volume per meter. The height of the shoreface nourishment is collected from the Jarkus survey. The median grain size was measured at the Noord-Holland-Egmond '99, Noord-Holland-Bergen '00 and Rijnland-Noordwijk '98, which is equal to 0.228 mm, 0.25 mm and 0.4mm respectively.

3.2.2. International nourishment projects

Information from international nourishment projects is obtained from nourishment reports and specifically the erosion rate, nourishment size, wave height and water depth etc. However, not all reports contain these useful data and therefore only 6 shoreface nourishment projects are selected (Table 3.2).

Table 3.2: International shoreface nourishment data

location	Approx depth of nourishment crest (m)	erosion rate (m^3/yr)	length (m)	local wave height (m)	dimensionless wave height (–)	wave period (s)	median grain size (mm)	reference
South Padre Island,Texas	6.9	73650	1220	0.78	0.11	6.7	-	Aidala et al. (1992)
Sliver Strand State Park, CA	3	37740	370	0.62	0.21	13.1	0.2	Larson and Kraus (1992) Juhnke et al. (1990)
Perdido Key, FL	4.5	160000	4000	0.6	0.13	6	0.3	Work and Otay (1996)
Brunswick, GA (Mound "C")	2.5	306000	1100	0.46	0.18	-	0.35	Johnson (2005) Gailani et al. (2007)
Ocean beach, SF	11.5	138000	800	2.5	0.22	12	0.18	Barnard et al. (2009)
New River Inlet NC	3	100500	210	0.55	0.18	7.3	0.49	Schwartz and Musialowski (1978)

* erosion rate: the method of calculation of the erosion rate of each international case is presented in Appendix A, local wave height: yearly-significant wave height on the nourishment area.

3.2.3. Calculation method of the erosion rate of the Dutch nourishments

Huisman et al. (2019) presented the measured volume change of the initial nourishment region. A linear line is fitted over the initial nourishment region (Figure 3.1 (b)). The erosion rate of shoreface nourishments is defined by a decrease in the volume within the bounds of the initial nourishment area (Figure 3.1 (a), dV_{nour}/dt). The erosion rate per meter is determined by the volume change over time in the cross-shore averaged volume along with the nourishment (Figure 3.1 (c), $dV_{nour}/dt/L_{length}$, L_{length} is the initial alongshore length of the nourishment).

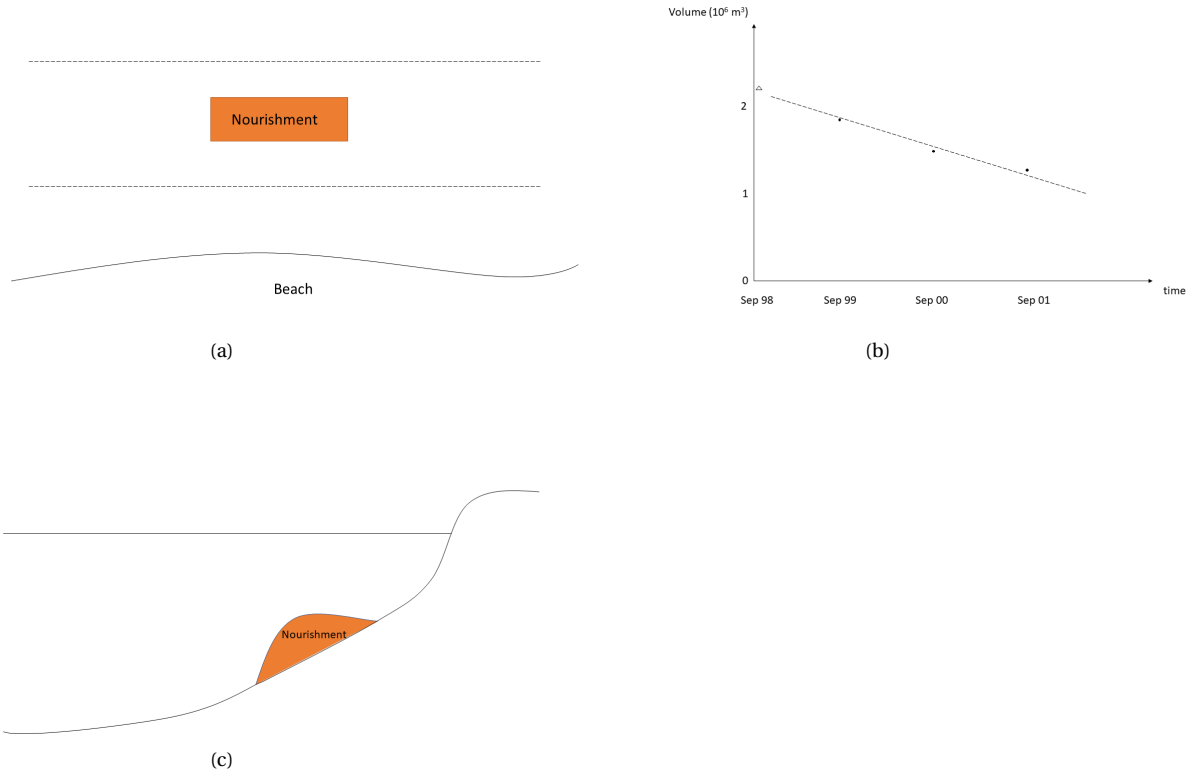

Figure 3.1: (a) an example of the defined initial nourishment region, orange rectangular box is the initial nourishment region; (b) measured volume change after implementation of the nourishment triangle is the official nourishment volume and circle dot is the measured volume in the initial nourishment region; (c) an example of the cross shore averaged volume of the nourishment

The erosion/ filling rate of the dump site/ pits is determined by the ratio of total dumped/ dredged volume of the dump sites/ pits and characteristic time scale. Boers (2005) presents the calculation method of the characteristic time which is based on the assumption that the dredged or dumped volume shows an exponential decrease (V_0: initial volume, V_t: back-filling volume at time t, T_k: characteristic time scale): $V_t = V_0(1 - e^{(-t/T_k)})$. This function is fitted through the volumes in time, to determine the characteristic time scale, at which time the volume has decreased by 62 %. The average erosion/ filling rate of the dump sites/ pits can be calculated by $0.62V_0/T_k$ (Figure 3.2).

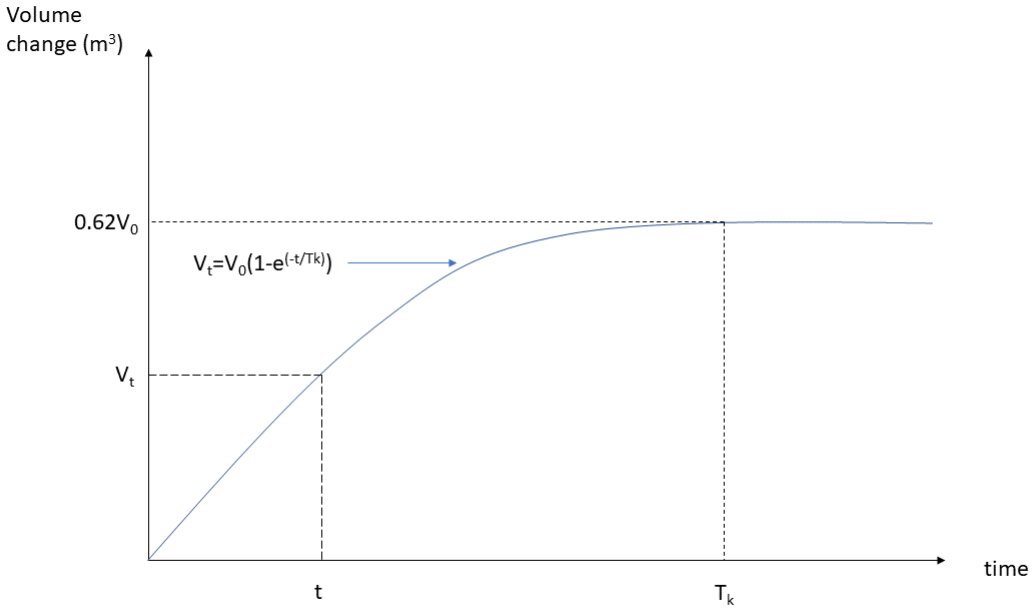

Figure 3.2: example of the volume change of the dump sites/ pits, V_t can be obtained from measured data, T_k is calculated through the characteristic time scale function.

3.3. Wave data along the Dutch coast

The wave condition at each nourishment project needs to be collected. According to Wijnberg (2002), the mean monthly wave heights (H_{m0}) as well as annual wave heights are very similar for wave stations ELD, YM6 and EUR which means wave heights along the Dutch coast do not vary a lot; however, the nearshore wave station MPN is relative lower (Figure 3.3). The wave condition of the shoreface nourishments can be obtained by a wave look-up table which has been developed within the Building with Nature project. This table transforms offshore wave data to an arbitrary location nearshore along the Dutch coast. EUR (Euro platform) wave station represents the wave condition of deeper dump sites/ pits (>9.5 m).

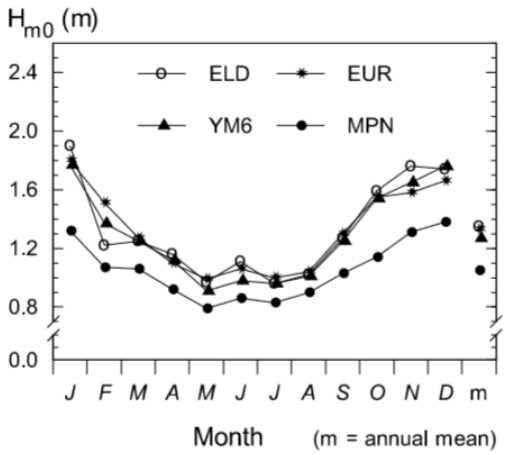

Figure 3.3: Mean monthly wave height and mean annual wave height along the Holland coast (source: rijkswaterstaat).

From Euro platform, the time series of significant wave data can be obtained. Then the yearly averaged significant wave height: $H_{s,ave} = \frac{1}{N}\sum_{j=1}^{N} H_j$. The significant wave height at Euro platform is averaged from 1987 to 2002 (Table 3.3). The significant wave height in two successive years after the placement of the shoreface nourishments or dump sites/pits is calculated to represent the wave condition. The wave data before 1987 is not available. The yearly difference of significant wave heights at Euro platform is approximate to 5% so it is possible to average the significant wave heights between 1987 and 2002 at Euro platform to represent the wave condition of dump sites/ pits which were placed before 1987.

For shoreface nourishments, the time series of significant wave heights on the specific nearshore location can be obtained by a wave look-up table. It has been developed by Deltares within Building with Nature. The validation has been done for the significant wave height at the Lichteiland Goeree and Meetpost Noordwijk stations (Figure 3.4) for a period of 22 years and the correlation factiors are 0.94 and 0.97, respectively (Fockert and Luijendijk, 2011).

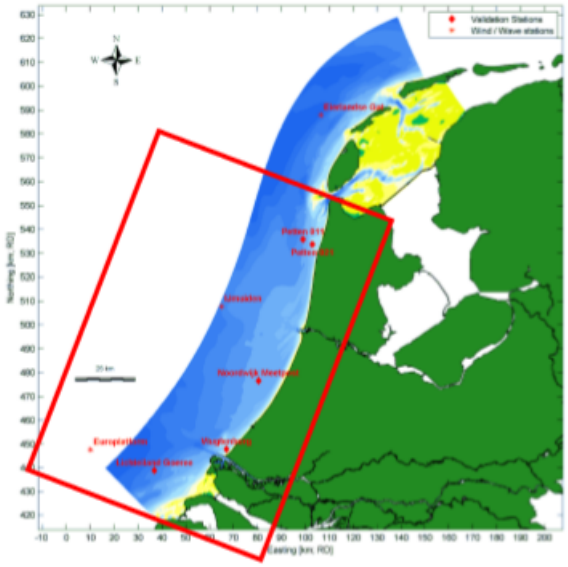

Figure 3.4: overview locations of wave stations (red points are wave stations)

The significant wave height in Table 3.4 is also calculated by averaging significant wave heights in two successive years after the placement of the shoreface nourishments.

Table 3.3: significant wave heights at Euro platform

year	significant wave height (m)
1987	1.20
1988	1.37
1989	1.23
1990	1.39
1991	1.20
1992	1.23
1993	1.30
1994	1.26
1995	1.29
1996	1.22
1997	1.09
1998	1.36
1999	1.29
2000	1.23
2001	1.25
2002	1.23

Table 3.4: significant wave heights of each shoreface nourishment case

ID	significant wave height (m)
1	0.93
2	0.89
3	0.92
4	0.97
5	0.92
6	0.92
7	0.79
8	0.88
9	0.80
10	0.87
11	0.89
12	0.76
13	0.91
14	0.94
15	0.95
16	0.93
17	0.96

There are three Dutch nourishment cases combining with international nourishment projects to test the influence of the mobility parameter, then the wave period is required. The peak wave period in two successive years after the placement of the shoreface nourishments is calculated for Noord-Holland-Egmond '99, Noord-Holland-Bergen'00 and Rijnland-Noordwijk '98 cases, which is equal to 5.84s, 5.81s and 5.9s respectively.

3.4. Definition of dimensionless wave heights in the measured data

The dimensionless less wave height is calculated for each nourishment project (shoreface nourishments and dump sites/ pits). The dimensionless wave height of the Dutch shoreface nourishment case is equal to the ratio of yearly-significant wave heights in two successive years after the placement of the shoreface nourishments at the local location of nourishment projects (Table 3.4) and the depth of the nourishment crest. The dimensionless wave height of each dump/ pit case is equal to the ratio of yearly-significant wave heights at Euro platform in two successive years after the placement of the dump sites/ pits (Table 3.3) and the initial water depth before dumping or dredging (the water depth after dumping or dredging is not available). The dimensionless wave height of the international shoreface nourishments is equal to the ratio of yearly-significant wave heights on the nourishment area and the depth of the nourishment crest.

3.5. Analysis method

For the Dutch cases, the dump sites and shoreface nourishments are combined together to test the relation between the erosion rate and water depth/ dimensionless wave height. Then the shoreface nourishment data are divided into different subsets. The shoreface nourishments with the same characteristics (volume, length or volume per meter) are classified into the same subset. Then the related graphs between erosion rate/ erosion rate per meter and shoreface nourishment size (such as length, volume, cross section area and berm height)/ hydrodynamic condition (such as water depth, dimensionless wave height) are plotted to test if any relation can be found.
Data of the Dutch shoreface nourishments and international shoreface nourishments are combined together to test the relation between the dimensionless wave height/ mobility parameter and erosion rate/ erosion rate per meter.

3.6. Correlation method

3.6.1. Linear regression

Linear regression is used to examine a linear relationship between a dependent variable and independent variables and used widely in practical applications. The linear regression is applied if we expect a linear trend between dependent variables and independent variables. The nourishment dataset is limited and variables are too much compared to each nourishment case. The linear trend is the best choice for the limited data and much easier to fit than the non-linear regression. Therefore, the linear trend is expected in the measured data.
However, the linear regression is only appropriate when the variances along the line of best fit remain similar as moving along the line. In this research, if the variances are not homogeneous along the trend line then the linear regression is not applied and the trend line is not presented. For the other cases, the linear regression is applied to test if any relation can be found.

3.6.2. R^2 and $p-value$

The R^2 value and $p-value$ is calculated for each linear relation between 2 parameters. The R^2 value is a measure of how well the linear regression model explains the data. In this research, there are a lot of variables (such as length, volume, volume per meter and height etc) that may influence each shoreface nourishment case. Therefore, it is relatively difficult

to get a high value of R^2 . In this case, the relatively lower value of R^2 also indicates some valuable information.

The $p-value$ is the probability of obtaining test results at least as extreme as the results actually observed during the test, assuming that the null hypothesis is correct (Wasserstein et al., 2016). The null hypothesis states that there is no relationship between the two variables being investigated (Everitt, 1998). It states the results are due to chance and are not significant in supporting the idea being studied. In general, the smaller $p-value$, the higher statistical significance will be that we can reject the null hypothesis. In this research, a threshold value or statistical significance level for $p-value$ is 0.05. If $p-value$ is less than 0.05 means the level of statistical significance is achieved.

3.6.3. Outliers

The linear regression is sensitive to the existed outliers, especially for the small sample size. In this research, the Dutch nourishment data will be divided into several subsets which will result in a relative small sample size (n≤ 8). Outliers in each subset may significantly influence the slope and sign of the trend line. And the existed outlier will also influence the trend in the large sample size (n≥ 14). It is therefore necessary to detect the ouliters for each sample size.

The method of detecting the ouliter is to calculate the Mahalanobis distance which can detect the outlier for multi-variate. The Mahalanobis distance is a measure to calculate the distance between a specific point D and a distribution E. It measures how many standard deviation the specific point D away from the mean of E. The Mahalanobis distance of each point x_i ($i = 1,2,3....$) is computed for detecting the outliers (Equation 3.1, Equation 3.2). If this distance is equal to zero then the specific point D is at the mean of E and it grows if the specific point D moves away from the mean along each axis. In this research, the Mahalanobis distance is larger than 4 regarded as the outliers which are removed in each small sample size (n≤ 8). The influence of the outliers is less strong for the large sample size, therefore the outliers of the large sample size is determined when the Mahalanobis distance is larger than 7.

$$V = \frac{1}{n-1}\sum_{i=1}^{n}(x_i-\bar{x})(x_i-\bar{x})^T \tag{3.1}$$

Then

$$MD_i = \sqrt{(x_i-\bar{x})^T V^{-1}(x_i-\bar{x})} \tag{3.2}$$

Where x_i is the observation point, $\bar{x}$ is the mean value of the observation point, V is the covariance matrix, MD_i is the Mahalanobis distance.

3.7. Modelling approach

3.7.1. Model description

A next step was to investigate morphological changes of the nourishments through the Xbeach model. A simplified model to represent the Dutch coast without natural bars. The stationary case (constant wave height) is applied and long waves are not included. Waves are breaking around the nourishment area which lead to both cross-shore and longshore sediment transport. To minimize the effect of model errors, the validation of hydrodynamics and morphological conditions is necessary. But a full validation is not possible as there are no observations of the simplified case. Instead, the hydrodynamics and morphological conditions are verified in combination with previous studies. The schematisation of model will be introduced in more detail in Chapter 5.
All modelling scenarios were executed with the Xbeach model V21. The XBeach model uses the shallow water equations for the low-frequency and mean flows and wave action balance equations for short waves and solves the coupled equations for wave propagation, flow, sediment transport and bottom changes. For a more detailed description can be found through the Xbeach manual (XBeach Model Description and Manual).

3.7.2. Model setting

For the stationary case (constant wave height), the Baldock formulation was applied. And the breaker parameter γ needs to be increased to be 0.78 instead of the default value of 0.55 when using the Baldock formulation (Van Bemmelen, 2017). The formulation to calculate the breaking wave height is in Equation 3.3:

$$H_b = \frac{0.88}{k} tanh\left[\frac{\gamma kh}{0.88}\right] \tag{3.3}$$

This research is focused on the initial phase of sedimentation and erosion of the nourishments instead of morphological change. Then the shorter simulation time is set which is equal to 1 hour. And a morphological acceleration factor of 10 was applied to accelerate bed changes for saving computational times. The time step is calculated based on the courant number which is set to be 0.7. The default value is used for the paramters which are not specified above (see Appendix II).

3.7.3. Bathymetry

In this study, the simulations are executed on a linearly sloping bottom profile of 1:150, similar to the average bed slope in the nourished area reported in Bruins (2016). The simulation model consists of a coastal area of 3900 meters in cross shore direction and 7500 meters in alongshore direction. The bathymetry of the nourishment is determined by the distance between the crest of the nourishment and water level. The different bathymetries of the nourishments are applied in this research. In this case, the maximum water depth of 25 m is at the seaward boundary.

The x-axis represents the cross-shore direction, with positive directed onshore. The x=0m and the x=3900 m are the seaward and landward boundaries respectively (Figure 3.5). And the x-axis is perpendicular to the coastline. The orientation of the model area is from west to east, which the western boundary is the seaward boundary and the eastern boundary is the land boundary. The x=0 and x=3900 line is the location of the seaward boundary and landward boundary, respectively. The water level extends to x=3750 and the width of the beach is 150 meters. And the y-axis is in the alongshore direction y=0 corresponds with the southern boundary of the model.

Figure 3.5 shows a cross section of the nourishment with 250 meters in the cross shore direction. The crest of the nourishment is a flat plane with a width of 133.3 meters and the bathymetry of the crest is equal to 5 meters. The height of the nourishment is about 2 m with the front and the back slope are around 1:30 and 1:20, respectively, this makes the cross section area of the nourishment is approximate to 408 m^3/m. In the alongshore direction the nourishment is 1000 m long with lateral slopes of 1:40. This is the reference scenario applied in this study, in the following steps the properties of the nourishment and the hydrodynamic conditions (water depth and wave heights) will be varied.

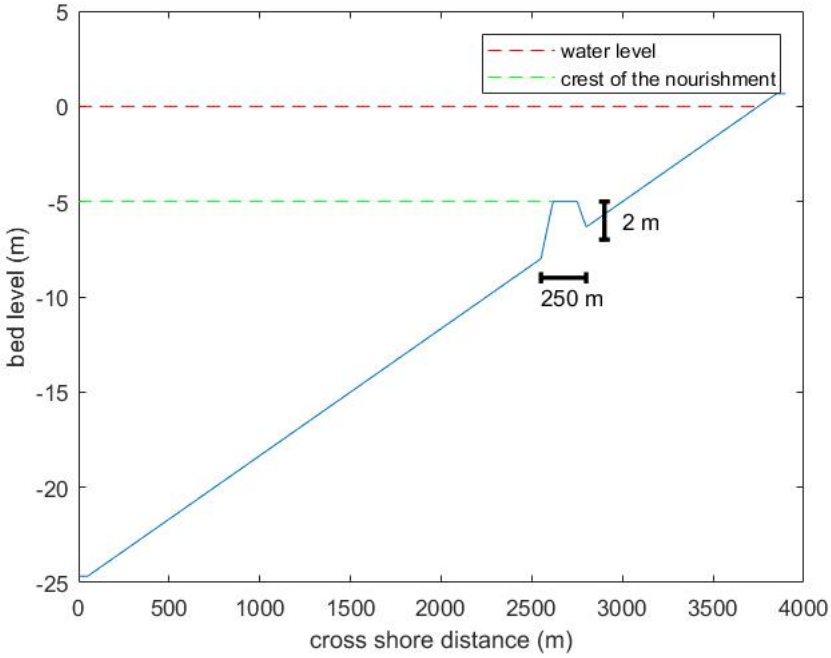

Figure 3.5: cross section of the nourishment, bed slope is 1:150, depth of the nourishment crest is 5m, cross section area of the nourishment is $408 m^3/m$

3.7.4. Computational grids

A computational grid is used that is locally refined at the location of the nourishment (Figure 3.6). Figure 3.6 shows the detail information of the computational grid. In order to get stable results of the nourishment, the grid size needs to be refined around the interest area with a refinement factor of 3. The refinement factor of the grid size, at the distance of 250 m away from the nourishment in the longshore and cross shore direction, is set to be 2 to avoid instabilities due to too large step size differences. In the other domain the grid size is set to be 50 meters. This results in the total number of grid cells equal to 19600, 98 and 200 in cross-shore and longshore direction respectively. This grid was constructed using RGFGRID. If the nourishment is placed at a different cross-shore location or with different lengths, then the area with a refined grid is moved accordingly.

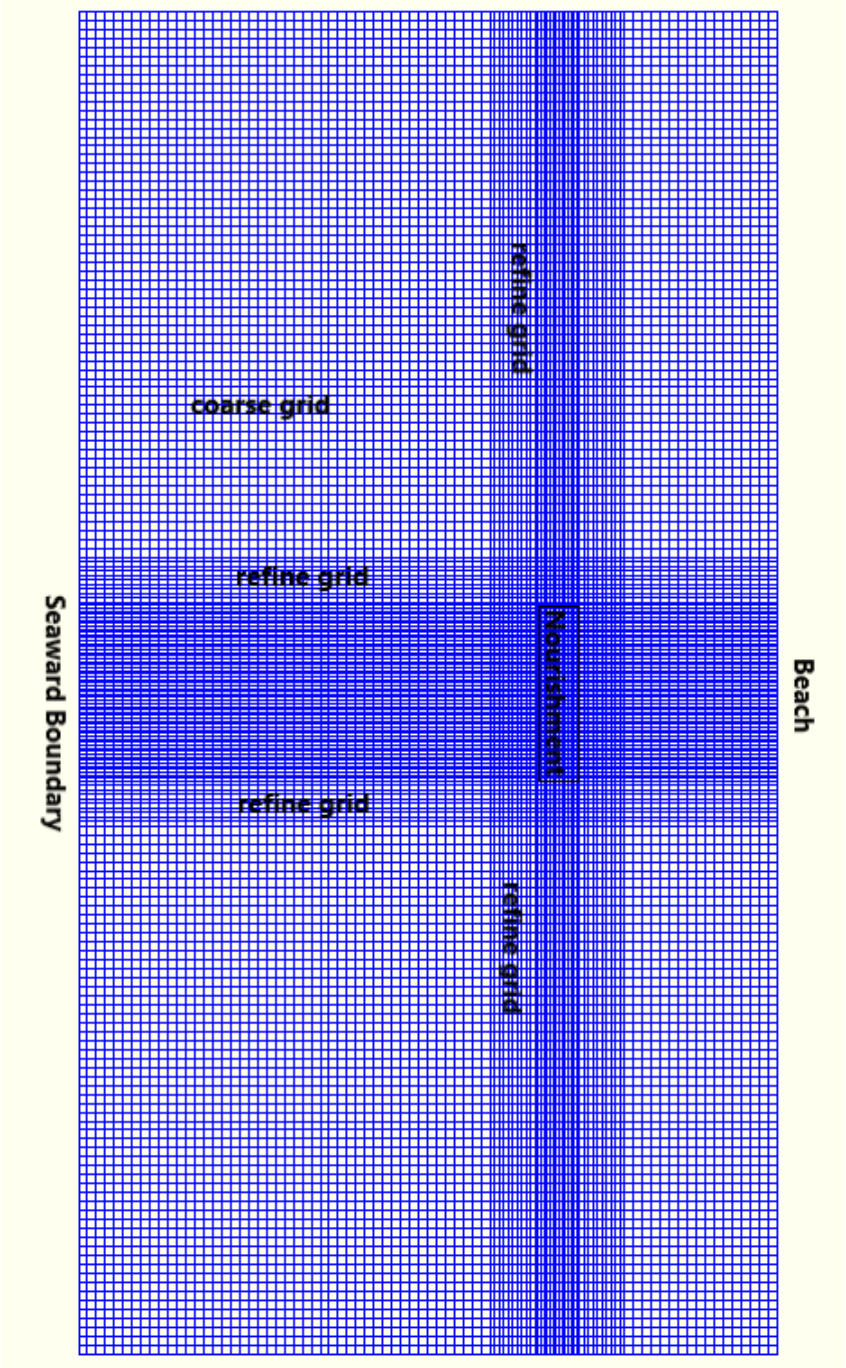

Figure 3.6: computational grids, the grid size is equal to 16.67m in the nourishment area, the grid size at the distance of 250m away from the nourishment in the longshore and cross shore direction is equal to 25m, the grid size in the remaining area is equal to 50m

3.7.5. Boundary conditions

• Wave: Waves are the most important driver for the cross-shore and longshore sediment transport around the nourishment. In this study, a constant wave condition is applied at the offshore boundary. In the reference case, the wave height of 2.25 m is set for validation

and according to Wijnberg (2002) the corresponding wave period is equal to 7.8 s. The other cases will be simulated in the following step to compare the results between each other. In Table 3.5 the wave properties for the reference case is presented.

Table 3.5: Wave properties of reference case

	H_{m0} (m)	T_P (s)	$\theta(deg)$
reference case	2.25	7.8	270

* H_m0 is the significant wave height at the seaward boundary, T_p is the peak wave period, θ is the wave direction and 270 deg is the direction towards the coastline.

•Water level: A constant water level (WL=0) is applied at the seaward boundary.
•Lateral boundary: The Neumann boundary is applied at the lateral boundary, which means there are no local variations of surface elevation and velocity. Neumann boundary prescribes the longshore water level gradient. The longshore gradient is determined by the difference in the water levels at the corner points, divided by the alongshore length of the model area.
•Flow: On the offshore boundary, the waves and currents will be generated locally which need to pass through the offshore boundary without any reflection. Then the option for the offshore boundary is to impose a weakly-reflective boundary condition. The beach width is around 150 m at the landward boundary, then no flux boundary condition is applied at x = 3900m.

3.7.6. Model scenarios

In the reference case, only one condition has been applied and it can be compared with other different cases. The water depths on the crest vary from 3m to 20m. The properties of each condition are summarized in Table 3.6.

Table 3.6: variation of water depth

		Hm0 (m)	Tp (s)	water depth of the nourishment crest (m)
reference case		2.25	7.8	5
depth secnario	condition 1a	2.25	7.8	3
	condition 1b	2.25	7.8	7
	condition 1d	2.25	7.8	9
	condition 1e	2.25	7.8	10
	condition 1f	2.25	7.8	12
	condition 1g	2.25	7.8	13
	condition 1h	2.25	7.8	15
	condition 1i	2.25	7.8	17
	condition 1j	2.25	7.8	20

The variation of wave heights on the offshore boundary is between 0.4m and 4m. For the

significant wave height in deep water, the wave period has been calculated by keeping the steepness of the waves at approximately 2.5 % (Koster, 2006). The calculation method is presented in Equation F.1 and Equation F.2 in Appendix F. The properties of each condition are summarized in Table 3.7.

Table 3.7: variation of wave heights

		Hm0 (m)	Tp (s)	water depth of the nourishment crest (m)
reference case		2.25	7.59	5
wave scenario	condition 2a	0.4	3.20	5
	condition 2b	0.5	3.58	5
	condition 2c	0.7	4.23	5
	condition 2d	0.9	4.80	5
	condition 2e	1	5.06	5
	condition 2f	1.2	5.54	5
	condition 2g	1.4	5.99	5
	condition 2h	1.6	6.40	5
	condition 2i	1.8	6.79	5
	condition 2j	2	7.16	5
	condition 2k	3	8.77	5
	condition 2l	4	10.12	5

The lengths of the nourishments vary from 500m to 6000m. The properties of each condition are summarized in Table 3.8.

Table 3.8: variation of length

		Hm0 (m)	Tp (s)	water depth on the nourishment crest (m)	length (m)
reference case		2.25	7.8	5	1000
length scenario	condition 2a	2.25	7.8	5	500
	condition 2b	2.25	7.8	5	700
	condition 2c	2.25	7.8	5	900
	condition 2d	2.25	7.8	5	1500
	condition 2e	2.25	7.8	5	2000
	condition 2f	2.25	7.8	5	2500
	condition 2g	2.25	7.8	5	3000
	condition 2h	2.25	7.8	5	4000
	condition 2i	2.25	7.8	5	5000
	condition 2j	2.25	7.8	5	6000

The volume per meter of the nourishments vary from 200 m^3/m to 608 m^3/m. The properties of each condition are summarized in Table 3.9.

Table 3.9: variation of volume per meter

		Hm0 (m)	Tp (s)	water depth of the nourishment crest (m)	volume per meter (m^3/m)
reference case		2.25	7.8	5	408
volume per meter scenario	condition 3a	2.25	7.8	5	200
	condition 3b	2.25	7.8	5	238
	condition 3c	2.25	7.8	5	278
	condition 3d	2.25	7.8	5	307
	condition 3e	2.25	7.8	5	363
	condition 3f	2.25	7.8	5	456
	condition 3g	2.25	7.8	5	505
	condition 3h	2.25	7.8	5	556
	condition 3i	2.25	7.8	5	608

* In each scenario, the back and front slope of the nourishment is the same. The volume per meter of the nourishment is extending or decreasing towards the seaward or landward direction respectively based on the reference case.

3.7.7. Definition of dimensionless wave heights in the modelling test

The dimensionless wave height is calculated in each specific case of the model scenarios. The dimensionless wave height is the ratio of average wave heights on the nourishment area over the simulation time and the crest depth of the nourishment.

3.7.8. Definition of the erosion rate in the modelling test

The erosion rate of the nourishment is compared through the numerical data. The cumulative erosion/ sedimentation in per alongshore length of the nourishment area is obtained through the model results. The erosion rate is determined by the ratio of the cumulative erosion/ sedimentation in per alongshore length and the morphological time (simulation time multiply by a morphological factor).

Chapter 4

Data analysis

In this chapter, the influenced parameters about erosion rates of the shoreface nourishments and dump sites are analysed.

4.1. Combination of the Dutch dump sites and shoreface nourishments

The relation between the rate of volume change of the shoreface nourishments/ dump sites and water depth is examined in Figure 4.1.

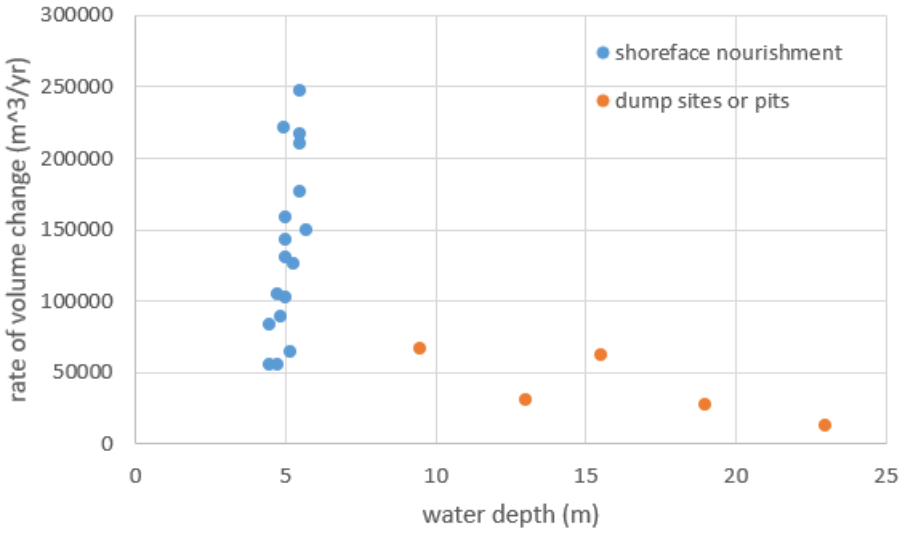

Figure 4.1: an overview of the Dutch shoreface nourishments and dump sites, the explanation of the water depth is presented in Chapter 3.2

The variables are not homogeneously spread over water depth and therefore a linear regression is not applied. The variation of erosion rates of shoreface nourishments is quite large (between 50000 and 250000 m^3/yr). And most of the rate of volume change of shoreface nourishments is larger than the erosion/filling rates of dump sites or pits (Figure 4.1).

The relation between the erosion rate/ erosion rate per meter of the Dutch shoreface nourishments and depth of the nourishment crest is presented in Figure 4.2 and Figure 4.3.

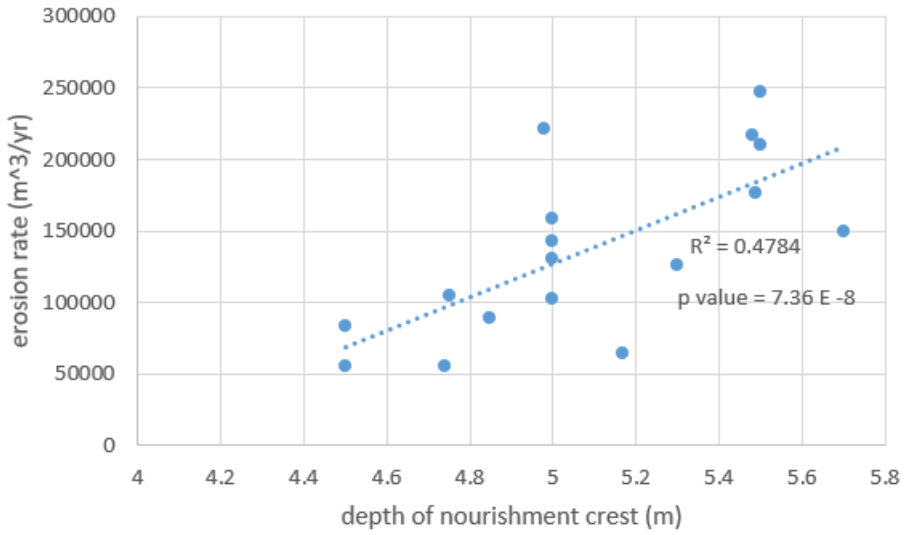

Figure 4.2: the relation between the erosion rate of the Dutch shoreface nourishment and depth of the nourishment crest

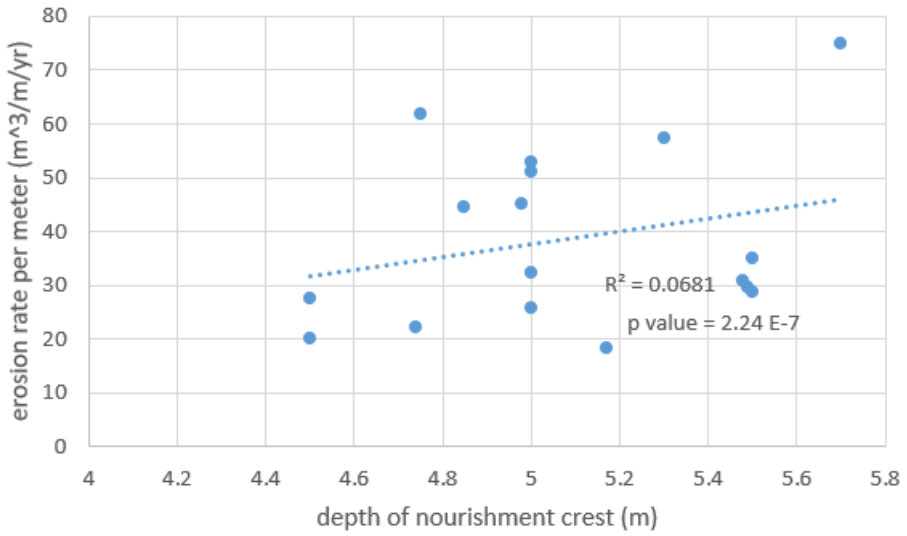

Figure 4.3: the relation between the erosion rate per meter of the Dutch shoreface nourishment and depth of the nourishment crest

Figure 4.2 shows that larger depths of the nourishment crest result in a larger erosion rate of the Dutch shoreface nourishments (with R^2 of 0.48, Figure 4.2) which is not the same as the expected results. While the erosion rate per meter is not highly dependent on the water depth (with R^2 of 0.068, Figure 4.3).

In the next step the influence of the nourishment geometry (e.g, length, width, volume, cross sectional area), wave conditions (the temporal and spatial variation of wave heights) will be tested.
Then the relation between the rate of volume change of the shoreface nourishments/ dump

sites and dimensionless wave height is examined.

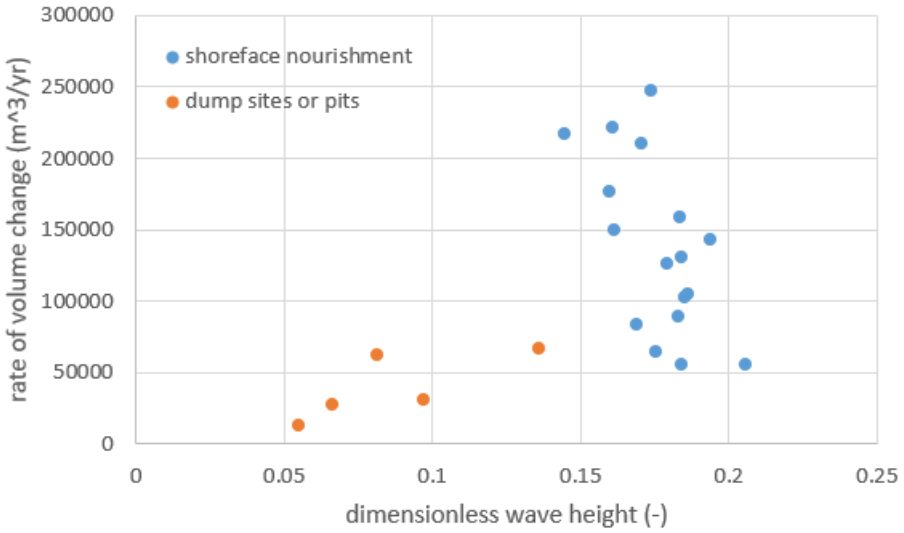

Figure 4.4: the relation between dimensionless wave heights and erosion rate for the Dutch nourishments, the definition of the dimensionless wave height is presented in Chapter 3.4

The variables are not homogeneously spread over dimensionless wave height and therefore a linear regression is not applied. Figure 4.4 shows that the rate of volume change is not highly dependent on the dimensionless wave height. Most of the rate of volume change of shoreface nourishments is larger than dump sites/pits (Figure 4.4).

The relation between the erosion rate/ erosion rate per meter of the Dutch shoreface nourishments and dimensionless wave heights is presented in Figure 4.5 and Figure 4.6

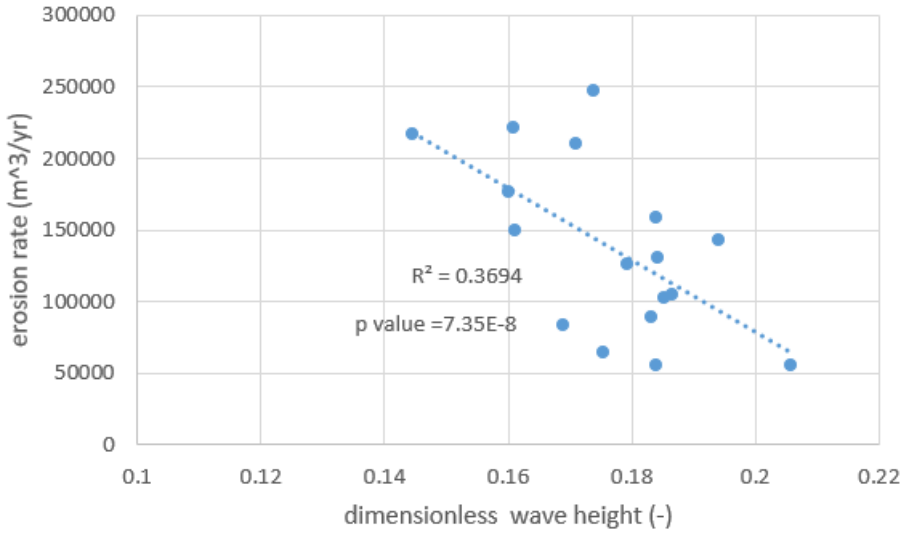

Figure 4.5: the relation between dimensionless wave heights and erosion rate for the Dutch shoreface nourishments

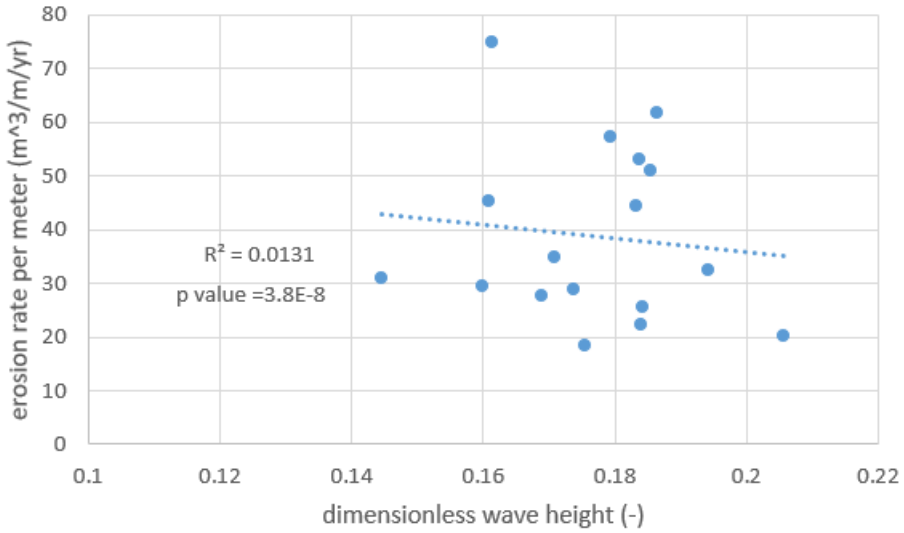

Figure 4.6: the relation between dimensionless wave heights and erosion rate per meter for the Dutch shoreface nourishments

Figure 4.5 shows that larger dimensionless wave heights result in a larger erosion rate of the Dutch shoreface nourishemnts (with R^2 of 0.37, Figure 4.5) which is not the same as the expected results. The erosion rate per meter of the nourishments is not highly dependent on the dimensionless wave height (with R^2 of 0.013, Figure 4.6).

The reason why the variation of erosion rate of shoreface nourishments is too large could be explained by the different geometries of shoreface nourishments. The following steps will focus more on the geometrical parameters of nourishment. To find how these parameters influence the erosion rate of the shoreface nourishments, a more detailed data analysis of the shoreface nourishment data is done using subsets.

4.2. Subsets of the Dutch shoreface nourishment case studies

Because nourishment geometrical parameters vary a lot compared to each other, the nourishment data is divided into subsets of nourishment cases of approximately similar length, volume or volume per meter to test if any relation can be found. And the Mahalanobis distance of each point in each related graph has been calculated (Table E.1 to Table E.12 in Appendix E),the point has been removed if the Mahalanobis distance is larger than 4 for the small sample size (n≤ 8) and 7 for the large sample size (n≥ 14).

4.2.1. Subset of volume

Nourishment cases are divided into three subsets based on the volume with each subset of nearly the same volume of shoreface nourishment (Table 4.1). Subsets have nourishment volumes of about 843500 m^3 (subset A), 1500000 m^3 (subset B) and 2600000 m^3 (subset C).

Table 4.1: Subset of shoreface nourishment volume

subset	ID	volume (m^3)
A	2	882605
	4	882055
	5	753338
	10	509913
	15	880100
	16	994000
	11	1002956
B	1	1425780
	6	1266028
	12	1301565
	13	1972272
C	3	2970879
	7	2645601
	8	2508887
	9	2203427
	17	3106812
	14	2315360

The relation between the volume and erosion rate/ erosion rate per meter is shown in Figure 4.7 and Figure 4.8

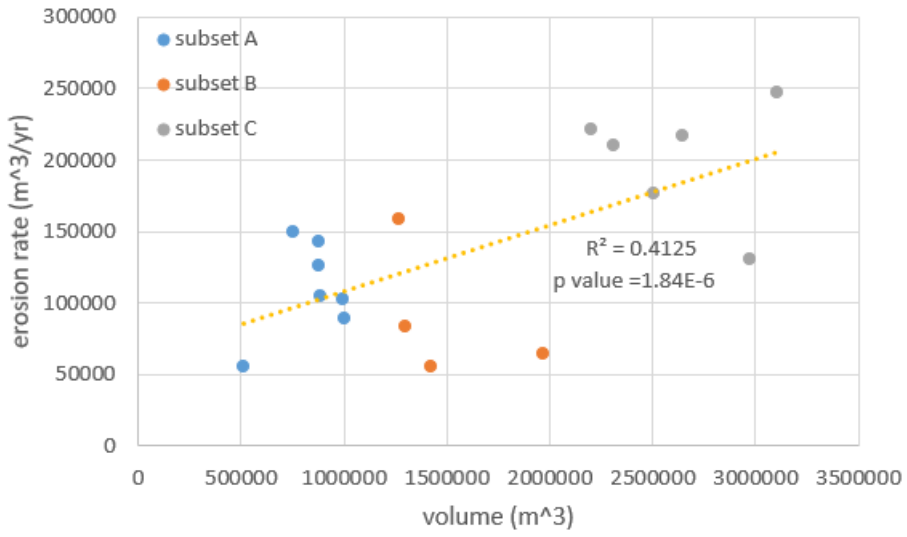

Figure 4.7: the relation between volume and erosion rate, different colors represent different subsets, the same clusters have the nearly same volume

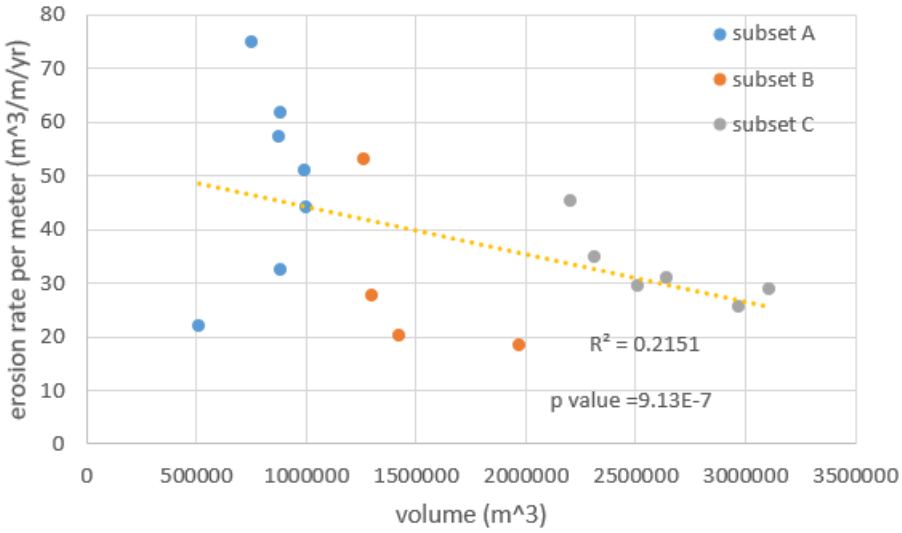

Figure 4.8: the relation between volume and erosion rate per meter

The larger volume of shoreface nourishments results in a larger erosion rate (Figure 4.7, with $R^2 = 0.41$). The variation of erosion rate of subset B is quite large but the average value of erosion rate of subset B ($130000 m^3/yr$) is a little bit lower than subset C ($18300 m^3/yr$). The relation between the erosion rate per meter and volume shows the opposite trend that larger volumes result in a lower erosion rate per meter (Figure 4.8, with $R^2 = 0.22$).

The relation between the length and erosion rate/ erosion rate per meter is shown in Figure 4.9 and Figure 4.10

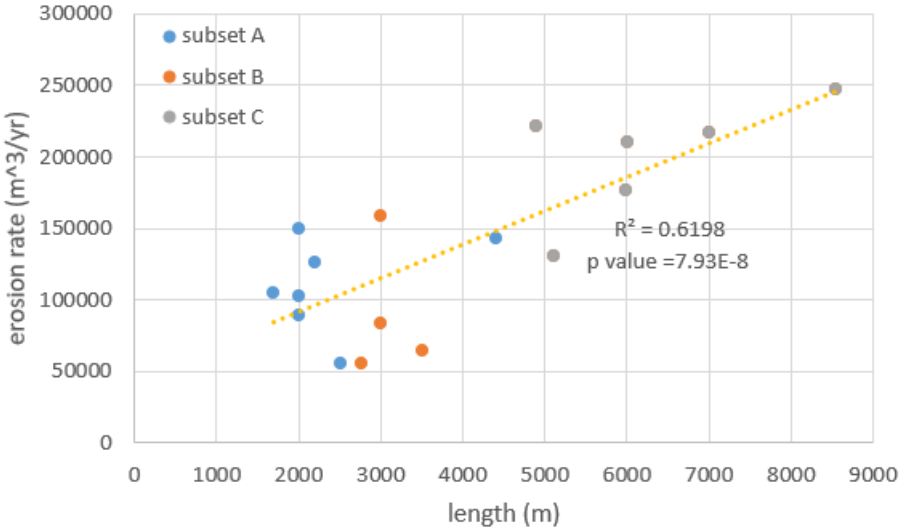

Figure 4.9: the relation between length and erosion rate

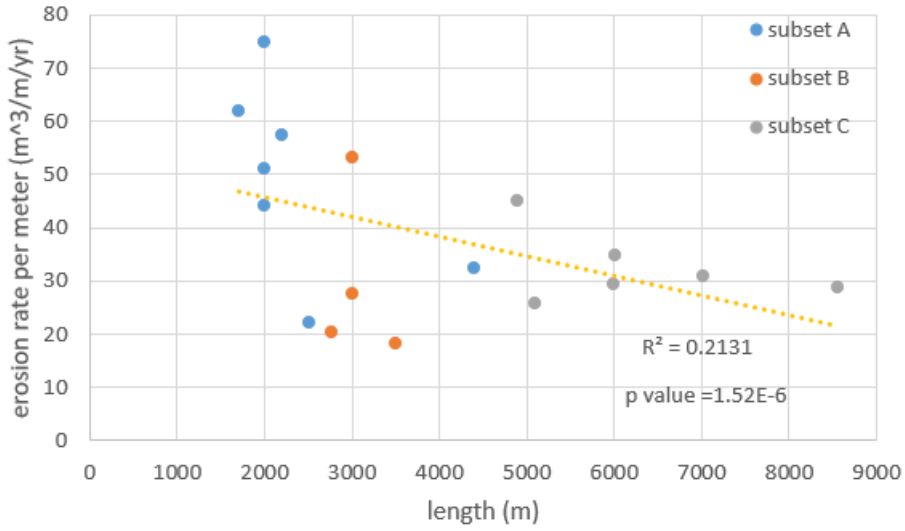

Figure 4.10: the relation between length and erosion rate per meter

The erosion rate is highly dependent on the length of the shoreface nourishments. The larger length of the shoreface nourishment results in a larger erosion rate (Figure 4.9, with $R^2 = 0.62$). Figure 4.10 shows that the erosion rate per meter is also dependent on the length (with $R^2 = 0.21$) that the larger length of the shoreface nourishments results in a smaller erosion rate per meter. While there is no clear relation in each subset (Figure D.2 in Appendix D).

The relation between the erosion rate/ erosion rate per meter and volume per meter is shown in Figure 4.11 and Figure 4.12.

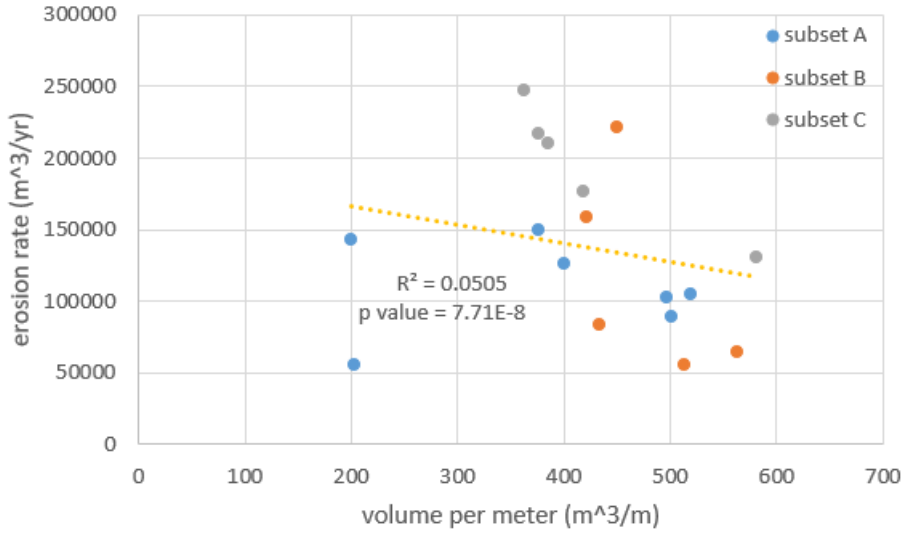

Figure 4.11: the relation between volume per meter and erosion rate

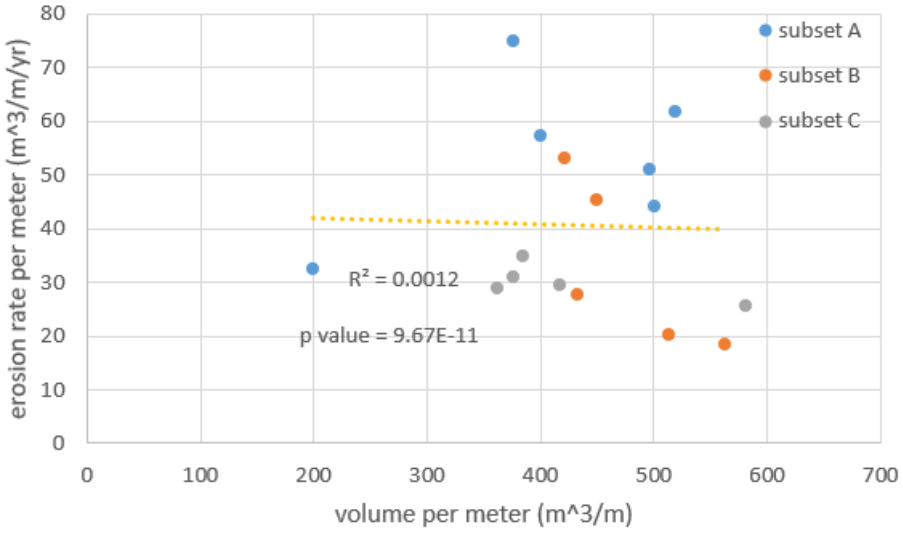

Figure 4.12: the relation between volume per meter and erosion rate per meter

Figure 4.11 and Figure 4.12 both show that there is no clear relation between the erosion rate/ erosion rate per meter and volume per meter of the combined results. But the decreased trend between the erosion rate and volume per meter can be found in subset A, B and C. It indicates that for the determined volume of the shoreface nourishments, a larger volume per meter of the nourishment results in a lower erosion rate (Figure D.3 in Appendix D).

The relation between the erosion rate/ erosion rate per meter and berm height is shown in Figure 4.13 and Figure 4.14.

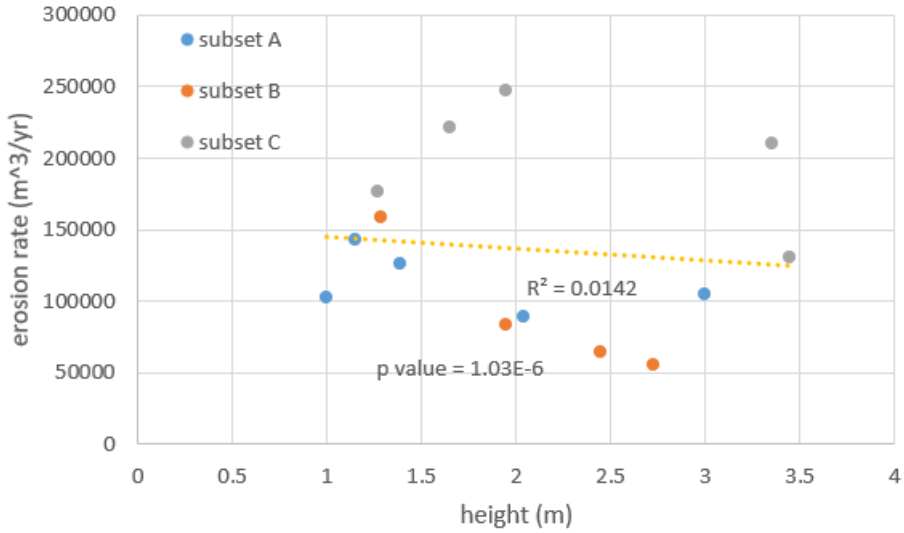

Figure 4.13: the relation between nourishment height and erosion rate

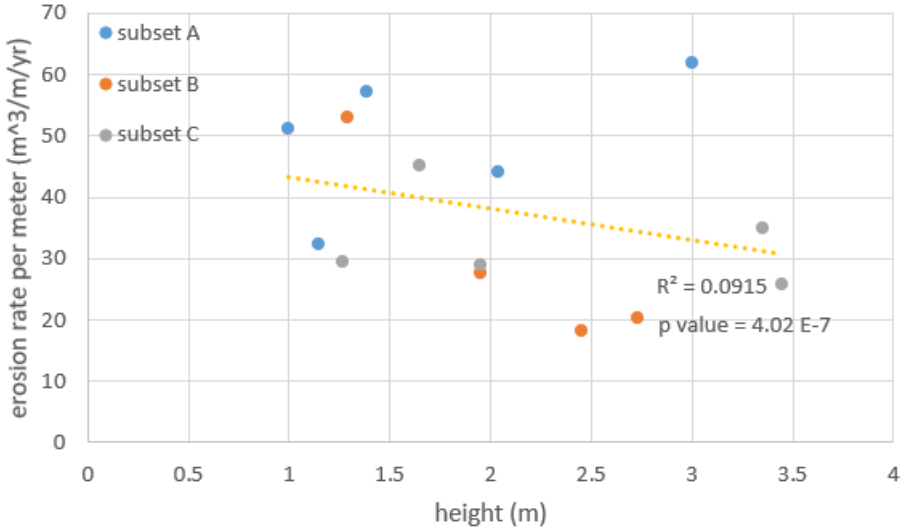

Figure 4.14: the relation between nourishment height and erosion rate per meter

The erosion rate/ erosion rate per meter is not highly dependent on the height of the shoreface nourishment (Figure 4.13 and Figure 4.14 with relative low value of R^2). And the relation is also not clear in each subset (Figure D.5 and Figure D.6 in Appendix D).

4.2.2. Subset of volume per meter

Additionally, the area of volume per meter is also divided into three subsets, where for each subset the area of volume per meter of the shoreface nourishment is in the same range (Table 4.2). Subsets have the nourishment volume per meter of about 530 m^3/m (subset A), 425 m^3/m (subset B), 320 m^3/m (subset C). The increasing trend between the length/ volume of the nourishemnts and erosion rate and the decreased trend between the length/ volume of the nourishments and erosion rate per meter is expected in each subset.

Table 4.2: subset of volume per meter of shoreface nourishment

subset	ID	volume per meter (m^3/m)
D	1	514
	2	519
	11	501
	16	497
	3	582
	13	563
E	6	422
	8	418
	9	450
	15	400
	12	433
F	4	200
	10	203
	17	363
	14	385
	5	376
	7	377

The relation between erosion rate/ erosion rate per meter and nourishment size (length, volume, height) is plotted for each subset, but there is no obvious relation can be found in all subsets (Figure D.8 to Figure D.12 in Appendix D).

4.2.3. Subset of length

The length of the shoreface nourishment can also be divided into three subsets, where for each subset the length of the shoreface nourishment is in the same range (Table 4.3). Subsets have shoreface nourishment lengths of about 1980 m (subset G), 3600 m (subset H), 6900 m (subset I). The increasing trend between volume and erosion rate and the decreased trend between length and erosion rate per meter is expected in each subset.

Table 4.3: Subset of shoreface nourishment length

subset	ID	length (m)
G	2	1701
	5	2004
	11	2002
	15	2200
	16	2000
H	1	2774
	4	4410
	9	4897
	12	3006
	6	3000
	13	3503
	3	5105
	10	2512
I	7	7018
	8	6002
	14	6014
	17	8559

The relation between the erosion rate/ erosion rate per meter and nourishment size (length, volum, height) is plotted for each subset, but there is no obvious relation can be found in all subsets (Figure D.13 to Figure D.18 in Appendix D).

4.2.4. Analysis of the Dutch shoreface nourishments

Above results show that the volume and length of the shoreface nourishments highly influence the erosion rate/ erosion rate per meter of the shoreface nourishments with nearly the same correlation patterns (Figure 4.9 to Figure 4.10). It indicates that a larger volume of shoreface nourishments also have a longer length (Figure 4.15 (a), with R^2 of 0.78). While the length and volume per meter of the shoreface nourishments are not strongly correlated (Figure 4.15 (b), with R^2 of 0.034).

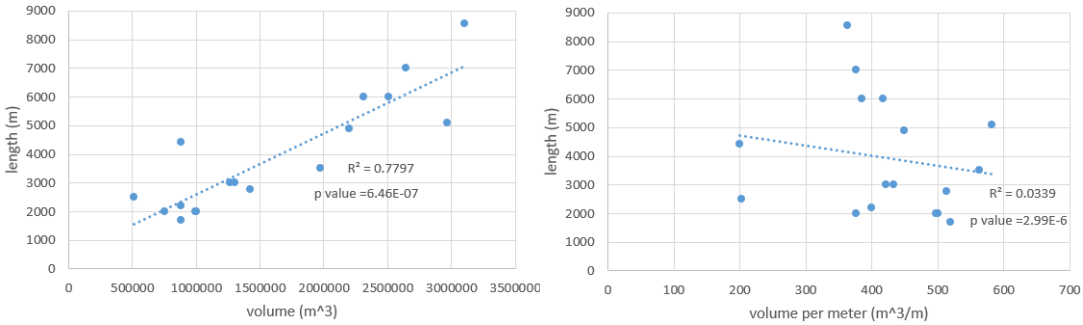

(a) the relation between volume and length of the Dutch shoreface nourishments

(b) the relation between length and volume per meter of the Dutch shoreface nourishments

Figure 4.15: the geometric relation of the Dutch shoreface nourishments

4.2.5. Summary of the Dutch shoreface nourishments

The correlation coefficient value of each related graphs of the Dutch shoreface nourishment is presented in Table 4.4.

Table 4.4: the correlation coefficient value of each related graphs of the Dutch shoreface nourishments

		erosion rate (m^3/yr)				erosion rate per meter (m^3/m/yr)			
		trend (+/-)	R^2	p value	sample size	trend (+/-)	R^2	p value	sample size
volume (m^3)		+	**0.4125**	**E-06**	17	-	**0.2151**	**E-07**	17
length (m)		+	**0.6198**	**E-08**	17	-	**0.2131**	**E-06**	17
volume per meter (m^3/m)		-	0.0505	E-08	17	-	0.0012	E-11	17
height (m)		-	0.0142	E-06	14	-	0.0915	E-07	14
volume dataset	water depth A	+	0.5726	E-04	7	+	0.4555	E-04	7
	water depth B	+	0.1149	3.00E-02	4	+	0.0559	5.00E-02	4
	water depth C	+	0.2051	E-05	6	-	0.1196	E-04	6
	dimensionless wave height A	+	0.1723	E-04	6	-	0.1261	E-04	6
	dimensionless wave height B	-	0.0342	3.00E-02	4	-	0.0109	3.40E-02	4
	dimensionless wave height C	-	0.174	E-05	6	-	0.105	E-05	6
	length A	-	0.2282	E-05	6	-	0.5011	E-03	6
	length B	-	0.0164	3.00E-02	4	-	0.0603	E-04	4
	length C	+	0.4028	E-03	6	-	0.1609	E-04	6
	volume per meter A	**-**	**0.6543**	**E-05**	6	+	0.3985	E-04	7
	volume per meter B	**-**	**0.5422**	**3.00E-02**	4	-	0.6115	E-03	4
	volume per meter C	**-**	**0.7069**	**E-03**	5	-	0.0362	E-04	6
	height A	-	0.1999	E-04	5	+	0.2847	E-04	5
	height B	-	0.7326	3.00E-02	4	-	0.6197	4.40E-02	4
	height C	-	0.1737	E-04	5	-	0.0901	E-03	5
volume per meter dataset	water depth D	+	0.0907	E-04	6	-	0.0105	E-03	6
	water depth E	+	0.2256	E-03	5	+	0.0722	E-03	5
	water depth F	+	0.5703	E-03	6	+	0.4377	E-04	5
	dimensionless wave height D	+	0.5897	E-04	5	+	0.6359	E-03	5
	dimensionless wave height E	-	0.1797	E-03	5	+	0.4919	E-03	5
	dimensionless wave height F	-	0.2396	E-03	6	-	0.1045	E-03	6
	length D	-	0.7465	E-03	5	-	0.5141	E-03	6
	length E	+	0.4556	E-03	5	-	0.7954	E-03	5
	length F	+	0.745	E-03	6	+	0.2085	E-03	4
	volume D	-	0.6749	E-03	5	-	0.4767	E-03	6
	volume E	+	0.4945	E-03	5	-	0.2873	E-03	5
	volume F	+	0.9834	1.90E-02	5	+	0.4378	2.00E-02	4
	height D	+	0.0367	E-04	6	-	0.1121	E-03	6
	height E	-	0.1741	E-03	5	-	0.2105	E-03	5
	height F	+	0.2577	2.20E-02	3	+	0.2987	E-03	3
length dataset	water depth G	+	0.8799	E-04	5	+	0.5169	E-04	5
	water depth H	+	0.6089	E-03	7	+	0.0658	E-03	7
	water depth I	+	0.109	E-04	4	+	0.0535	E-04	4
	dimensionless wave height G	-	0.7964	E-04	5	-	0.6088	E-04	5
	dimensionless wave height H	-	0.1880	E-03	8	-	0.1055	E-04	8
	dimensionless wave height I	+	0.1107	E-04	4	+	0.016	E-04	4
	volume G	-	0.8635	E-04	5	-	0.9466	E-05	5
	volume H	+	0.126	E-03	8	nan	3.00E-05	E-04	8
	volume I	+	0.5529	E-04	4	-	0.569	E-04	4
	volume per meter G	-	0.8382	E-04	5	-	0.424	E-04	5
	volume per meter H	nan	0.0001	E-03	8	-	0.0176	E-04	8
	volume per meter I	-	0.9558	E-04	4	nan	0.0001	E-05	4
	height G	-	0.0639	E-04	4	+	0.1704	E-04	4
	height H	-	0.2216	E-03	7	-	0.4578	E-03	7
	height I	+	0.0836	E-03	3	+	0.8329	E-03	3

* The following index with each parameter means the corresponding subsets (water depth A means the water depth of nourishment crest in subset A). Nan means there is no clear trend. The bold font means relative good correlation values. The related graphs of different subsets are presented in Appendix C and Appendix D.

Table 4.4 shows that the larger volume/ length results in the larger erosion rate and smaller erosion rate per meter. And for the determine volume, the larger volume per meter results in the smaller erosion rate.

4.3. Combination of the international and Dutch shoreface nourishment projects

There are 6 international shoreface nourishments projects analysed in this research (Table Figure 3.2). In this case, the international and Dutch shoreface nourishments are combined and the relation between the dimensionless wave height and erosion rate/ erosion rate per meter is shown in Figure 4.16 and Figure 4.17. The outliers have been removed for Figure 4.16 and Figure 4.17, the Mahalanobis distance of each point in both graphs has been calculated (Table E.12 in Appendix E)

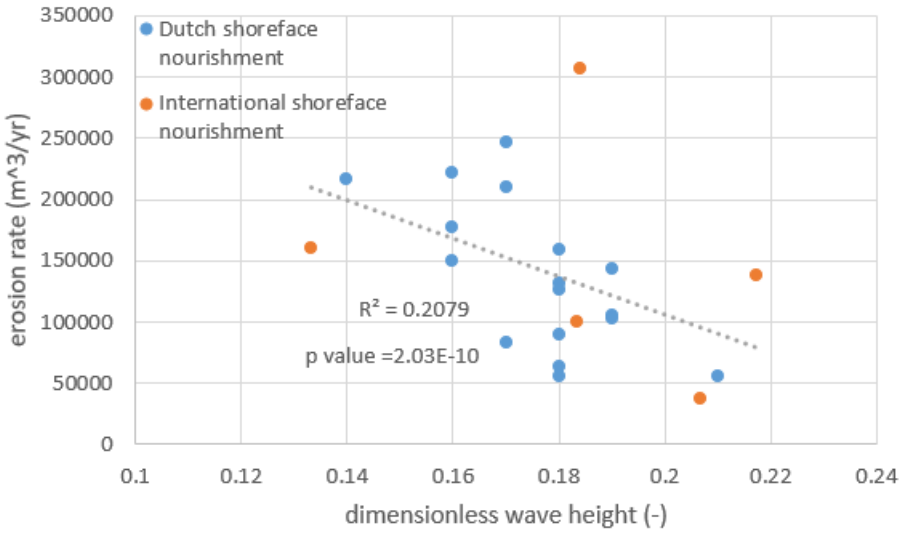

Figure 4.16: the relation between the dimensionless wave height and erosion rate, the definition of dimensionless wave heights of the Dutch and international shoreface nourishment cases are presented in Chapter 3.4

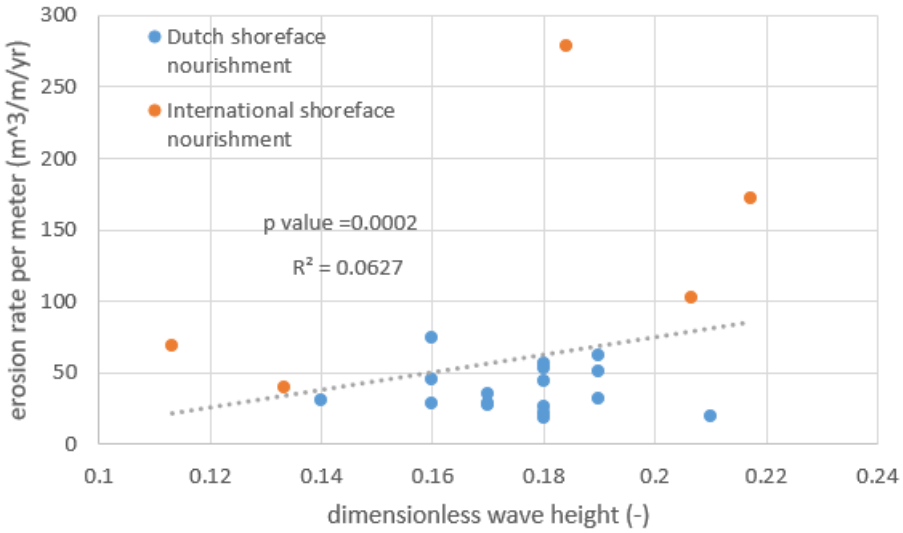

Figure 4.17: the relation between the dimensionless wave height and erosion rate per meter

Figure 4.16 shows that larger dimensionless wave heights result in a smaller erosion rate which is opposite as the expect. While the relation between erosion rate per meter and dimensionless wave height is not clear yet (with R^2 of 0.063). There are 2 international nourishment cases having much higher erosion rates per meter than the Dutch nourishments. The dimensionless wave height of all shoreface nourishment cases is between 0.1 and 0.22.

The relation between the mobility parameter (Equation 2.4 to Equation 2.5 in Appendix F) and erosion rate/ erosion rate per meter is shown in Figure 4.18 and Figure 4.19. There are only 3 Dutch cases (Noord-Holland-Egmond '99; Noord-Holland-Bergen '00 and Rijnland-Noordwijk '98) involved, for the other Dutch cases the data of the sediment diameter is not available. And 3 international cases (South Padre Island, TX and Brunswick, GA (Mound "C")) are excluded due to the unavailable wave periods and sediment diameter. The outliers have been tested for each related graph, the Mahalanobis distance of each point in each related graph has been calculated (Table E.11 in Appendix E), and the point has been removed if the Mahalanobis distance is larger than 4. Larger mobility parameters result in a larger erosion rate/ erosion rate per meter of nourishments is expected.

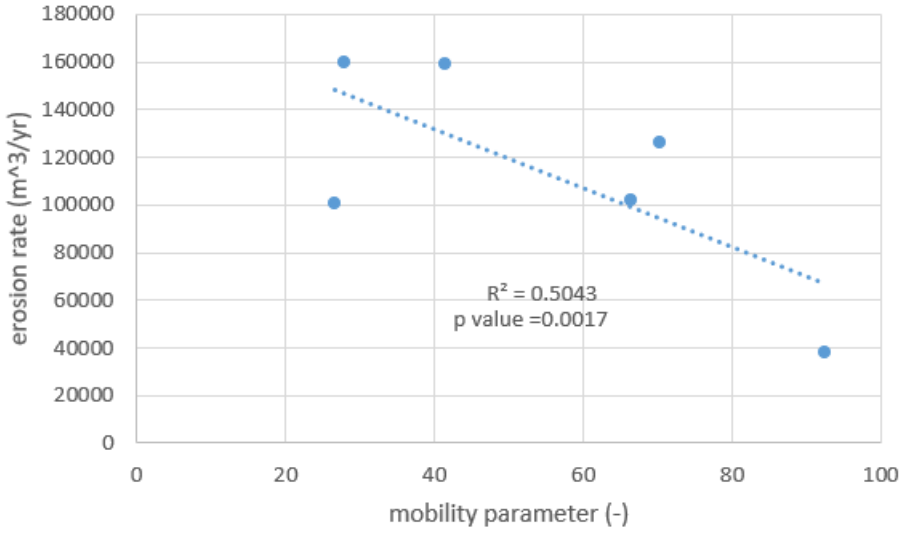

Figure 4.18: the relation between mobility parameter and erosion rate

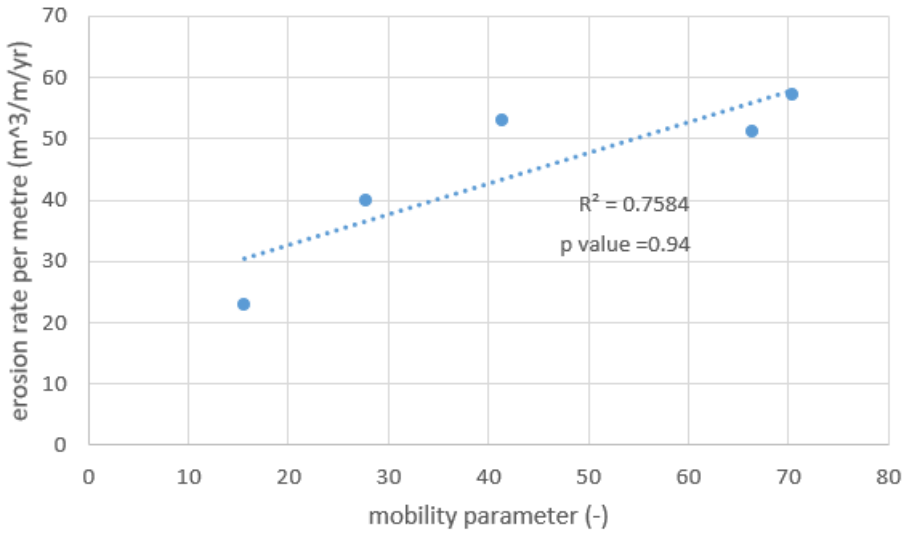

Figure 4.19: the relation between mobility parameter and erosion rate per meter

The larger mobility parameter results in the smaller erosion rate (with R^2 of 0.5 Figure 4.18), which is not the same as the expected results. The R^2 value of 0.76 (Figure 4.19) is found in the relation between the mobility parameter and erosion rate per meter. But the $p-value$ is larger than 0.05, therefore the relation is not in statistical significance.

Chapter 5

Modelling test

5.1. Verification of model performance: Hydrodynamic response for the reference case

The hydrodynamics around the nourishments are quite complex. Wave heights, resulted longshore, cross-shore velocities and varied water levels influence the hydrodynamic characteristics. The total effects of hydrodynamic conditions determine the evolution of the nourishment.

5.1.1. Expected hydrodynamic response

• Wave: Waves start to break and decrease around the nourishment area in the cross shore direction. In the longshore direction, wave heights decrease on the nourishment area which is lower than the deeper area just next to the nourishment.
• Cross shore velocities: Figure 2.3 (Haas et al., 1999) presented the horizontal circulation cells around the bar. In the cross shore direction, cross shore velocities increase till the nourished area and then start to decrease. Due to the horizontal circulation, cross shore velocities are in the offshore direction just onshore of the nourishment.
According to Figure 2.4 (Koster, 2006), onshore velocities are expected on the nourishment crest. The peak velocity is at the tip of the nourishment. And the offshore velocities can be found in the deeper area just next to the nourished area.
• Longshore velocities: According to Figure 2.5 (Koster, 2006), longshore flow velocities are split into two symmetrical parts of the nourishment where the currents flow through in opposite directions.
• Water level: Wave energy is dissipating on the nourishment which is compensated by set-up of water level. Then the water level of the nourishment is much higher than the deeper area just next to the nourishment.

5.1.2. Verified method

In the reference case, the wave properties of the reference case (significant wave height of 2.25 m, peak wave period of 7.8 s) is imposed. The detailed dimension of the nourishment has already been described in Chapter 3.5.2. This simulation is used for examining the hydrodynamic conditions, if the model results are reasonable then the same model settings, boundary conditions and grid size will be applied in the other scenarios.
In order to get the detailed information of the hydrodynamic conditions around the nourishment, the cross section of the nourishment has been divided into three parts (Figure 5.1).

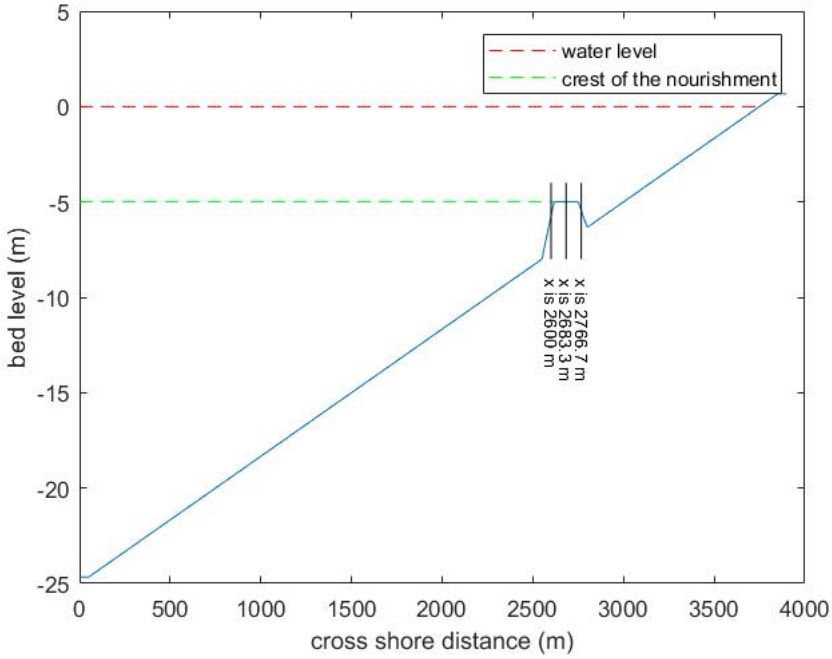

Figure 5.1: cross section of the reference case, the crest depth is 5m, black lines are different sections of the nourishment

5.1.3. Wave conditions

The wave height in the cross shore direction is shown in Figure 5.2.

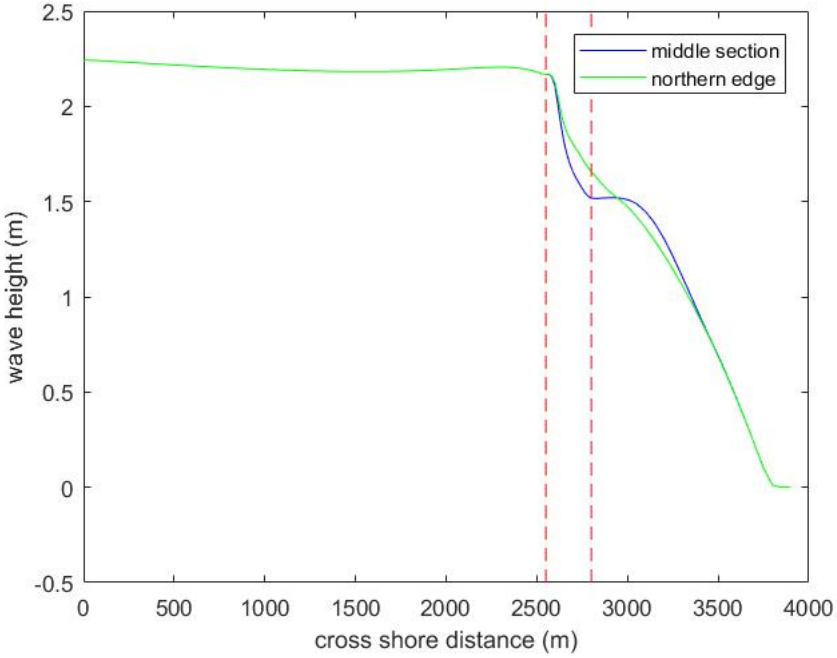

Figure 5.2: wave heights in the cross shore direction (red dotted line is the location of the nourishment in the cross shore direction)

Figure 5.2 shows that the wave heights decrease around the nourished area. The blue line and green line represent the middle and northern edge of the nourishment respectively. The wave heights in the northern edge are a little bit higher than the middle part.
The wave heights in the longshore direction of different cross sections are plotted in Figure 5.3.

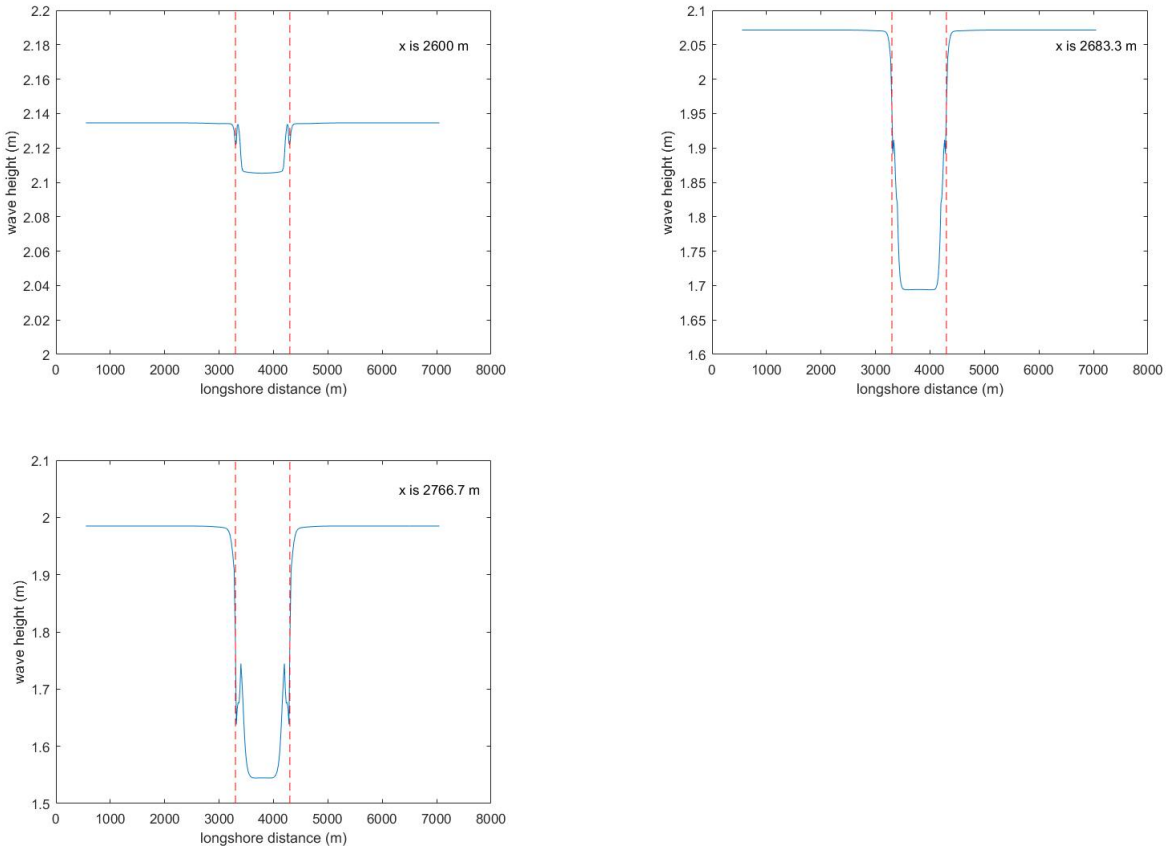

Figure 5.3: wave heights at the cross sections (x=2600 m is just offshore from the crest, x=2683.3 m is on the crest, x=2766.7 is just onshore from the crest,red dotted line is the location of the nourishment in the alongshore direction)

The wave height has the maximum value on the offshore location of the nourishment (x=2600 m) and then decreases towards the onshore area (Figure 5.3). The lower wave height is observed around the crest of the nourishment due to wave breaking effects. As a result of wave refraction, an abrupt change of wave heights is observed at the tips of the nourishment. The detailed explanation is presented in Appendix G.

5.1.4. Longshore and cross-shore flow velocities

The cross shore velocities in the alongshore direction and cross-shore direction are plotted in Figure 5.4 and Figure 5.5 respectively.

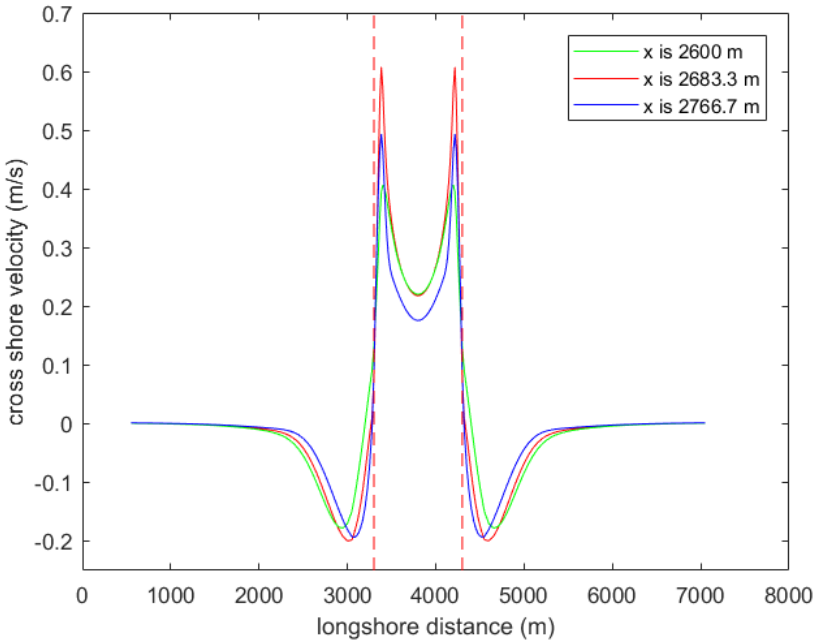

Figure 5.4: cross shore velocities in different cross sections, x=2600 m is just offshore from the crest (x=2683.3 m is on the crest, x=2766.7 is just onshore from the crest, red dotted line is the location of the nourishment in the longshore direction)

The magnitude of the cross shore velocities are relative larger at the crest of the nourishment and have its peak value at the tips (Figure 5.4). Around the nourished area, a large percentage of waves is breaking and results in the onshore velocities. In the deeper area just next to the nourishment is the location with offshore velocities. The largest cross shore velocity is at the tip of the nourishment, this is mainly caused by a relatively large water level gradient here leading to larger longshore and cross shore current velocities.

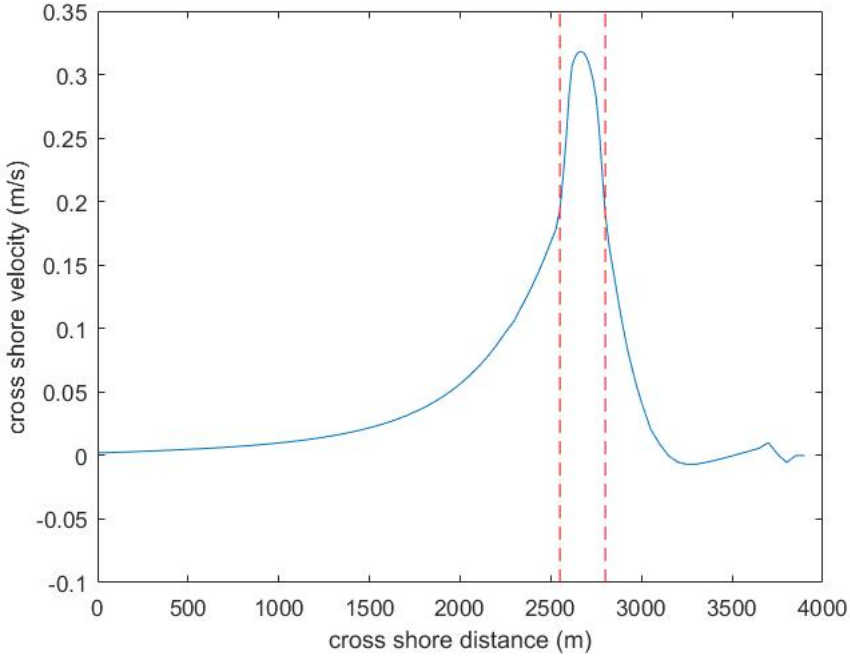

Figure 5.5: cross shore velocities averaged over the longshore direction (positive values are in the onshore direction, negative values are in offshore direction, red dotted line is the location of the nourishment in the cross shore direction)

Figure 5.5 shows that the onshore velocities increase when close to the nourishment, a strong decrease can be found just onshore of the nourishment. The cross shore velocities are in the offshore direction when moving the onshore area of the nourishment.
The longshore velocities in different cross sections are plotted in Figure 5.6.

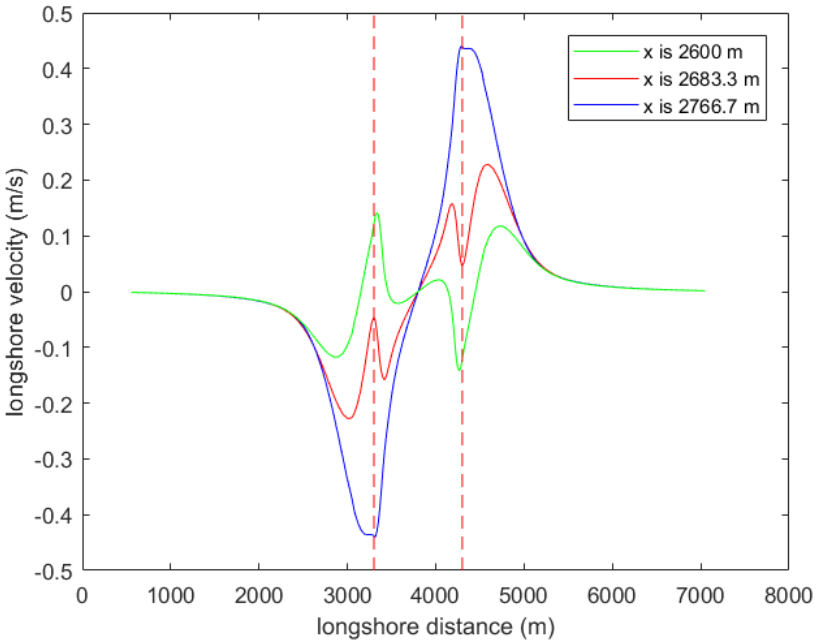

Figure 5.6: longshore velocities in the longshore direction (red dotted line is the location of the nourishment in the longshore direction)

The longshore velocities vary a lot through the nourishment, the largest longshore velocities is just onshore of the crest. It is obvious in Figure 5.6 that the longshore currents split at the half distance of the nourishment where the currents flow through in opposite directions just onshore of the nourishment. In the other two cross sections, the magnitude of the longshore velocities is relatively smaller.

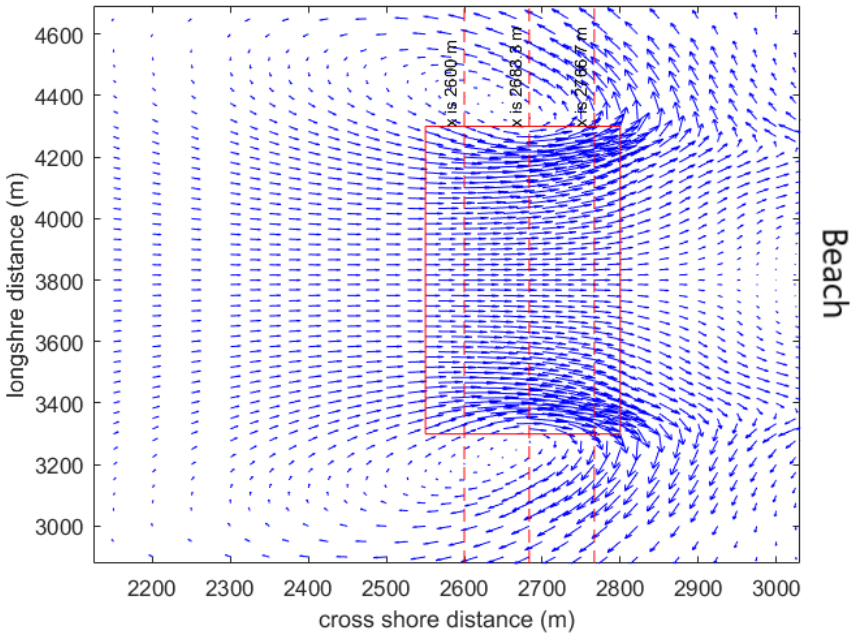

Figure 5.7: vector of the velocity (red box is location of the nourishment, red dotted line is the transect of the nourishment at the location of x=2600m, x=2683.3m, x=2766.7m)

Figure 5.7 shows on the shoreward area of the nourishment crest (around the location of x= 2766.7m), a large percentage of currents above the nourishment tends to flow into the ripple channel. The currents return back to the nourishment at the offshore side of the nourishment. Consequently, on the seaward area of the nourishment crest (around the location of x= 2600m), the currents flow toward the nourishment. At the location of x= 2683.3m, a small percentage of currents flow into the ripple channel. It results in a smaller longshore velocity at the tip of the nourishment at x= 2683.3m. Meanwhile, the currents are away from the nourishment in the ripple channel (deeper area just next to the nourishment).

5.1.5. Water level

The water level in the longshore direction is plotted in Figure 5.8.

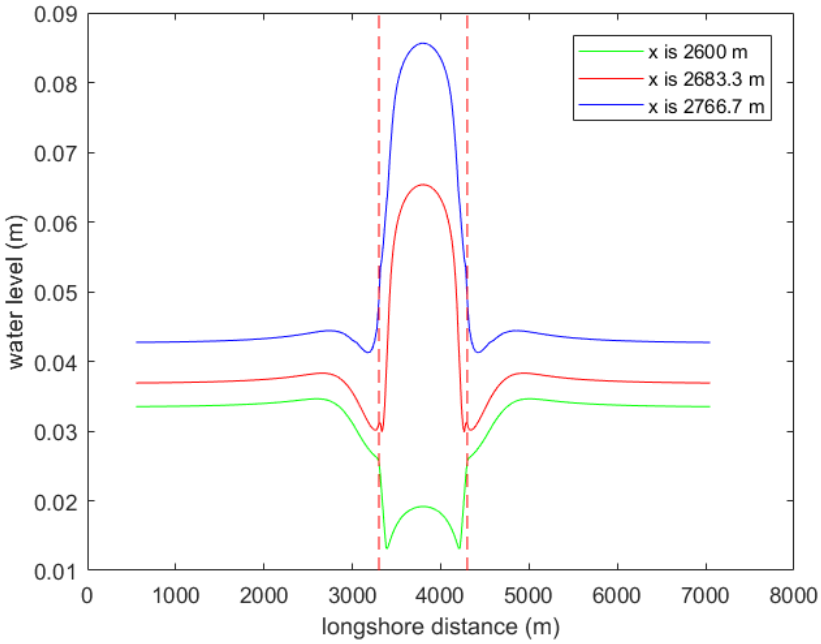

Figure 5.8: water levels in the cross shore sections (red dotted line is the location of the nourishment in the longshore direction)

Figure 5.8 shows that the water level increases in the middle section of the nourishment and also decreases abruptly just next to the nourishment. The minimum and maximum water level in the middle section of the nourishment is at x = 2600 m and 2766.7 m respectively, the water level is increasing across through the nourishment. The reason why the water level on the nourishment area is smaller than the deeper area just next to the nourishment at x=2600m (the offshore area of the nourishment) is explained in Appendix G.

5.1.6. Summary of hydrodynamic response

Above all, the general trend of the hydrodynamic response is nearly the same as the expected results. Wave heights decrease around the nourished area. The onshore direction of cross shore velocities can be observed around the nourishment area and set up water level is obvious on the crest. The longshore velocities also split at half distance of the nourishment just onshore of the crest.

5.2. Verification of model performance: Morphodynamic response for the reference case

The hydrodynamics around the nourishment were presented in chapter 5.6. And in this chapter the related cross-shore and longshore sediment transports will be discussed.

5.2.1. Expected morphological response

• Cross shore sediment transport: In the cross shore direction, cross shore sediment transports increase to its maximum value on the nourished area and then decrease till the onshore area of the nourishment. In the onshore area of the nourishment, the cross shore sediment transport is in the offshore direction.
In the longshore direction, cross shore sediment transports are in the onshore direction on the nourished area and have the maximum value at the tips. In the deeper area just next to the nourishment, the cross shore sediment transport is in the offshore direction.
• Longshore sediment transport: Longshore sediment transport splits at the half distance of the nourishment where the sediment transports into the opposite direction. This effect is significant when the bed topography disturbs a lot compared to the initial condition.
• Erosion and sedimentation pattern of the nourishment: According to Koster (2006) (Figure 2.8), both erosion and sedimentation patterns can be observed on the nourished area. Due to edge effects, the maximum erosion rate is at the tips of the nourishment.

5.2.2. Longshore and cross-shore sediment transport

Figure 5.9 presents the cross-shore sediment transport in the cross-shore direction.

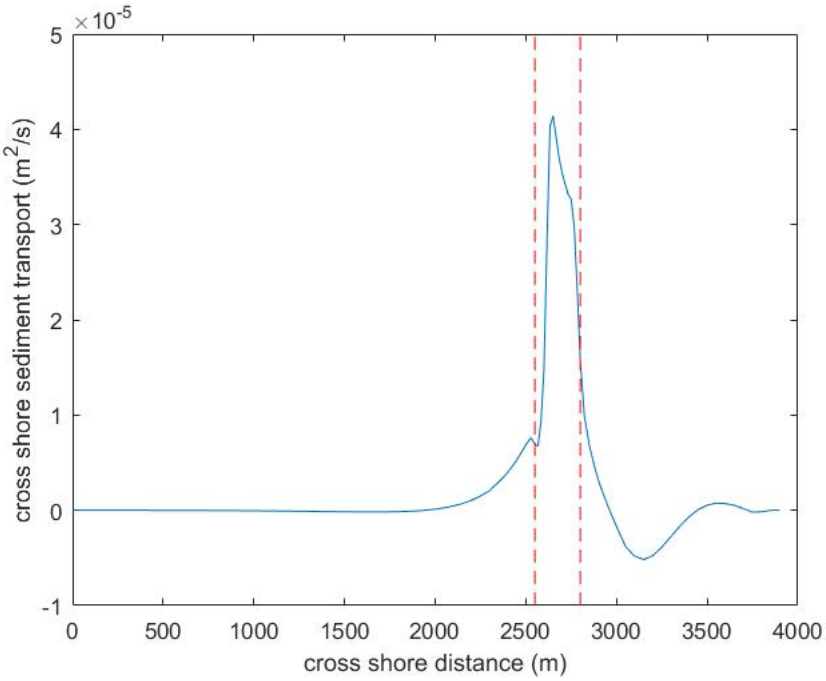

Figure 5.9: cross-shore sediment transport averaged over the longshore direction, (positive value is in the onshore direction, red dotted line is the location of the nourishment in the cross-shore direction)

Around the nourished area, the cross-shore sediment transport increases to its peak value at x is 2666.7 m (on the crest of the nourishment) and then starts to decrease. In the onshore area of the nourishment, the sediment transport toward offshore.

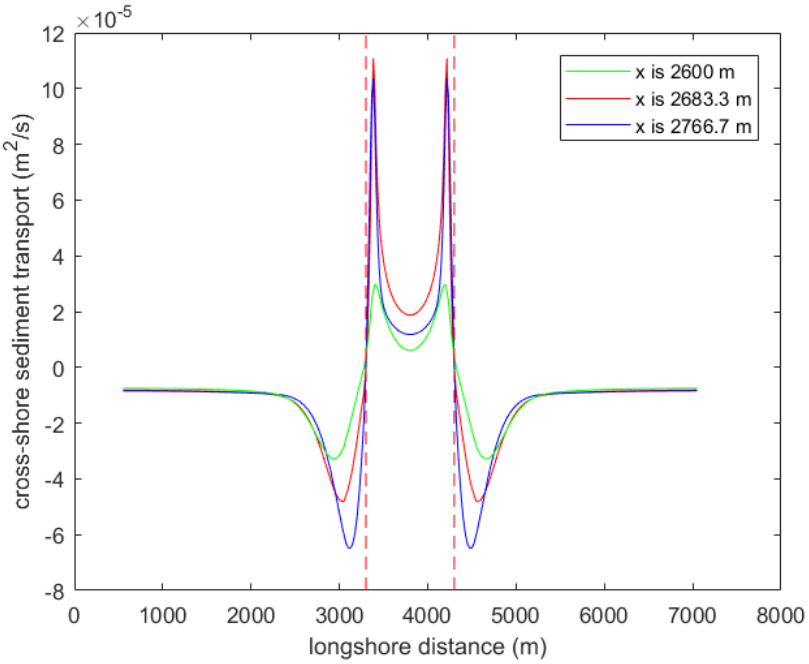

Figure 5.10: cross-shore sediment transport in longshore direction (positive values are in onshore direction, negative values are in offshore direction, red dotted line is the location of the nourishment in the longshore direction)

According to Figure 5.10 ,the cross-shore sediment transport has its minimum value at x= 2600 m (just offshore of the crest). The onshore sediment transport is observed on the crest of the nourishment and the maximum value is at the tips of the nourishment. The opposite direction is in the deeper area just next to the nourishment. In the other two sections (x=2683.3m and x=2766.7m), the cross shore sediment transports almost have the same value of the onshore sediment transport.

The longshore sediment transport is presented in Figure 5.11.

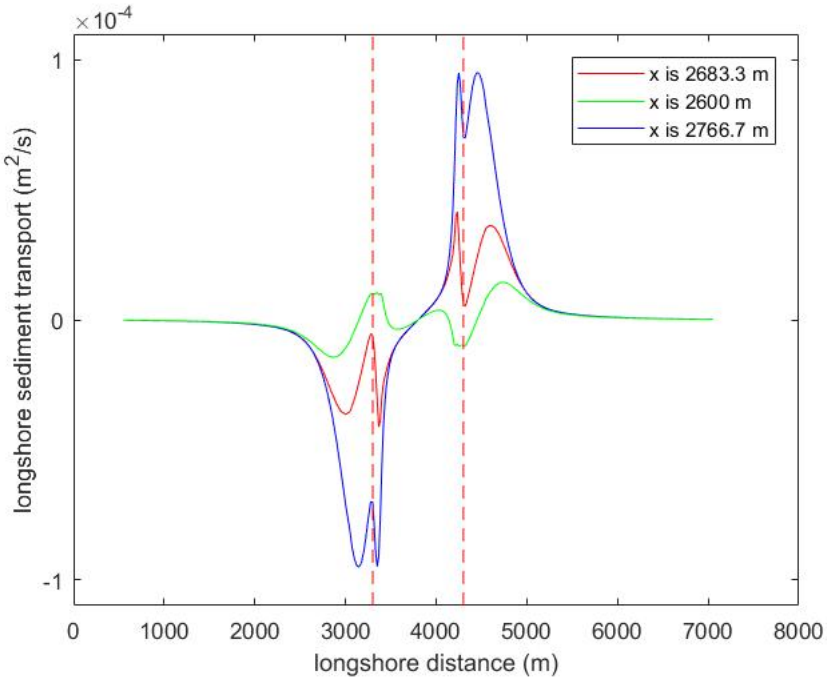

Figure 5.11: longshore sediment transport in longshore direction (red dotted line is the location of the nourishment in the longshore direction)

The largest longshore sediment transport is at x = 2766.7 m (just onshore of the crest). The longshore sediment transport also splits at the half distance of the nourishment at this location (Figure 5.11). The pattern of the longshore sediment transport is nearly the same as the longshore velocity. The detailed explanation of the abrupt change at the tip of the nourishment at x= 2766.7m is presented in Appendix G.

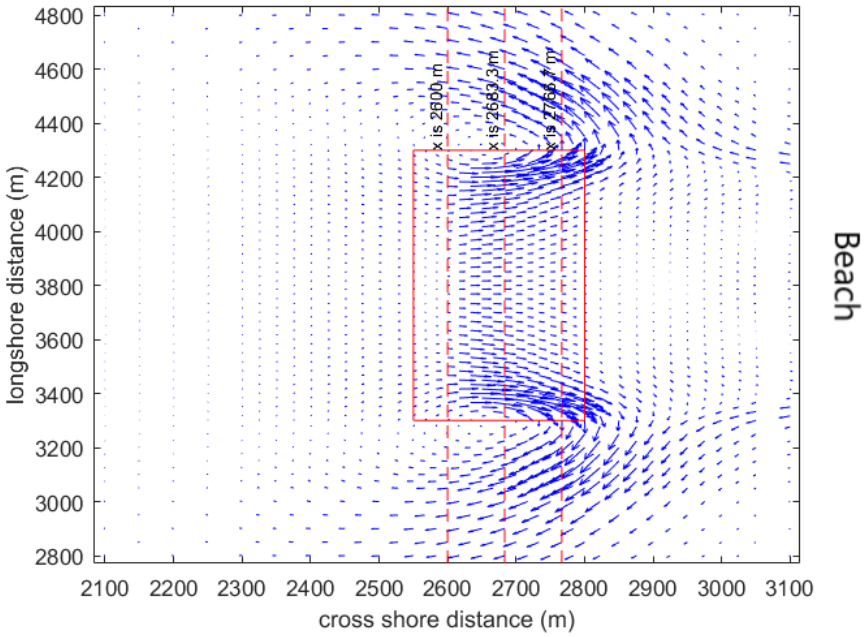

Figure 5.12: vector of the sediment transport (red box is location of the nourishment, red dotted line is the transect of the nourishment at the location of x=2600m, x=2683.3m, x=2766.7m)

Figure 5.12 shows that the largest sediment transport is on the edge area of the nourishment. The onshore sediment transport is observed on the nourishment area. On the onshore are of the nourishment crest, the sediments transport into the ripple channel. In the ripple channel, the sediment transport is in the offshore direction.

5.2.3. Erosion and sedimentation of the nourishment

According to Figure 5.13, it can be seen that the erosion pattern occurs just offshore of the crest and along the edge of the crest. The cumulative erosion at the tips is larger than the middle section. The significant erosion patter can be observed in the onshore area of the nourishment and the sedimentation pattern can be observed in the deeper area just next to the nourishment. The sedimentation pattern is observed in the major area of the nourishment crest with a relatively lower magnitude than the erosion pattern.

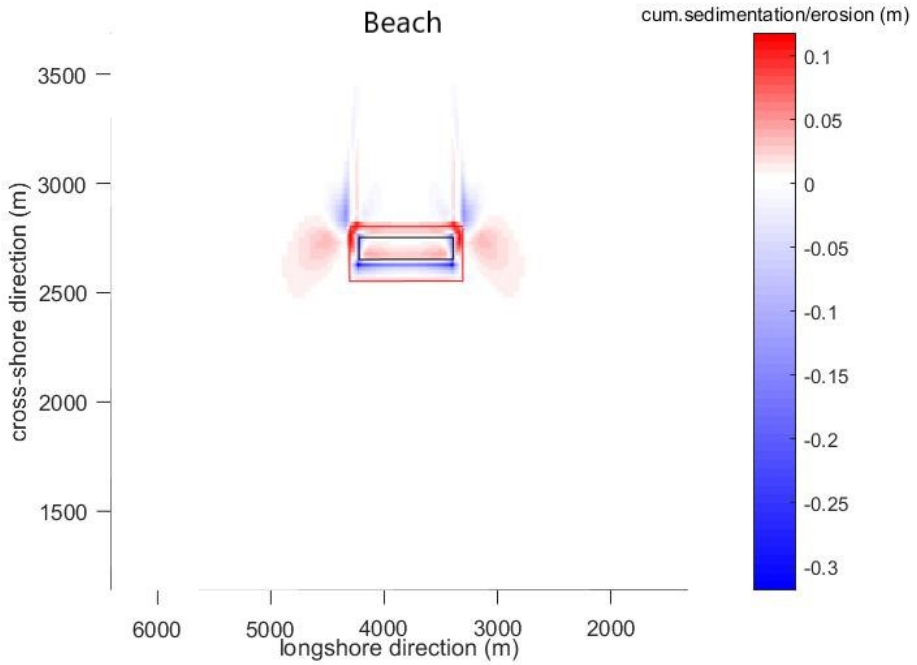

Figure 5.13: sedimentation and erosion of the sandy mound (red box is the location of the nourishment, black box is the location of the nourishment crest)

5.2.4. Summary of morphological response

The general trend of the cross shore, longshore sediment transport and erosion sedimentation pattern is nearly the same as the expected results. The onshore sediment transport on the crest and the offshore sediment transport in the surrounding area of the nourishment can be observed. The maximum cross shore sediment transport is at the tips and the longshore sediment transports also split at the half distance. There is an abrupt change of the longshore sediment transport at the tips due to the horizontal circulation. Both the erosion and sedimentation pattern can be observed on the nourishment, the maximum erosion pattern can be observed at the tips which are the same as expected.

5.3. Numerical experiments: Varying water depth and wave height

The erosion and sedimentation of the nourishments is highly dependent on the hydrodynamic conditions. In this section, the combined results of different scenarios are presented.

5.3.1. Variation of water depth on the crest of the nourishment

The different scenarios of water depths have been tested, the detailed information of each scenario is presented in Table 3.6. Wave height is identical for all cases, $H_s = 2.25m$ at the offshore boundary. The relation between the erosion/ sedimentation rate and water depth from the modelling test is plotted in Figure 5.14.

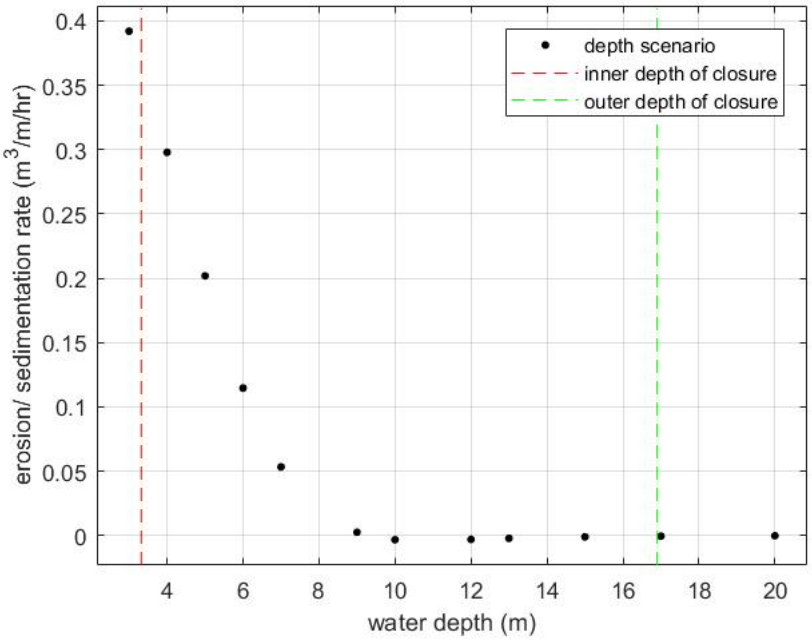

Figure 5.14: the relation between erosion/ sedimentation rate and water depth (positive value is erosion, negative value is sedimentation), the inner depth of closure is equal to 3.32m, the outer depth of closure is equal to 16.9m, the detailed calculation method of the depth of closure is presented in Appendix F

Figure 5.14 shows that larger water depths result in a smaller erosion rate of the nourishment. The erosion/ sedimentation rate is relatively sensitive when the water depth is smaller than 9 m. The erosion/ sedimentation is approximate to zero in deep water.

The relation between the erosion/ sedimentation rate and dimensionless wave height of each depth scenario is plotted in Figure 5.15.

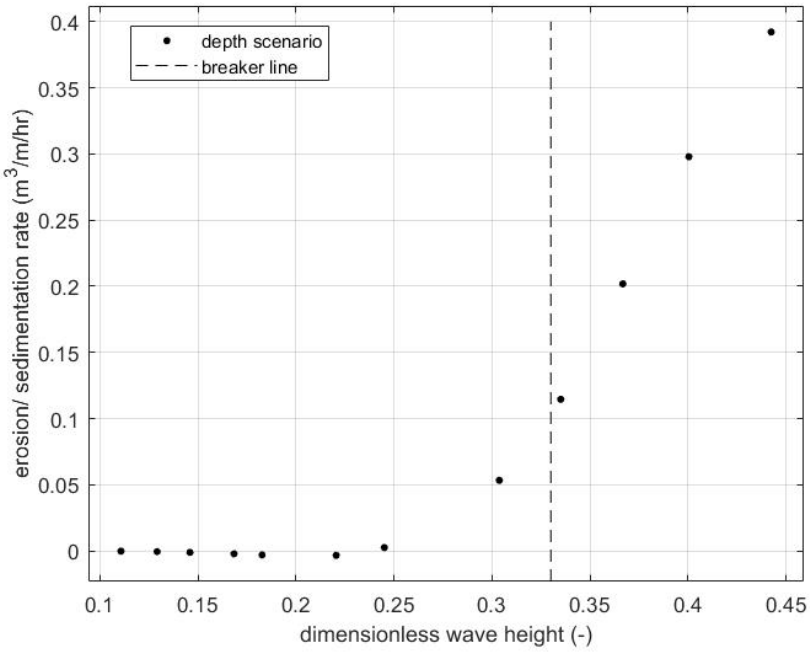

Figure 5.15: the relation between erosion/ sedimentation rate and dimensionless wave height (positive value is erosion, negative value is sedimentation, the definition of the dimensionless wave height in the modelling test is presented in Chapter 3.7.7)

The dimensionless wave height is averaged over the nourishment area for each depth scenario. The breaker line (the dimensionless wave height is equal to 0.33) is the outer limit of the surf zone. The larger dimensionless wave height results in the larger erosion/ sedimentation rate of the nourishments. The erosion/ sedimentation rate is relatively sensitive when the dimensionless wave height is larger 0.3 (almost inside the surf zone). Outside the surf zone (the dimensionless wave height is smaller than 0.25), the erosion/ sedimentation rate is almost the same.

To detect how sediment processes vary in different depth scenarios, components of the sediment processes (Eulerian velocity, orbital motion, turbulence intensity) are tested. The relation between each component and dimensionless wave height/ water depth is tested. According to Equation 2.11, the power trend is expected between the Eulerian velocity and water depth ($u_E \sim h^{-2}$). Based on Equation 2.14, the orbital velocity relates to the dimensionless wave height with the relation of $u_{rms} \sim \frac{H/h}{sinh(1+H/h)}$. The exponential trend is expected between the dimensionless wave height and turbulence intensity (Equation 2.15, $k_b \sim exp(H/h)$).

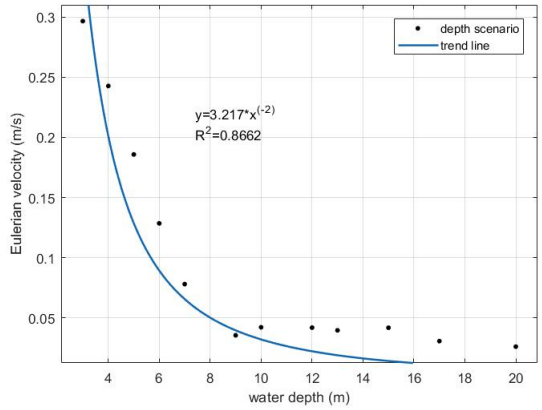

(a) the relation between Eulerian velocity and water depth

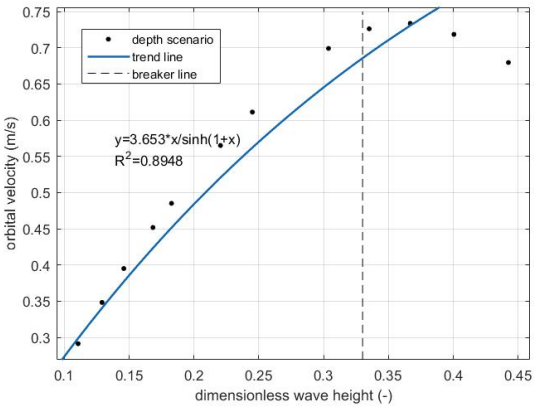

(b) the relation between orbital velocity and dimension less wave height

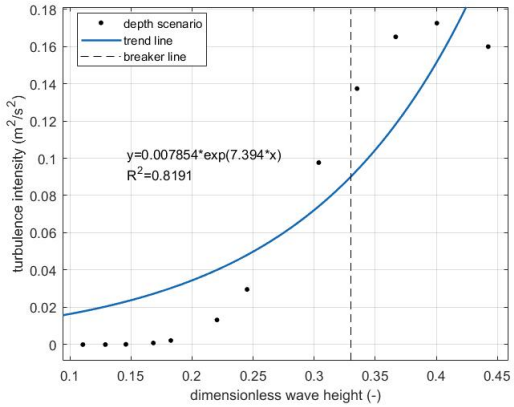

(c) the relation between turbulence intensity and dimensionless wave height

Figure 5.16: the relation sediment transport processes and hydrodynamics of depth scenarios, all components are averaged over the nourishment area in the simulation time

The power trend is found between the Eulerian velocity and water depth (with R^2 of 0.87, Figure 5.16 (a)). The trend line fits well over the water depth from 3m to 9m. While in deep water, the data is far away from the trend line. The Eulerian velocity decreases when the water depth increases from 3m to 9m. The small fluctuation of the Eulerian velocity is observed in deep water. The simplified relation of $u_{rms} \sim \frac{H/h}{sinh(1+H/h)}$ fits well between the dimensionless wave height and orbital velocity (with R^2 of 0.89, Figure 5.16 (b)). The orbital velocity increases over the dimensionless wave height from 0.1 to 0.37 and starts to decrease as the dimensionless wave height is larger than 0.37. The orbital velocity is also proportional to the wave height, waves have already broken in the seaward area of the nourishment for the shallow depth scenarios. As a result, the smaller orbital velocity is observed for the shallow water depth scenarios. The exponential trend is found between the turbulence intensity and dimensionless wave height (with R^2 of 0.82, Figure 5.16 (c)). The turbulence intensity is sensitive when the dimensionless wave height is larger than

0.25. However, it is decreasing as the dimensionless wave height increases from 0.4 to 0.45 (inside the surf zone). According to Equation 2.15, the turbulence intensity is also proportional to the roller dissipation. For the shallow water depth scenario, a large percentage of waves has already broken in the seaward area of the nourishment. It could lead to a smaller roller dissipation around the nourishment area. For the deep depth scenario (dimensionless wave height is smaller than 0.2), the turbulence intensity is approximate to zero.

All components have effects on the evolution of the nourishment in different depth scenarios. As the crest depth gets deeper, the impact of the turbulence intensity decreases to zero. While the Eulerian velocity and orbital velocity still have some impacts on the evolution of the nourishment. In deep water, the Eulerian velocity and turbulence intensities tend to be stable, but the orbital motion still shows the decreased trend.

5.3.2. Variation of wave height

The different conditions of wave heights have been tested and the detailed information of each scenario is presented in Table 3.7. Nourishment profile is constant with crest level at a water depth of 5m. The relation between the erosion/ sedimentation rate and dimensionless wave height of wave scenarios is plotted in Figure 5.17.

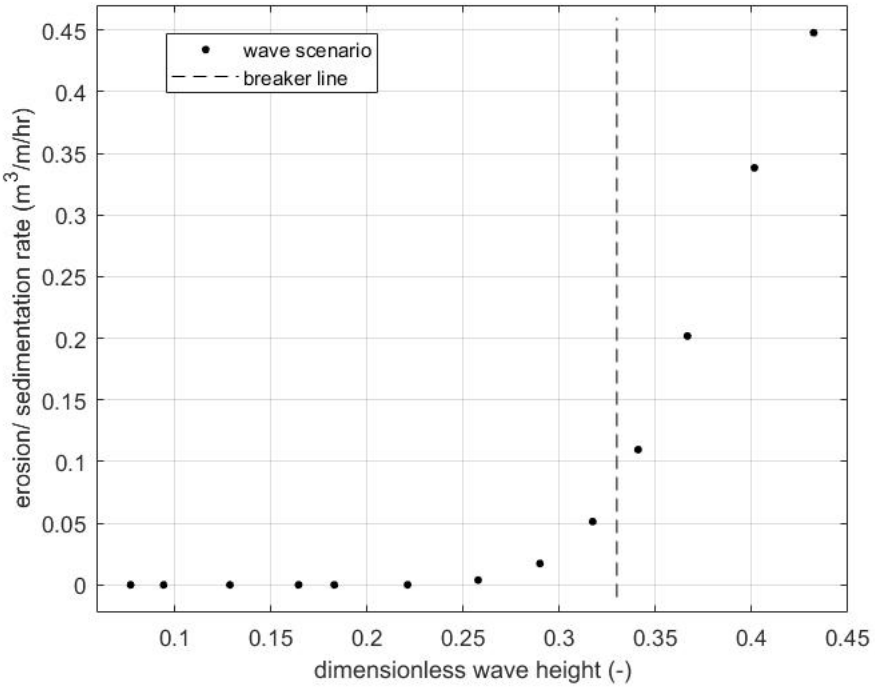

Figure 5.17: the relation between the erosion/ sedimentation rate and dimensionless wave height

Figure 5.17 shows that the erosion/ sedimentation rate is highly dependent on the dimensionless wave height while inside the surf zone (dimensionless wave height is larger than 0.33). Outside the surf zone, the dimensionless wave height has less impact on the evolution of the nourishment. The erosion/ sedimentation rate tends to be the same.

To detect the detailed sediment processes of different wave heights, different components of the sediment processes are tested for each wave scenario (orbital motion, turbulence intensity and Eulerian velocity). The relation between the Eulerian velocity and dimensionless wave height is expected as: $u_E \sim (\frac{H}{h})^2$.

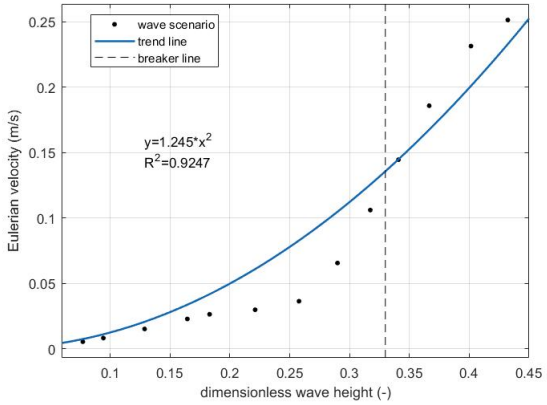

(a) the relation between Eulerian velocity and dimmensionless wave height

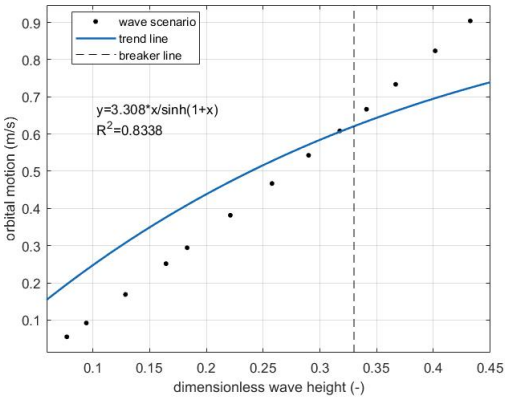

(b) the relation between orbital velocity and dimensionless wave height

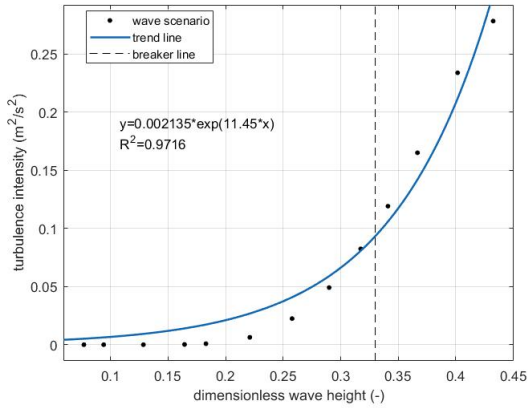

(c) the relation between turbulence intensity and dimensionless wave height

Figure 5.18: the relation sediment transport processes and hydrodynamics of wave scenarios, all components are averaged over the nourishment area in the simulation time

The power trend is fitted between the Eulerian velocity and dimensionless wave height (Figure 5.18 (a), with R^2 of 0.9247). The Eulerian velocity shows a high dependency on the dimensionless wave height while inside the surf zone. The Eulerian velocity is still decreasing outside the surf zone but with a relatively lower decreasing rate. The orbital velocity

decreases over the dimensionless wave height from 0.45 to 0.05. The turbulence intensity decreases over the dimensionless wave height with an exponential trend (with R^2 of 0.9716, Figure 5.18 (c)). The turbulence intensity decreases to zero as dimensionless wave heights get lower. For different wave scenarios, all components have effects on the evolution of the nourishment, especially for the dimensionless wave height is larger than 0.33. As wave heights get lower, the impact of the turbulence intensity decreases to zero. While the Eulerian velocity and orbital motion still have some effects on the evolution of the nourishment.

Compared with the depth scenarios, the decreasing trend is not observed of the turbulence intensity and orbital motion when the dimensionless wave height is larger than 0.33. For the wave scenario, the crest depth of the nourishment is constant. In this case, the most percentage of waves is breaking around the nourishment area and a small percentage of waves is breaking at the seaward area of the nourishment. Then the larger wave heights at the offshore boundary, the larger breaking effects around the nourishment area will be.

5.4. Numerical experiments: Varying geometry

The sedimentation and erosion of nourishments is also dependent on the nourishment size. In this case, the different length and volume per meter of nourishments have been tested.

5.4.1. Variation of length

The length varies from 500m to 6000m. The properties of each condition are summarized in Table 3.8. The decreased trend between the length of the nourishment and the erosion rate is expected. The relation between the erosion/ sedimentation rate and the length of the nourishment is plotted in Figure 5.19.

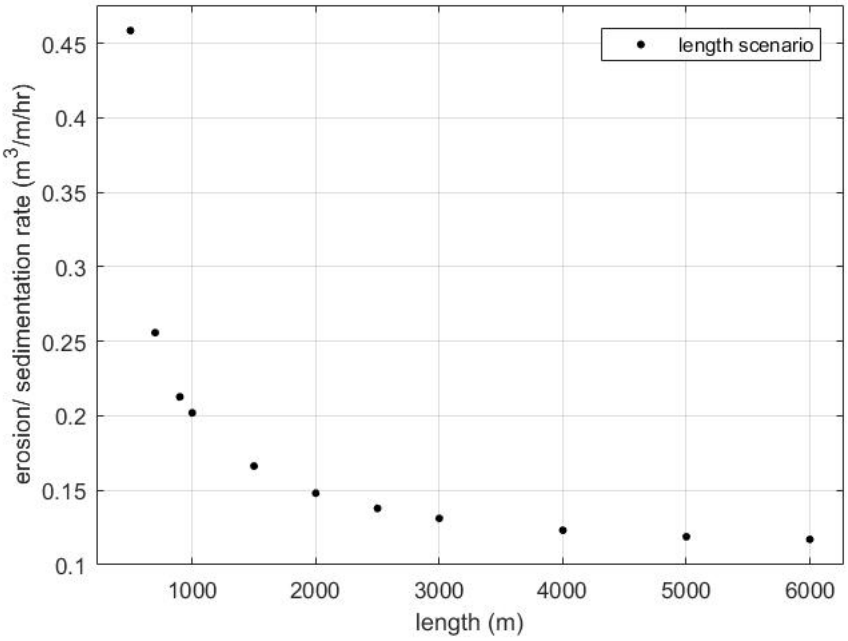

Figure 5.19: the relation between erosion/ sedimentation rate and length of the nourishment (positive value is erosion, negative value is sedimentation)

Figure 5.19 shows that a shorter nourishment is eroded more compared to a longer one. When the length is larger than 2000m, the erosion rate of the nourishment remains stable but does not decrease to zero.

To detect the detailed sediment processes with the increasing length of the nourishment, different components of the sediment processes are tested for each length scenario (orbital motion, turbulence intensity and Eulerian velocity).

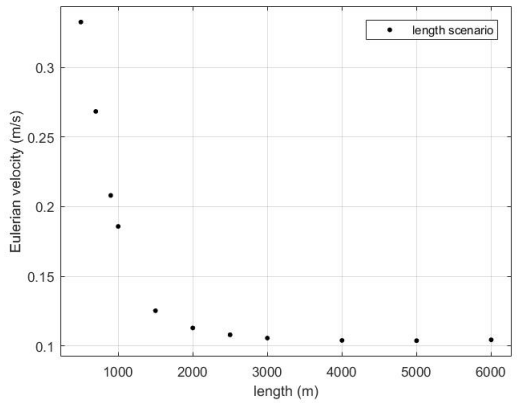

(a) the relation between Eulerian velocity and length

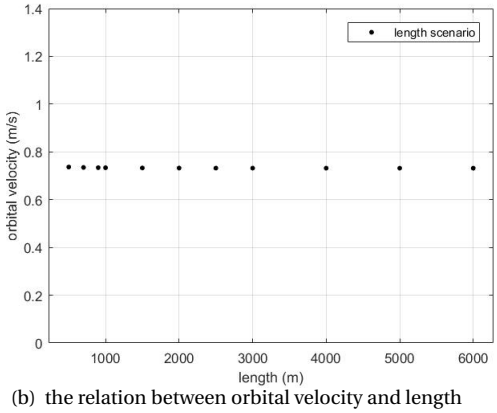

(b) the relation between orbital velocity and length

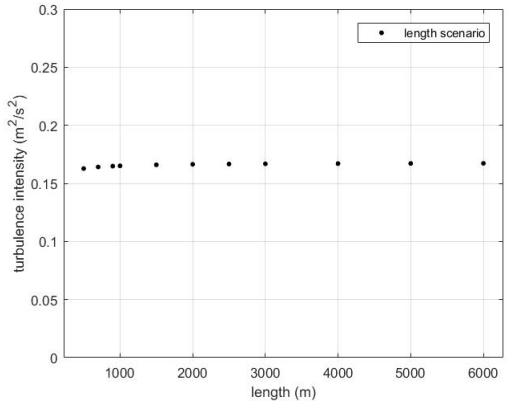

(c) the relation between turbulence intensity and length

Figure 5.20: the relation between sediment transport processes and length, all components are averaged over the nourishment area in the simulation time

Figure 5.20 shows that only the Eulerian velocity varies with the increasing length. The Eulerian velocity decreases with an increasing length. It tends to be stable when the length is larger than 2000m. While the turbulence intensity and orbital velocity is nearly the same for different length scenarios. It indicates that for the shorter length of the nourishment, the stronger currents will be. The horizontal circulation mainly impacts on the edge area, the currents are much stronger at this specific area than the middle section. For the shorter length of the nourishment, the edge currents cover a larger percentage area compared to the longer one. It results in the larger Eulerian velocity and the associate larger erosion rate.

5.4.2. Variation of volume per meter

The range of the volume per meter varies from 200 m^3/m to 608 m^3/m. The properties of each scenario are summarized in Table 3.9. The increasing trend between the volume per meter of the nourishment and the erosion rate is expected. The relation between the

erosion/ sedimentation rate and volume per meter is plotted in Figure 5.21.

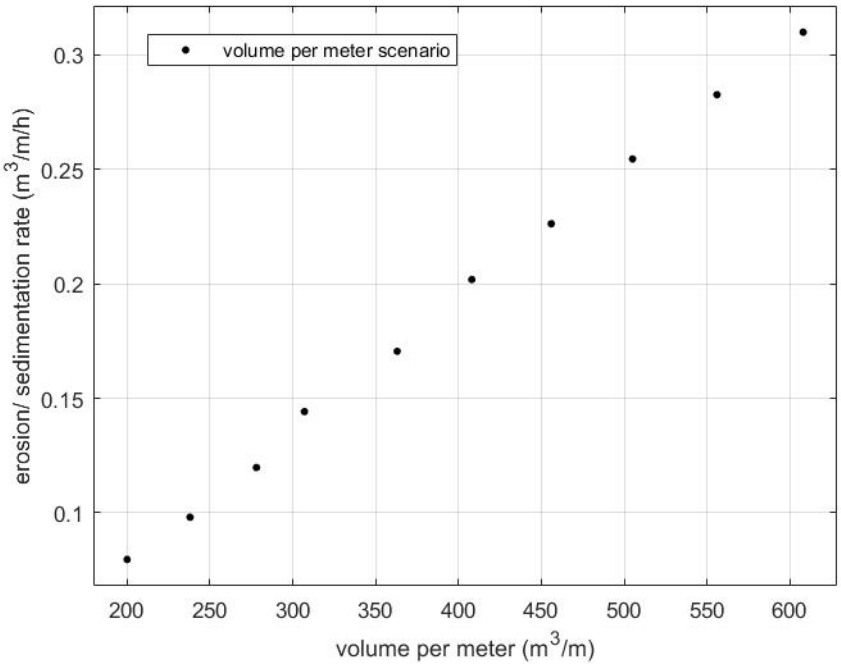

Figure 5.21: the relation between erosion/ sedimentation rate and volume per meter of the nourishment (positive value is erosion, negative value is sedimentation)

Figure 5.21 shows that the nourishment is eroded more with the increased volume per meter. The increasing trend can be found over the volume per meter increases from 200 m^3/m to 608 m^3/m.

To detect how the sediment processes vary when the volume per meter of the nourishment is increasing, the different components of the sediment processes will be tested for each volume per meter scenario (orbital motion, turbulence intensity and Eulerian velocity).

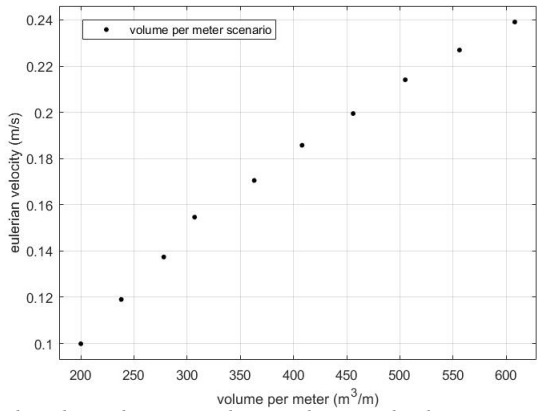

(a) the relation between Eulerian velocity and volume per meter

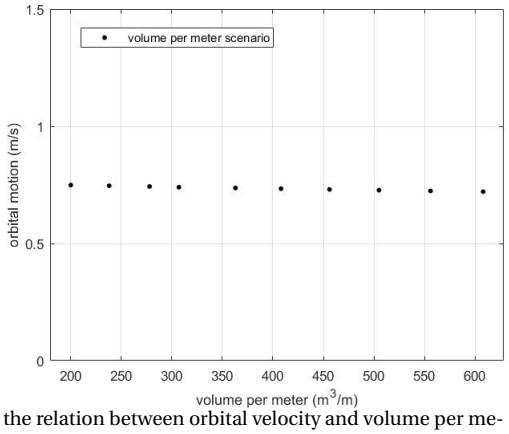

(b) the relation between orbital velocity and volume per meter

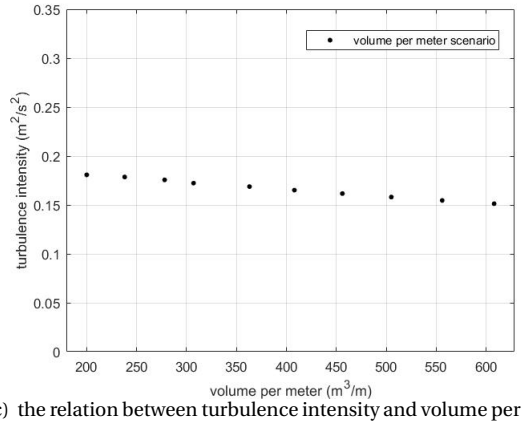

(c) the relation between turbulence intensity and volume per meter

Figure 5.22: the relation sediment transport processes and volume per meter, all components are averaged over the nourishment area in the simulation time

The Eulerian velocity increases over the volume per meter of the nourishment from 200 m^3/m to 608 m^3/m. While the orbital velocity is nearly the same for all volume per meter scenarios and the turbulence intensity shows a weaker decrease trend with the increased volume per meter. This indicates that the wave impact does not differ a lot between volume per meter scenarios. The larger volume per meter of the nourishment also has larger edge sections. The impacts of currents are becoming stronger with the larger edge sections as well. It leads to stronger edge effects and the associated larger erosion rate.

Chapter 6

Discussion

In this chapter, the assumptions and simplifications of this research are justified.This chapter summarizes the most important results in previous parts. It compares the similarities and differences between the results of data analysis and modelling test. The limitations of the methodology are also discussed.

6.1. Discussion of methodology

To get a better understanding about the behaviour of the nourishments, data analysis and XBeach model were performed in this research.

6.1.1. Limitation of data analysis

In the data analysis part, data of the nourishment cases are relatively limited. For the Dutch shoreface nourishment cases, all of them are placed in a similar water depth (4-6m). Therefore, the water depth may not influence the evolution of the nourishment a lot. And wave heights along the Dutch coast are approximately the same, the yearly-difference of the Dutch wave heights is also quite small. It results in nearly the same wave conditions of each Dutch nourishment project. And the evolution of nourishments can not be fully reflected on the yearly significant wave height. The yearly-significant wave height includes calm and storm periods. The nourishment tends to have a faster erosion process in storm periods than calm periods. It is hard to detect the evolution of the nourishment in different wave conditions just through the yearly wave condition. While the nourishment size (length, volume and volume per meter etc) differs a lot between each case. In this case, the effects of the nourishment size are more obvious for the Dutch nourishment projects.

In the measured data, the erosion rate of the Dutch shoreface nourishment is determined by a decrease in the volume within the bounds of the initial nourishment area. In this case, the migration of the nourishment also results in a volume loss in the bounds of the initial nourishment area. The shoreface nourishment possibly has a faster migration rate in deeper water. It may result in larger erosion rates of the shoreface nourishments in deeper

water.

6.1.2. Limitation of the XBeach Model

The modelling test has been performed to examine the behaviour of the nourishments through the XBeach model. The model is only an approximation of the reality and the performance of the model is limited by the basic assumptions that form the foundation of the model. The assumptions also arise from the users that make during the process of the model set-up. In this research, the model has been established in idealised conditions without complex bed topographies. The imposed offshore wave condition is stationary (extreme wave conditions) and tide effects are excluded, which may cause the mismatch of real conditions. After imposing the realistic wave boundary conditions which include mild and extreme periods, the active period of the nourishment will decrease in the simulation time. It results in a lower erosion rate of the nourishments compared to this simplified numerical model. This simplified model also excludes tide effects. Only waves and induced currents have impacts on the evolution of the nourishment. It leads to a nearly zero erosion rate of the nourishment in deep water. With imposing the tidal effects, the evolution of the nourishments could increase in deep water.

It should be noticed that the model results are obtained in certain model parameters. Based on the previous practice, the sediment transport depends on the settings of wave skewness and asymmetry. In this research, the default settings are used. Different factors of wave skewness and asymmetry could influence the magnitude of the sediment transport and erosion rate of the nourishment.

6.2. Interpretation of results

6.2.1. Interpretation of data analysis

The results of the Dutch and international shoreface nourishments are combined together to examine the influence of the dimensionless wave height. According to Hoekstra et al. (1997), non-fluxes only occurred for the dimensionless wave height is larger than 0.3-0.35. The dimensionless wave height of all shoreface nourishments is between 0.1 and 0.22 through the measured data. It indicates that the shoreface nourishments were stable for the most time of one year.

Figure 4.2 shows that the larger depth of the nourishment crest results in a larger erosion rate which is opposite to the expected results. It presents nearly the same trend as the

relation between the length/ volume of the shoreface nourishments and erosion rate. It indicates that the shoreface nourishment with a larger volume/ length tends to be placed in deeper depth (with R^2 of 0.17 in Figure 6.1 (a) and R^2 of 0.27 in Figure 6.1 (b)). That may be the reason why the larger depth of the nourishment crest results in a larger erosion rate.

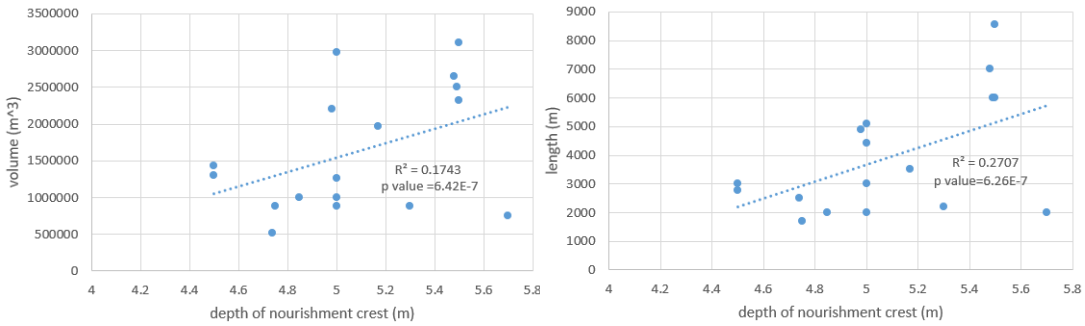

(a) the relation between the depth of the nourishment crest and volume of the Dutch shoreface nourishments

(b) the relation between the depth of the nourishment crest and length of the Dutch shoreface nourishments

Figure 6.1: the relation between the depth of the nourishment crest and geometric conditions (volume, length)

6.2.2. Interpretation of modelling tests

The results of the modelling tests have been presented in Chapter 5. Firstly, the validation of hydrodynamic and morphological conditions have been done. It is only a conceptual model, a full validation is not possible without real data. However, the general trend of the hydrodynamic and morphologic condition is the same as the expected results. And the erosion/ sedimentation pattern (Figure 5.13) through the modelling test can be compared with the results from Koster (2006) (Figure 2.8). Both the erosion/ sedimentation pattern is observed around the nourishment area and the maximum erosion pattern is at the edge section of the nourishment. In the Koster (2006) case, the wave direction is not perpendicular to the coastline. As a result, the erosion pattern in the onshore area of the nourishment is not symmetrical which is different from the shore normal case in this research.

After that, several model scenarios have been done to test how the influence of hydrodynamic and geometric conditions on the erosion rate of the nourishments. The different depths of the nourishment crest have been examined through the XBeach model. The results of the numerical data show that the erosion/ sedimentation rate tends to be zero when the water depth is larger than half the water depth of the outer depth of closure. It shows the same results as the measured data from Beck et al. (2012). However, this is only for the case of the offshore wave height is equal to 2.25m. The yearly-significant wave height through the measured data is used to determine the depth of closure. It includes the mild and extreme wave heights. The results from the numerical data of the depth scenario can only

represent the extreme case. For the mild wave condition, it could lead to a different result when compared to the Depth of Closure. The dimensionless wave height is examined for depth and wave scenarios, the erosion rate increases when the dimensionless wave height is larger than 0.3. Otherwise, the erosion rate is nearly zero. This supports the results of Hoekstra et al. (1997) that non-zero cross-shore sediment fluxes only occurred for the dimensionless wave height is larger than 0.3.

6.2.3. Combined results of data analysis and modelling test

In the measured data, a multitude of parameters varies between cases, obscuring the view on relationships. While in the modelling test, the isolated parameter of the nourishments can be explored. Therefore, the relation in the numerical data is much more obvious than the measured data. In the numerical data, the water depth, dimensionless wave height, volume per meter all have effects on the evolution of the nourishments. However, it is not the case in the measured data. Both the numerical data and measured data show that the larger length of the nourishments results in a lower erosion rate per meter. It indicates that the length is an important factor for the evolution of the nourishments in the measured data and numerical data.

Meanwhile, it is also possible to make a link between the measured data and numerical data. From the measured data, we have already collected wave data for the Dutch shoreface nourishment cases. Then the exceedance probability of the dimensionless wave height can be obtained by combining the wave data of all Dutch shoreface nourishment cases (Figure 6.2).

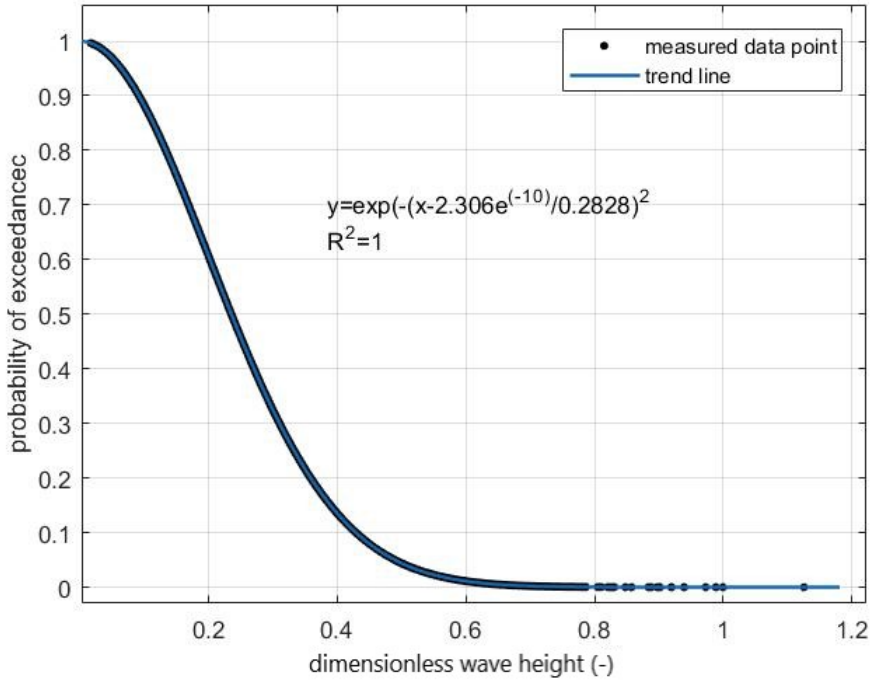

Figure 6.2: probability of exceedance of the dimensionless wave height (the water depth is assumed to be 5m; wave data is the combination of all Dutch shoreface nourishment cases, the detailed explanation is presented in Chapter 3.3)

The relation between the erosion rate and dimensionless wave height has already obtained through the numerical data (Figure 5.17). Assume the exceedance probability of the dimensionless wave height in the numerical data is the same as the measured data. In this case, the exceedance probability of the erosion rate in the numerical data is obtained (Figure 6.3).

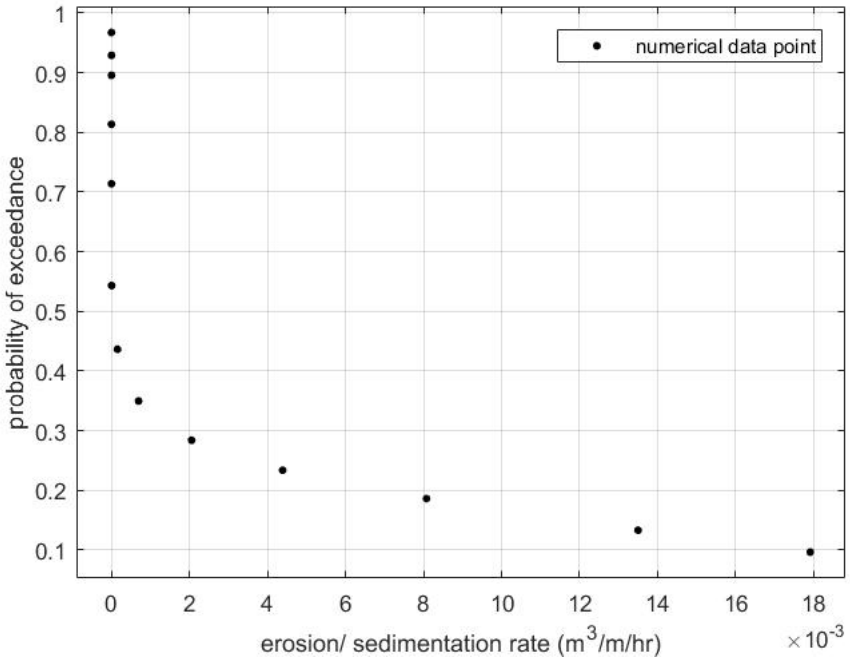

Figure 6.3: exceedance probability of the erosion rate in the numerical data

Figure 6.3 shows that a nourishment with a crest level of 5 m is about 45 % of the year active. During the remaining time, the nourishment tends to remain stable.

6.2.4. Practical Application

The main purpose of this research is to examine how erosion processes are influenced by different parameters of the nourishments. In this way, the nourishments can be applied much better. The design method of the nourishments (such as the length, displaced location) depends on the specific situation. If the coastal area has a high shortage of sediments and the erosion problem is quite serious due to coastal flood, it is suggested to implement the nourishment just inside the surf zone in a shallow water depth to compensate the coastline within a short period. On the other hand, if sediments are not highly demanded in the coastal area and the strategy is to maintain the coastline against the sea-level rise in the following decades. It is suggested to place a relatively long length/ large volume of the nourishment in a relatively deep water depth (outside the breaking zone). As a result, the nourishment can be kept for a longer time and sediments will be supplied in a sustainable method.

Chapter 7

Conclusions and recommendations

7.1. Conclusions

In this section, the research questions are discussed here.
This research aims to examine how the water depth/ dimensionless wave height and geometric conditions (length, volume, volume per meter of nourishments) influence the erosion rate of the shoreface nourishments. The research question is:

"How does the depth of the nourishment crest/ dimensionless wave height influence the erosion rate of the nourishments?"

For the measured data, the erosion rate of the shoreface nourishments varies a lot in a small range of water depths (4-6m), but most of them are larger than the dump sites and pits in deep water depth. Combined data of the international and Dutch shoreface nourishments show that the erosion rate is not highly dependent on the dimensionless wave height. The dimensionless wave height of all shoreface nourishment cases is between 0.1 and 0.22 (outside the surf zone).

Numerical data show a high dependency on water depths. For a specific wave condition ($H_s = 2.25m$, $T_p = 7.8s$ at the offshore boundary), the erosion rate is 8 times smaller if the water depth is 7m compared to the water depth is 3m. When the water depth is larger than 9m, the erosion rate is around zero (Figure 5.14). As the water depth gets deeper (from 3m to 20m), the impacts of the Eulerian velocity, turbulence intensity and orbital motion become much weaker with the deeper water depth.

The numerical data also show a high dependency on dimensionless wave heights. The dimensionless wave height highly influences the evolution of the nourishment when the dimensionless wave height is larger than 0.33 (inside the surf zone). As the dimensionless wave height is smaller than 0.25, the erosion rate is approximate to zero. Most erosion of the nourishment occurs during the storm wave condition (the dimensionless wave height is larger than 0.33).

"How does the nourishment size (length, volume, volume per meter etc) influence the

erosion rate of the nourishments?"

The effect of nourishment size has also been examined through 17 Dutch shoreface nourishments. The most influenced factors through the measured data are the volume and length. The larger volume/ length of the shoreface nourishments coincide with larger erosion rates (with R^2 of 0.41 and 0.62 respectively, Table 4.4). The relation between the volume/ length of the shoreface nourishments and erosion rate per meter shows the opposite trend that the larger length/volume leads to a smaller erosion rate per meter (with R^2 of 0.22 and 0.21 respectively, Table 4.4). While the erosion rate/ erosion rate per meter is not highly dependent on the volume per meter/ height of the shoreface nourishments through the measured data.

The numerical data show that the length is relatively important for the evolution of the nourishment. When the length is smaller than 2000m, the nourishment tends to have a faster erosion process. This is due to the strong circulations at end sections. The numerical data show that the volume per meter of the nourishment also has an effect of the evolution of the nourishment. With constant wave conditions ($H_s = 2.25m$, $T_p = 7.8s$) at the offshore boundary, changing the volume per meter of the nourishment from 200 m^3/m to 500 m^3/m impacts the erosion rate by factor 3. The nourishment has a larger volume per meter also has a larger edge section area. The impacts of currents are becoming stronger with the larger edge sections as well.

Practical Application

In this research, we get a better understanding of the nourishment behaviour. It helps us to implement the nourishment in a better way. The coastal area with a high shortage of sediments requires the nourishment to compensate the coastline in a short time scale. Then it is suggested to place the nourishment in a relatively shallow depth. If the goal is to compensate the coastline in a sustainable method, it is better to implement the nourishment with a longer length/ larger volume in deep water depth.

7.2. Recommendations

In this thesis, several important findings of the nourishments have been concluded through the measured and numerical data that can be useful for better understanding the behaviour of the nourishment. Recommendations are summarized to benefit the improvement of further research.

Accuracy of wave data

The numerical model proves that the erosion rate of the nourishments is nearly zero when the dimensionless wave height is smaller than 0.25. It indicates that the nourishments tend to be stable during calm periods and active during storm periods. For further research, it is recommended to detect how the nourishments behave under different wave conditions in short periods through the measured data. To achieve that, the daily nourishment behaviour should be recorded with a monitoring system. After that, time series of the volume change of nourishments and wave conditions can be obtained. Then it is possible to compare the difference of the nourishment evolution between calm and storm periods. It can help us get much more insights into the nourishment behaviour.

Tide effects

The tide effects also influence the behaviour of the nourishments, especially for the tide-dominated area. It is also worth to detect the difference of the impact of the tide and wave effects on the nourishment behaviour. This can be done by analysing two nourishment cases of the wave-dominated and tide dominated area with the measured data and numerical model respectively and compare the evolution and migration of the nourishments.

Realistic model

In this thesis, the model is constructed with simplified conditions. A full validation is not possible for this simplified model and the idealised condition does not exist in reality. Further research can focus on the actual behaviour of the nourishments with existing bathymetry and boundary conditions. The model can be calibrated with real data to give more realistic results and predict long term of the nourishments.

Response of coastline

This research only focuses on the evolution of the nourishment itself and the response of the landward area of the nourishment is excluded. Detect how the landward area of the nourishment and coastline evolve under different design parameters of the nourishments is also valuable. For the further research, the advice is to collect data along the Dutch coast through the Jarkus survey. Then it is possible to see how the coastline evolves under different nourishment projects and compare the results. Results of this comparison can be supported by a numerical model.

Appendix A

Method of calculating erosion rate of international nourishment projects

A.1. South Padre Island, Texas

Aidala et al. (1992) present the evolution of the nourishment which include the length, width, volume. The volume of the nourishment decreased from 125000 m^3 in January, 1989 to 26800 m^3 in May, 1990 (Figure A.1). The erosion rate is equal to the ratio of the volume loss of the nourishment and the corresponding period: $\frac{125000-26800}{1+4/12} = 76350(m^3/yr)$.

Parameter	Initial (Jan. 4, 1989)	Period 1 (Jan. 4 - Mar. 9, 1989)	Period 2 (Mar. 10 - Jun. 19, 1989)	Period 3 (Jun. 19, 1989 - May 14, 1990)
Berm bathymetry				
length (m)	1,220	975	850	460
width (m)	380	250	250	190
area (m^2)	259,000	207,200	207,200	77,700
max. relief (m)	1.4	1.3	1.2	0.6
volume (m^3)	125,000	94,800	88,000	26,800
crest movement (m) & direction	--	60, onshore	none	45, offshore
centriod movement (m) & direction	--	55, onshore 90, south	7.5, onshore 4.5, south	30, offshore 180, south

Figure A.1: Nourishment evolution of South Padre Island (Source: Aidala et al., 1992)

A.2. Sliver Strand State Park, CA

The measured volume and berm height of the middle section of Sliver Strand State Park, CA nourishment project is given in Figure A.2 ((Larson and Kraus, 1992)). Initially, the berm grew rapidly because the placement of the berm was continuing until the beginning of January. The total volume loss is equal to the volume loss per meter multiply the length of the berm. The erosion rate is determined by the ratio of the total volume loss and the corresponding period (year): $(600-480)*370/1.1765 \approx 37740(m^3/yr)$

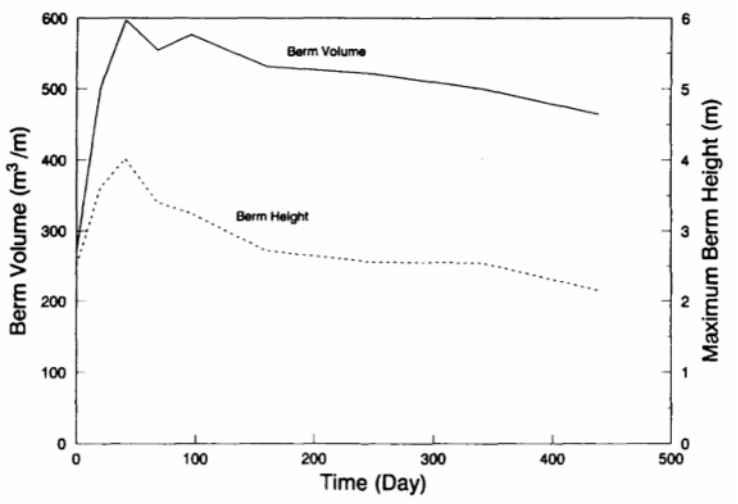

Figure A.2: Berm volume and height with respect to reference profile (Source: Larson and Kraus, 1992)

A.3. Perdido Key, FL

The remaining volume of sand was calculated as a record of nourishment performance. Three years after placement of the nourishment, there was 84% of the initial volume remaining (Figure A.3). The initial volume is around $3 \times 10^6 m^3$, then the erosion rate is equal to $\frac{3\times10^6\times0.16}{3} = 160000(m^3/yr)$.

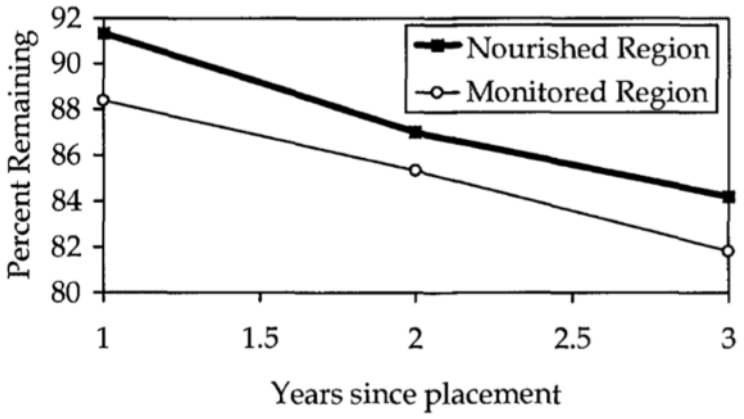

Figure A.3: Volume changes for Perdido Key, FL nourishment. Nourished region is a subset of the monitored region. (Source: Work and Otay, 1996)

A.4. Brunswick, GA(Mound "C")

The volume loss of Brunswick, GA nourishment was measured by the OBS Measurements. The OBS Measurements recorded the volume loss in two periods (April 2- June 4, 2003 and June 5- August 22, 2003) which is equal to $3.5 * 10^4 m^3/month$ and $1.5 * 10^4 m^3/month$,

respectively (Johnson, 2005). The 4 month volume loss can be transferred to yearly-volume loss which is equal to $306000 m^3/yr$.

A.5. Ocean beach, SF

Barnard et al. (2009) concludes that approximately half of the nourishment has eroded in the nearshore dredge-disposal site in 2.5 years. The total placed volume of the nourishment is equal to $690000 m^3$, the associated erosion rate is $138000 m^3/yr$.

A.6. New River Inlet, NC

Schwartz and Musialowski (1978) indicates that $26750 m^3$ of sand was transported to the disposal site. 40 % of the $26750 m^3$ had been removed from the offshore zone during the disposal period. 75 % of the $26750 m^3$ had been removed 34 days after disposal. These 35 % of the $26750 m^3$ had been transported by natural processes which is applied to calculate the erosion rate. The erosion rate is approximately to $275 m^3/day$ ($100500 m^3/yr$).

Appendix B

Parameters in Xbeach

The presented values and settings have been applied in this research.

Table B.1: Parameters in Xbeach

Model time parameters:	**Flow parameters:**
CFL = .7000	bedfriction = chezy
tstop = 86400.0000	bedfricfile = None specified
	C = 55.0000
Physical constants:	nuh = .1000
rho = 1025.0000	nuhfac = 1.0000
g = 9.8100	nuhv = 1.0000
depthscale = 1.0000	smag = 1
Initial conditions:	**Coriolis force parameters:**
zsinitfile = None specified	wearth = .0417
hotstartflo = 0	lat = .0000
Wave boundary condition parameters:	**Wind parameters:**
instat = stat	rhoa = 1.2500
taper = 100.0000	Cd = .0020
nmax = .8000	windfile = None specified
Hrms = 2.2500	windv = .0000
Tm01 = 7.8000	windth = 270.0000
Trep = 7.8000	
dir0 = 270.0000	**Bed composition parameters:**
m = 10	ngd = 1
leftwave = neumann	nd = 3

rightwave = neumann

Flow boundary condition parameters:
front = abs_2d
left = neumann
right = neumann
back = wall
ARC = 1
order = 2.0000
carspan = 0
freewave = 0
epsi = .0050
nc = 201
tidetype = velocity

Tide boundary conditions:
tideloc = 0
zs0 = .0000

Discharge boundary conditions:
disch_loc_f = None specified
disch_times = None specified
ndischarge = 0
ntdischarge = 0
beta = .1000

Wave breaking parameters:
break = baldock
gamma = .7800
alpha = 1.0000
n = 10.0000
gammax = 2.0000

por = .4000
D50 = .0002
D90 = .0003
rhos = 2650.0000
dzg = .1000
dzg1 = .1000
dzg2 = .1000
dzg3 = .1000
sedcal = 1.0000
ucrcal = 1.0000

Sediment transport parameters:
form = vanthiel_vanrijn
waveform = vanthiel
sws = 1
lws = 1
BRfac = 1.0000
facsl = 1.6000
z0 = .0060
smax = -1.0000
tsfac = .1000
facua = .1000
facSk = .1000
facAs = .1000
turbadv = none
turb = bore_averaged
Tbfac = 1.0000
Tsmin = .5000
lwt = 0
betad = 1.0000
sus = 1
bed = 1

delta = .0000
fw = .0000
fwcutoff = 1000.0000
breakerdela = 1
shoaldelay = 0
facsd = 1.0000
facrun = 1.0000

Roller parameters:
roller = 1
rfb = 0

Wave-current interaction parameters:
wci = 0
hwci = .1000
cats = 4.0000

bulk = 1
facDc = 1.0000
jetfac = .0000

Morphology parameters:
morfac = 10.0000
morfacopt = 1
morstart = 5400.0000
morstop = 86400.0000
wetslp = .3000
dryslp = 1.0000
hswitch = .1000
dzmax = .0500
struct = 0

Appendix C

Related graphs of hydrodynamic conditions for each subset

In this appendix, the relation between water depth/ dimensionless wave height and erosion rate/ erosion rate per meter is presented for each subset.
The relation between water depth and erosion rate/erosion rate per meter is shown as follows (Figure C.1 to Figure C.6) :

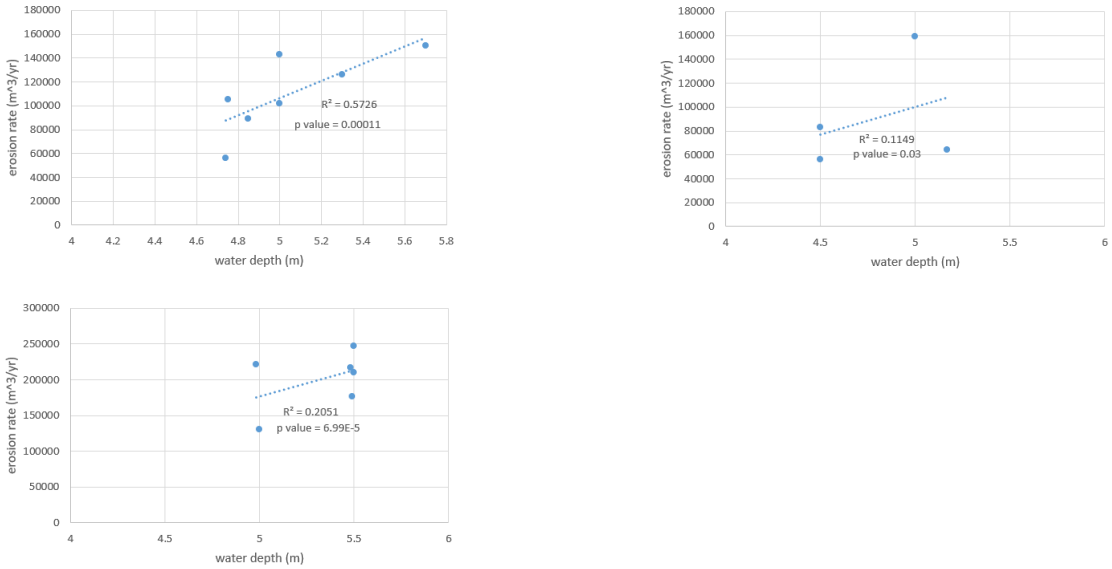

Figure C.1: the relation between water depth and erosion rate of subset A, B and C

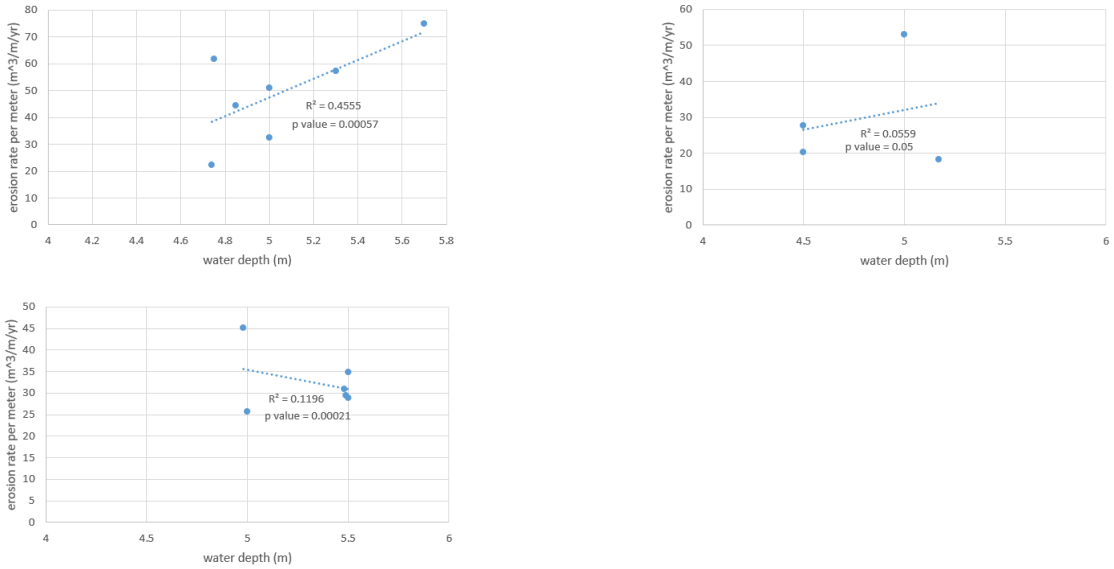

Figure C.2: the relation between water depth and erosion rate per meter of subset A, B and C

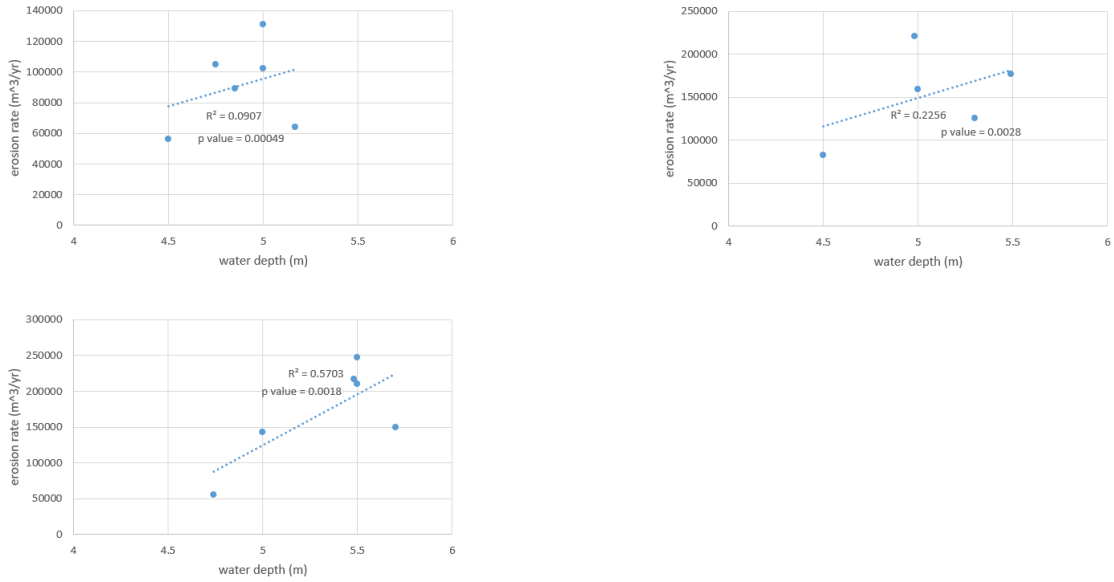

Figure C.3: the relation between water depth and erosion rate of subset D, E and F

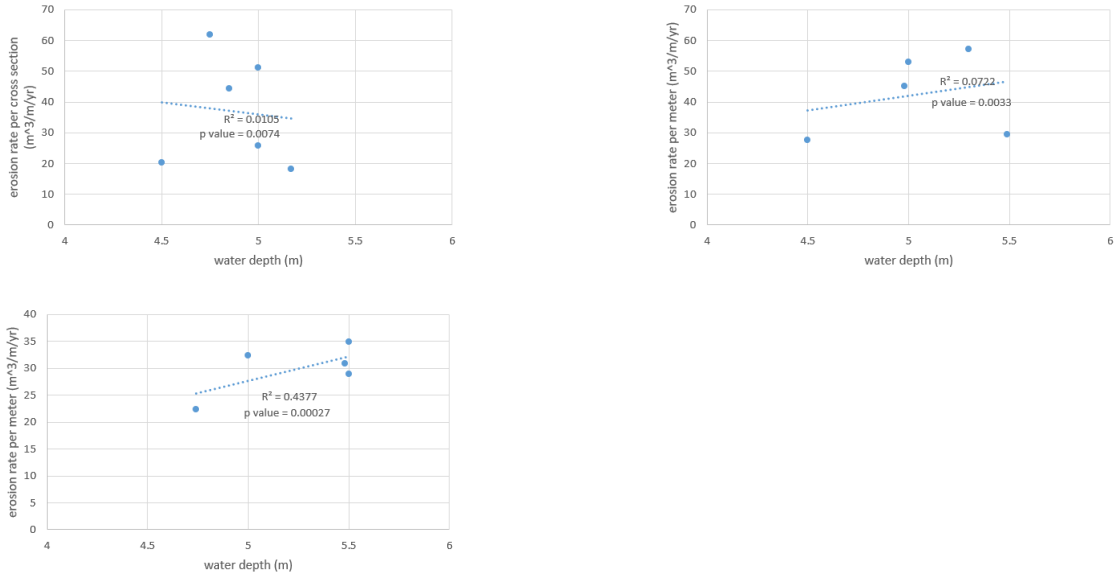

Figure C.4: the relation between water depth and erosion rate of subset D, E and F

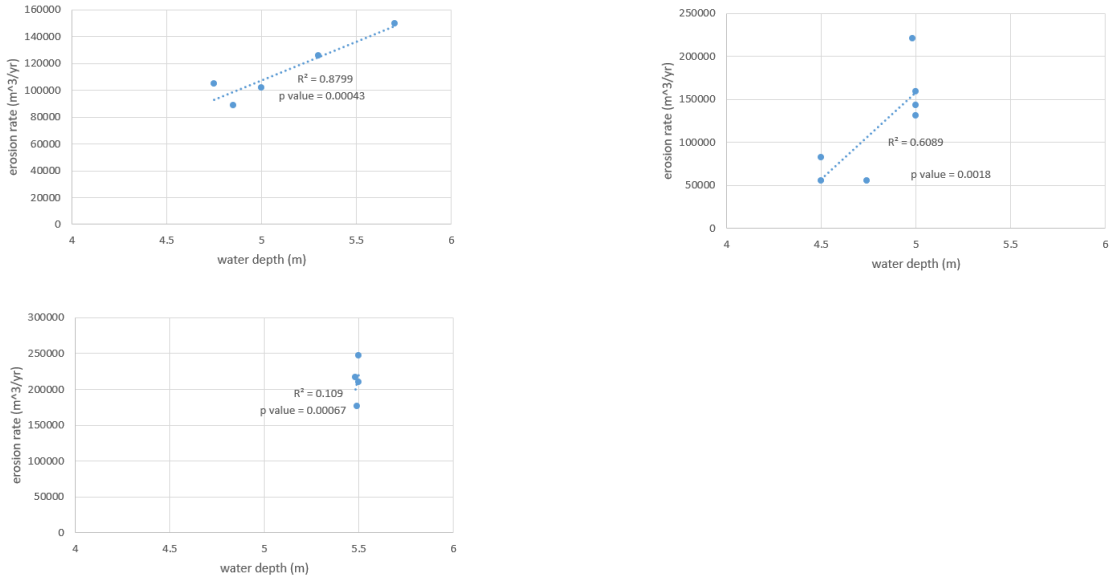

Figure C.5: the relation between water depth and erosion rate of subset G, H and I

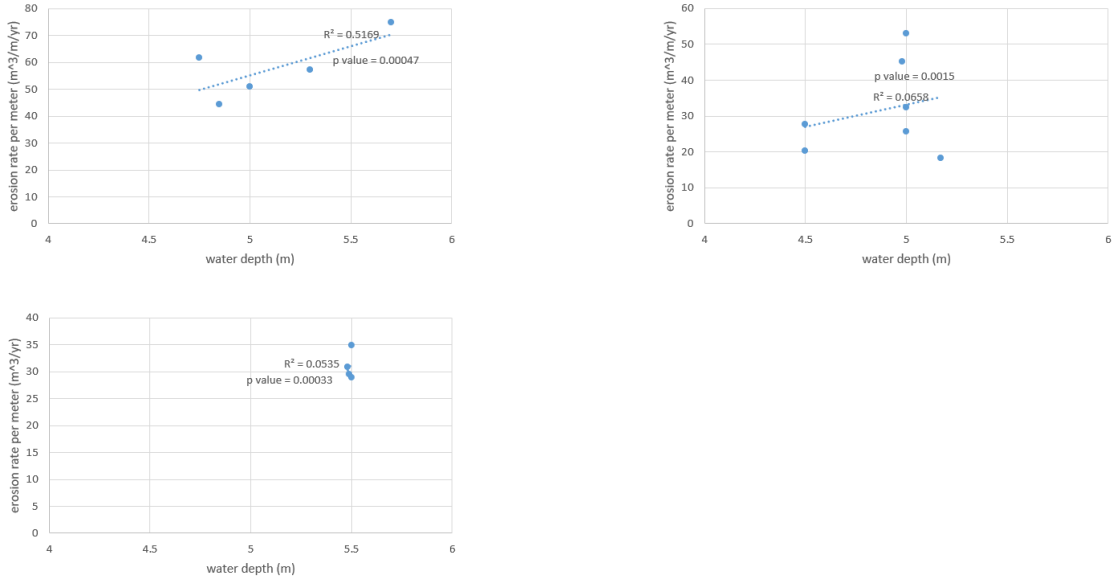

Figure C.6: the relation between water depth and erosion rate per meter of subset G, H and I

The relation between dimensionless wave height and erosion rate/ erosion rate per meter is shown as follows (Figure C.7 to Figure C.12):

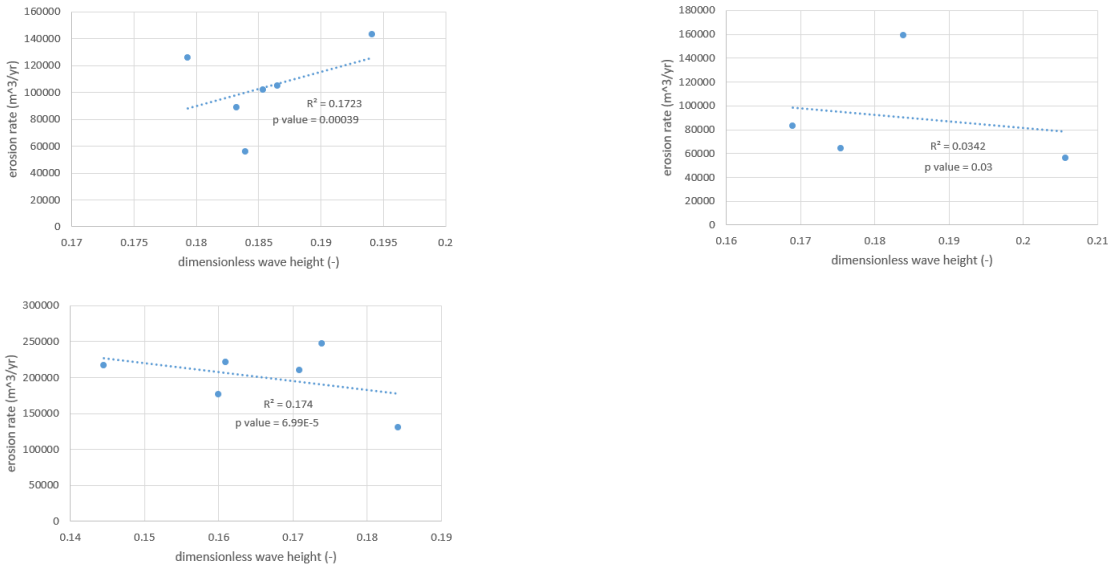

Figure C.7: the relation between dimensionless wave height and erosion rate of subset A, B and C

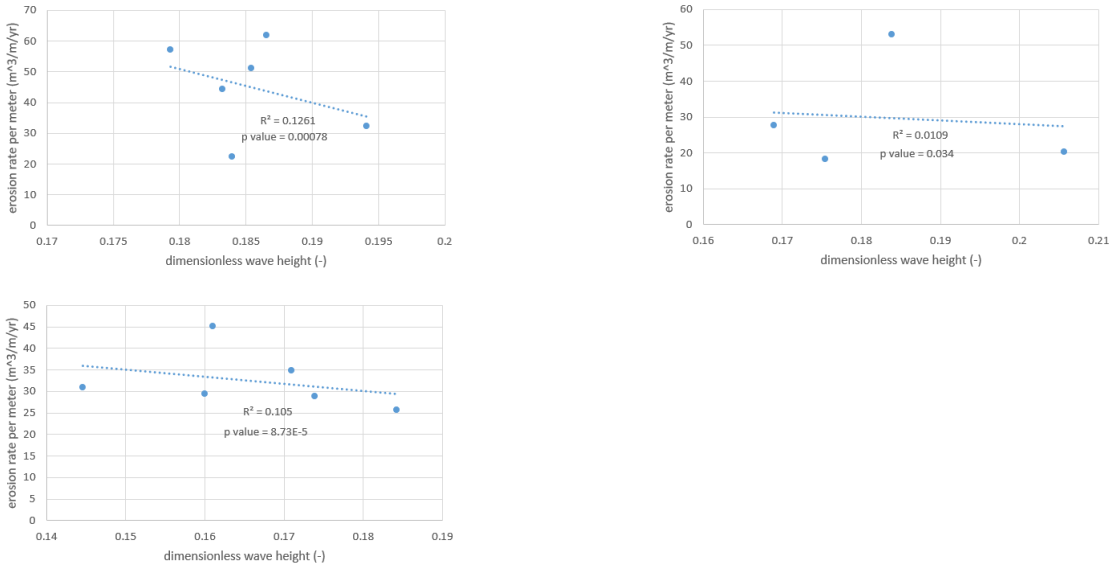

Figure C.8: the relation between dimensionless wave height and erosion rate per meter of subset A, B and C

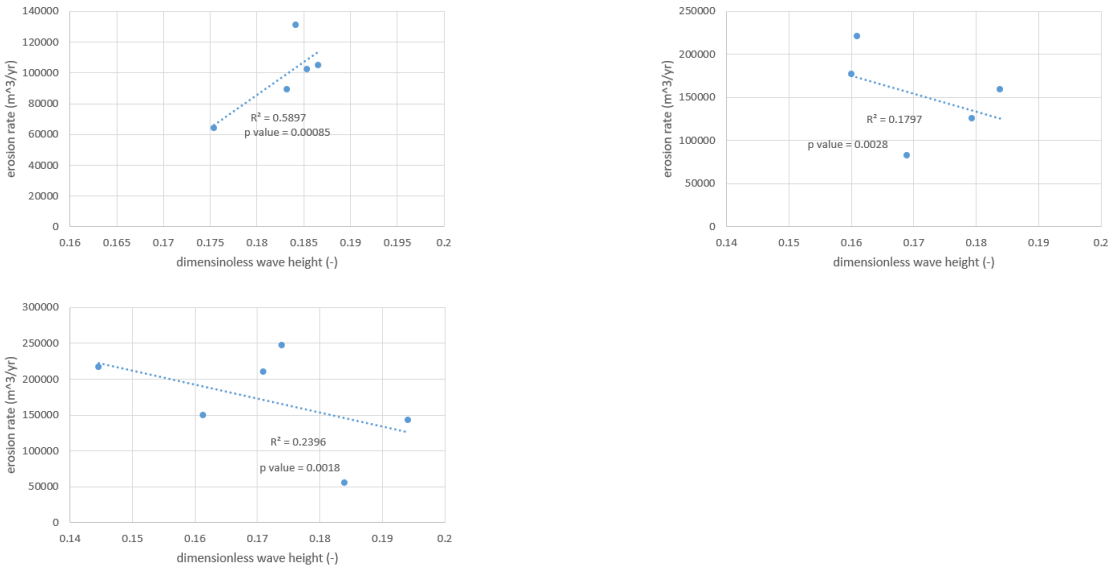

Figure C.9: the relation between dimensionless wave height and erosion rate of subset D, E and F

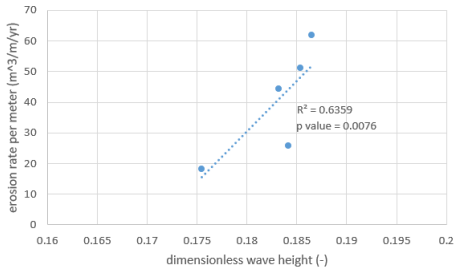

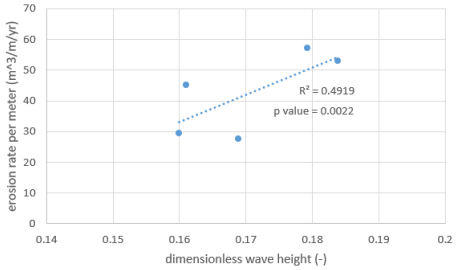

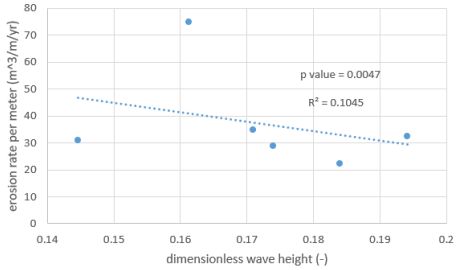

Figure C.10: the relation between dimensionless wave height and erosion rate per meter of subset D, E and F

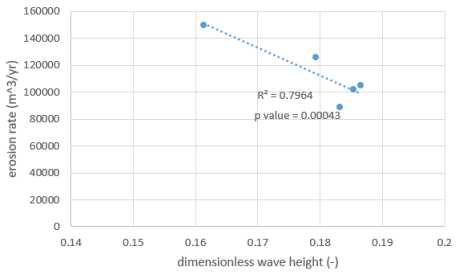

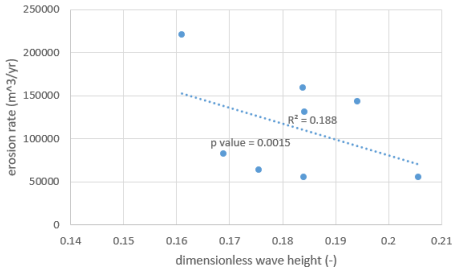

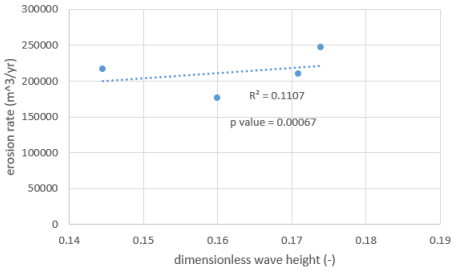

Figure C.11: the relation between dimensionless wave height and erosion rate of subset G, H and I

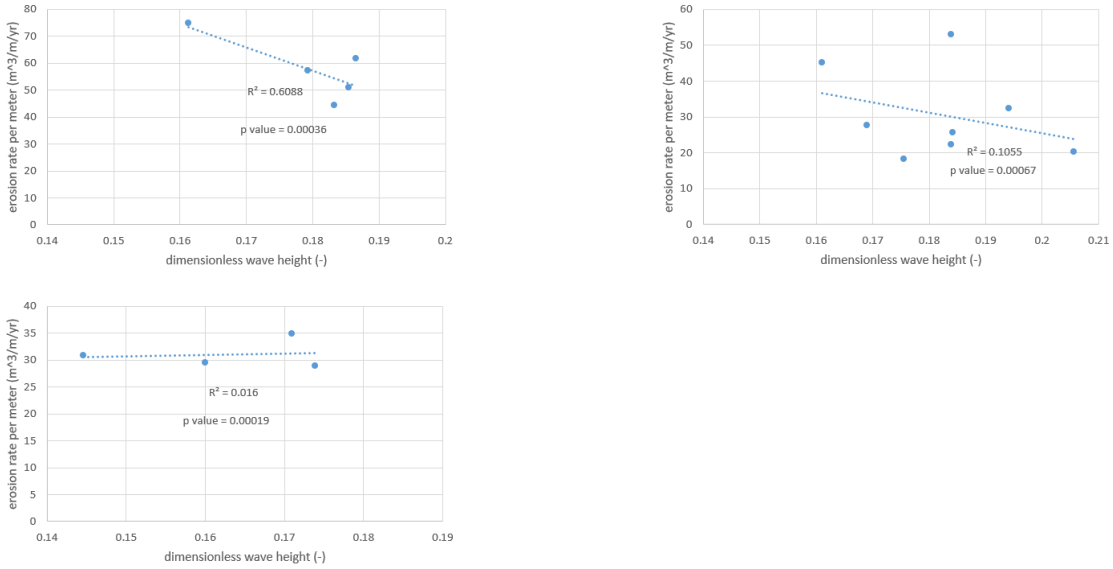

Figure C.12: the relation between dimensionless wave height and erosion rate per meter of subset G, H and I

Appendix D

Related graphs of geometrical conditions for each subset

In this appendix, the relation between erosion rate/ erosion rate per meter and nourishment size (length, volume per meter, volume and height) of each subset is presented (Figure D.1 to Figure D.18).

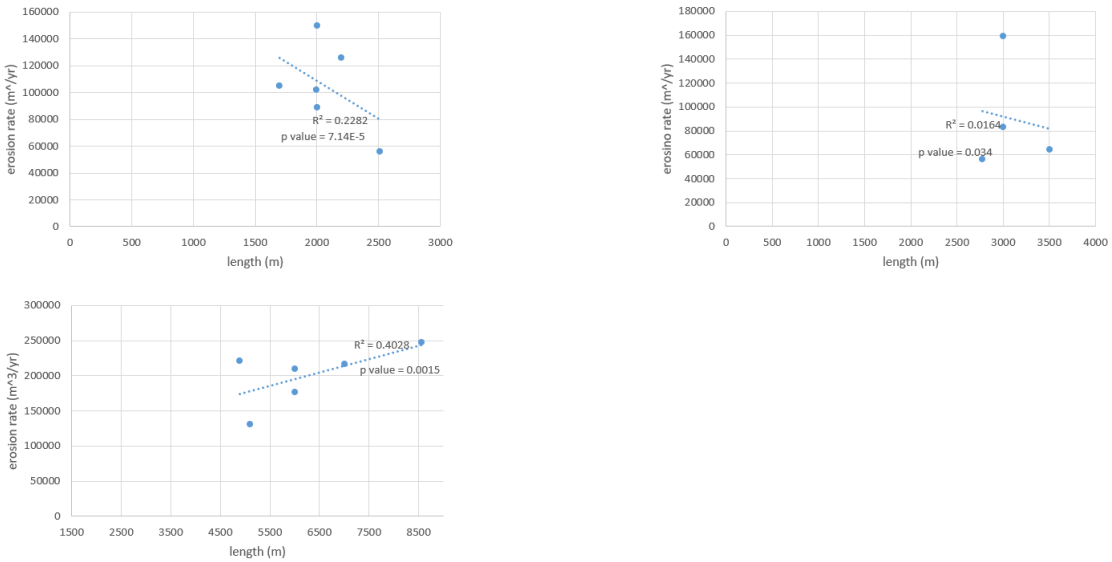

Figure D.1: the relation between length and erosion rate of subset A, B and C

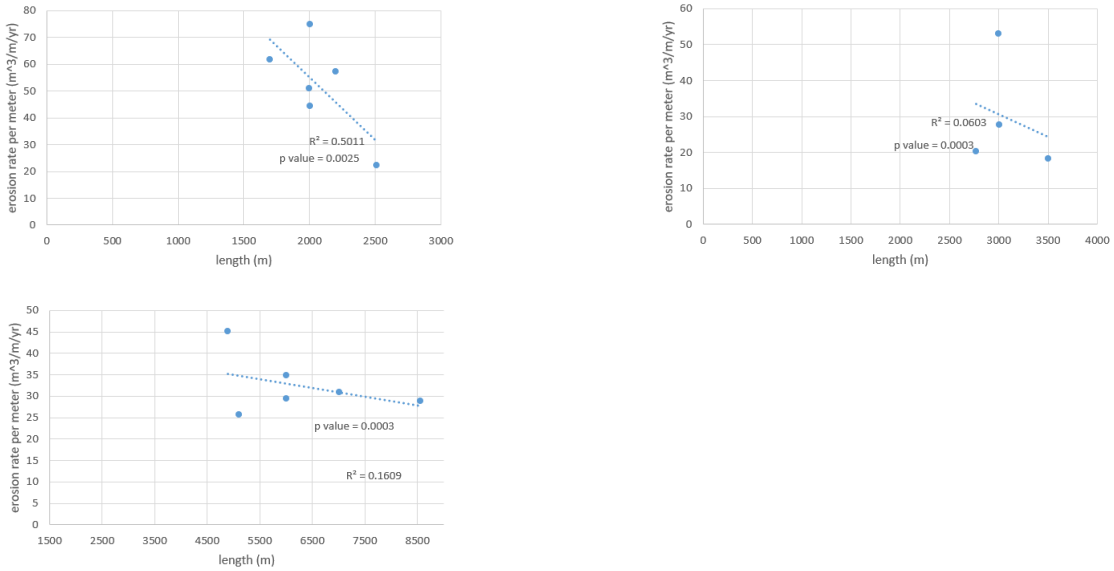

Figure D.2: the relation between length and erosion rate per meter of subset A, B and C

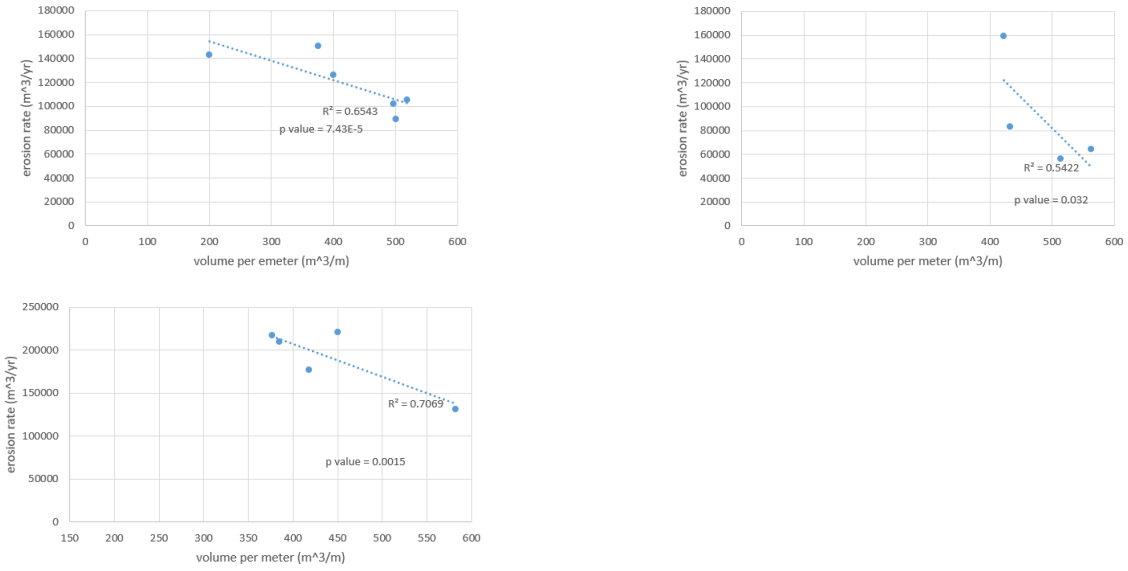

Figure D.3: the relation between volume per meter and erosion rate of subset A, B and C

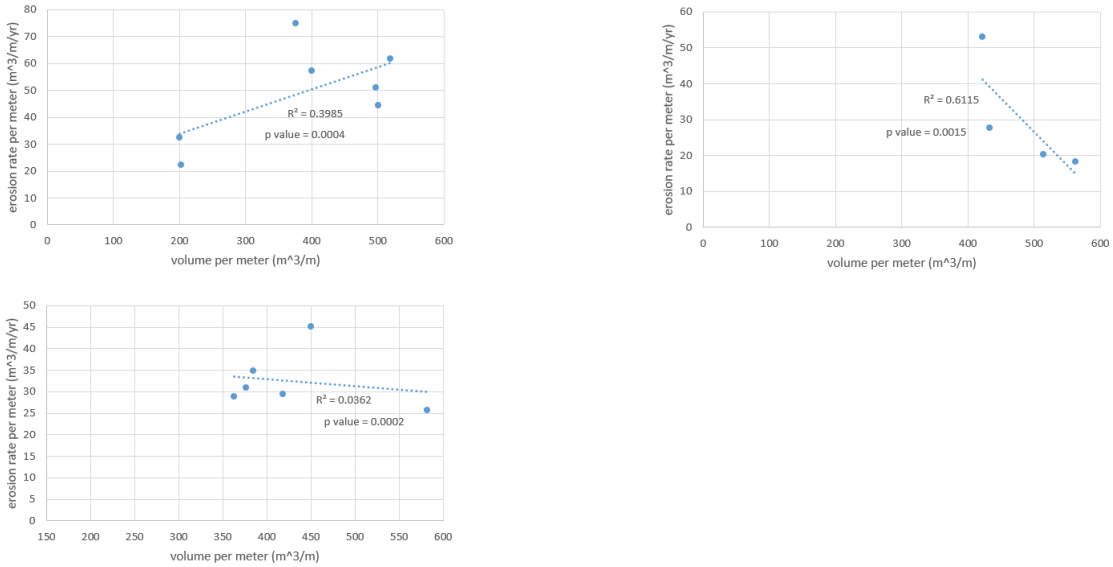

Figure D.4: the relation between volume per meter and erosion rate per meter of subset A, B and C

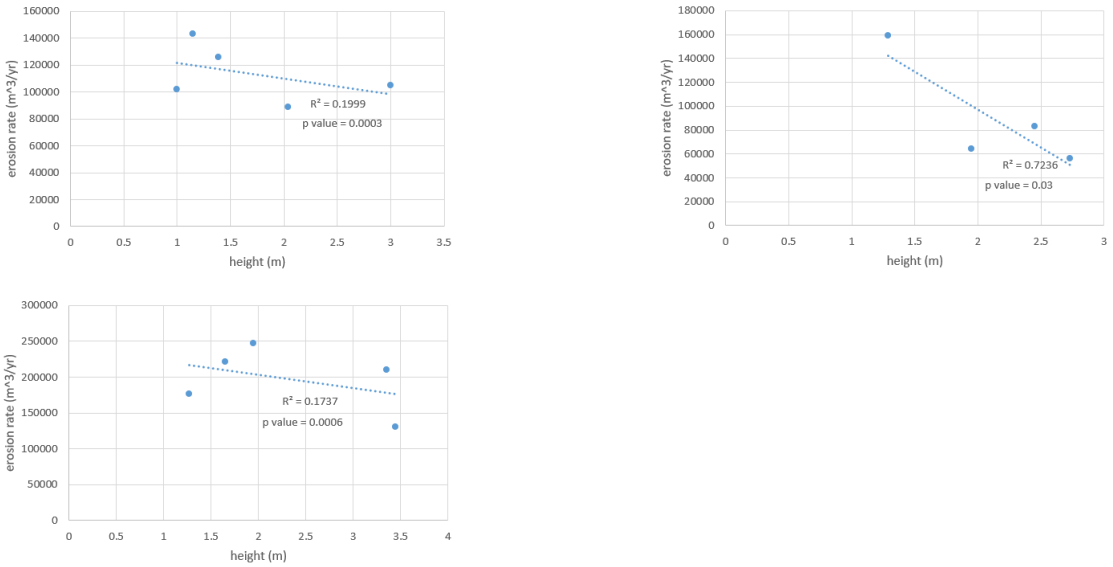

Figure D.5: the relation between height and erosion rate of subset A, B and C

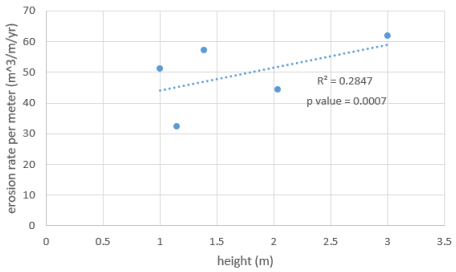

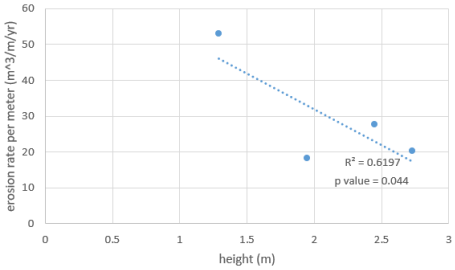

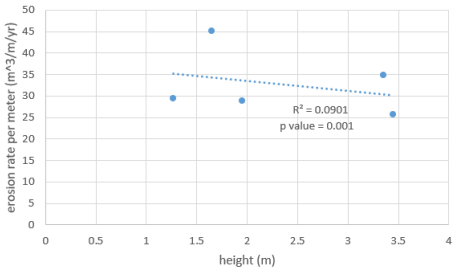

Figure D.6: the relation between height and erosion rate of subset A, B and C

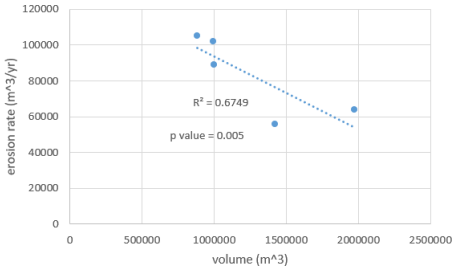

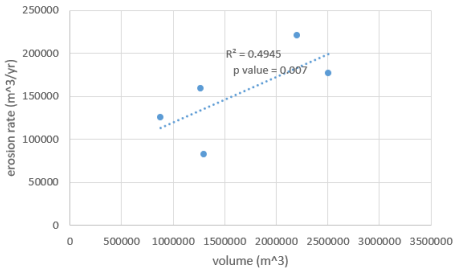

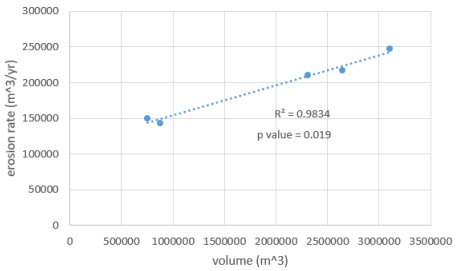

Figure D.7: the relation between volume and erosion rate of subset D, E and F

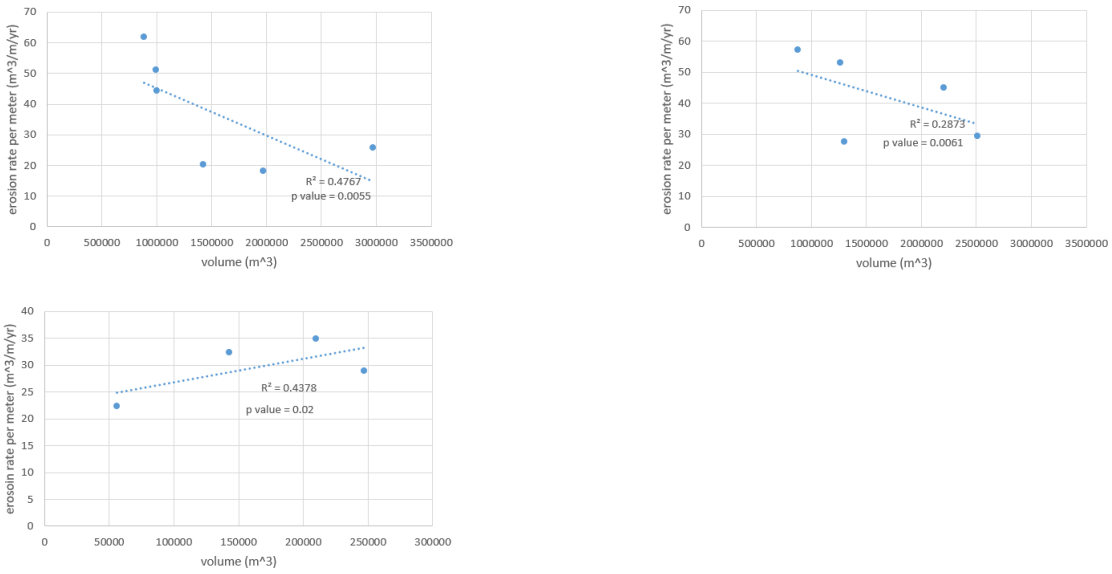

Figure D.8: the relation between volume and erosion rate per meter of subset D, E and F

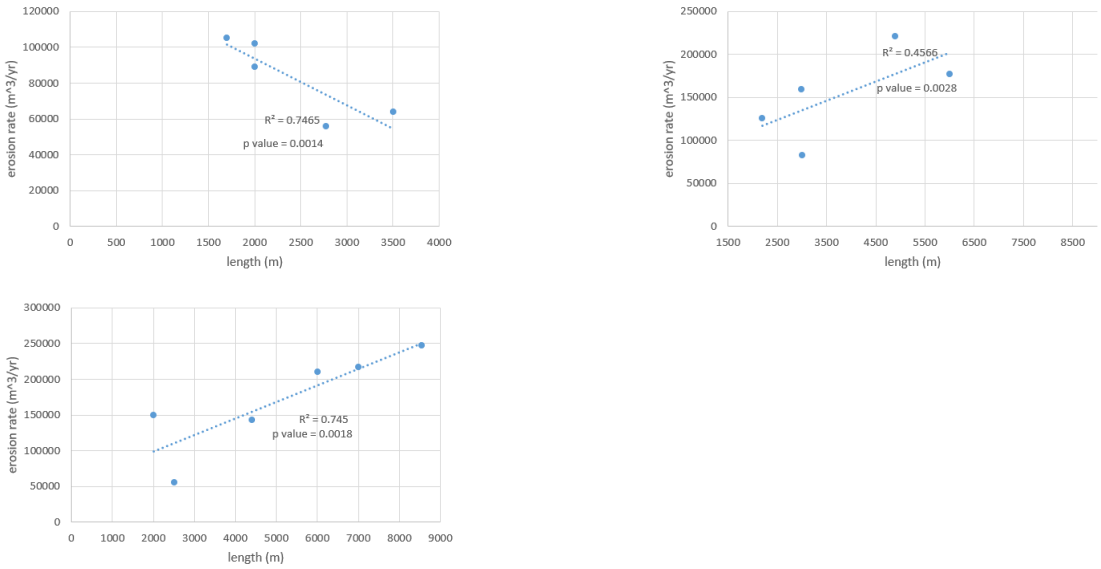

Figure D.9: the relation between length and erosion rate of subset D, E and F

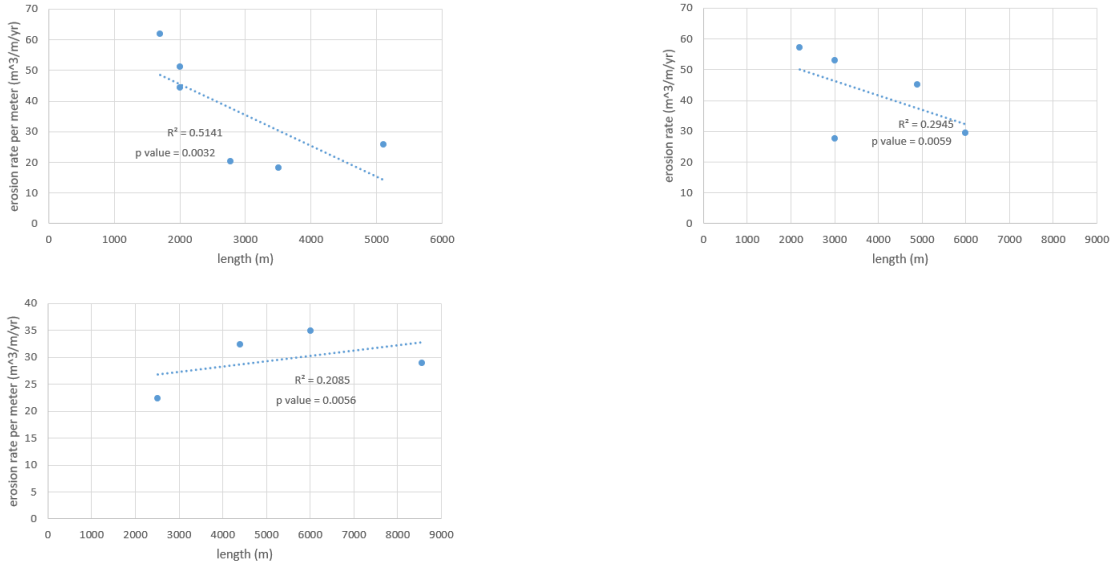

Figure D.10: the relation between length and erosion rate per meter of subset D, E and F

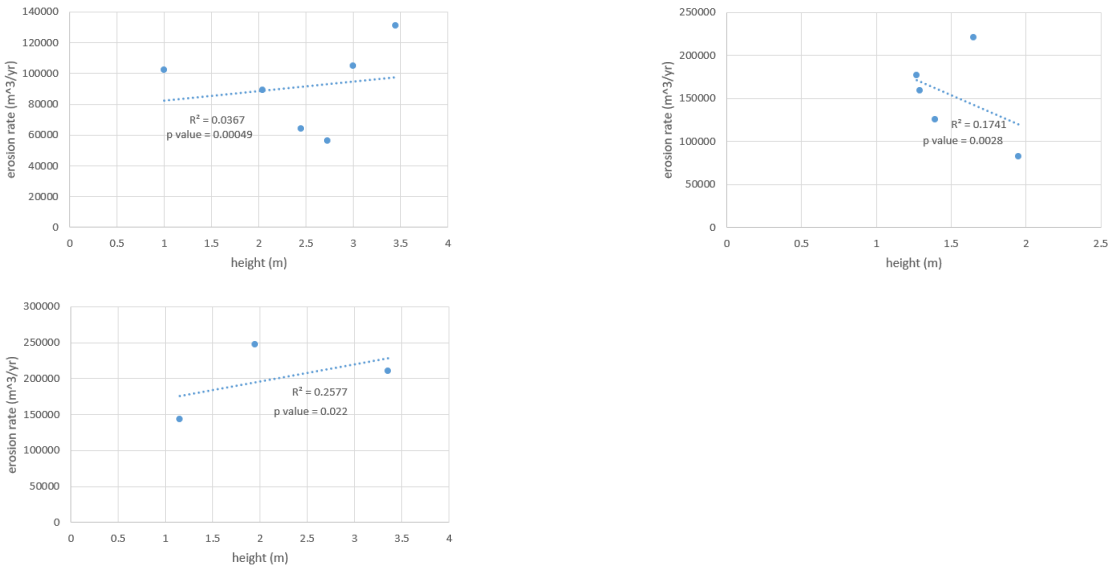

Figure D.11: the relation between height and erosion rate of subset D, E and F

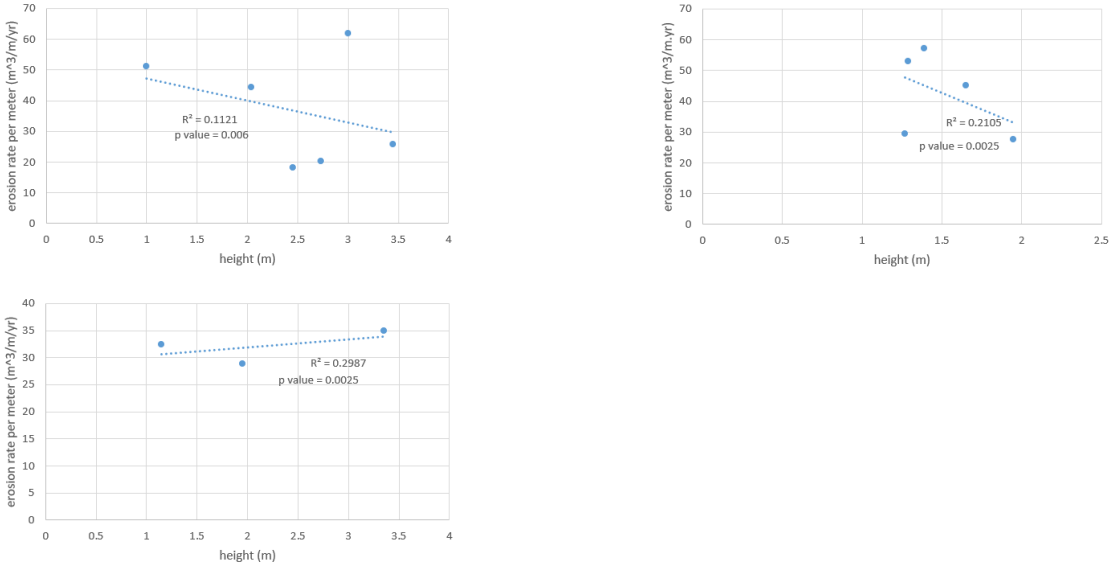

Figure D.12: the relation between height and erosion rate per meter of subset D, E and F

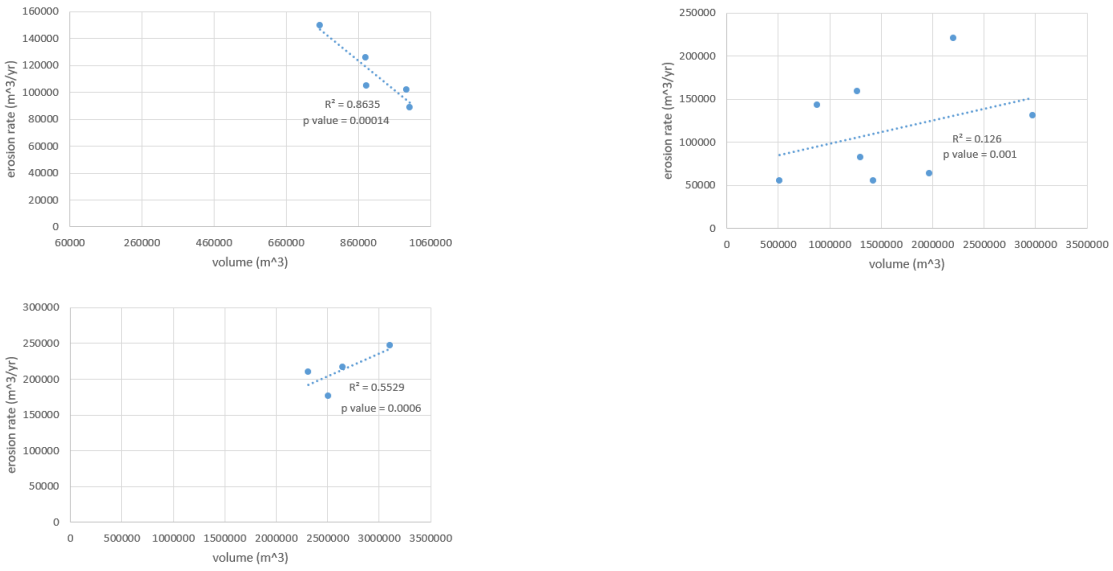

Figure D.13: the relation between volume and erosion rate of subset G, H and I

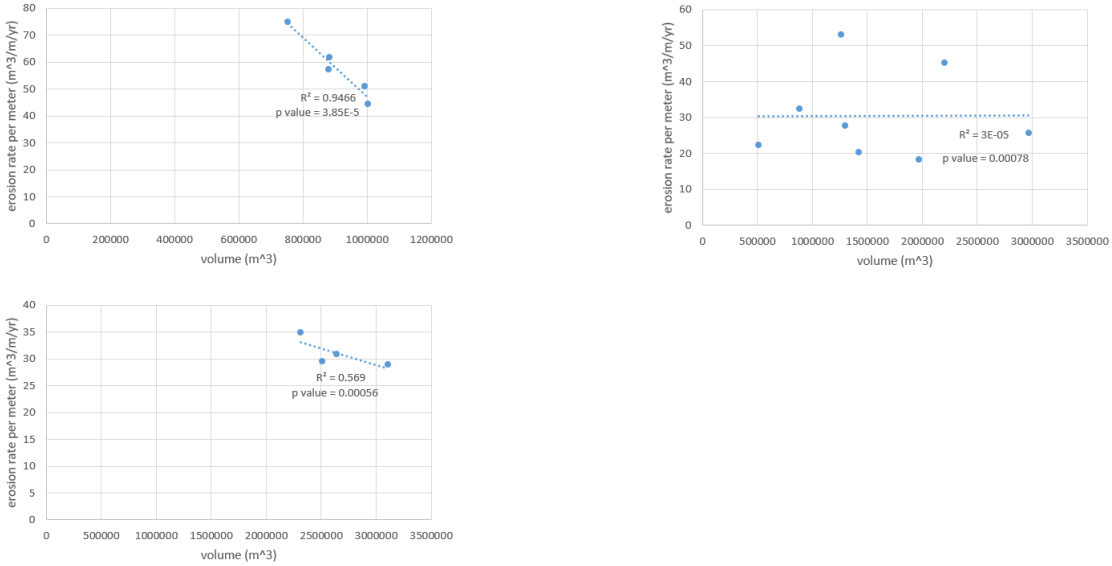

Figure D.14: the relation between volume and erosion rate per meter of subset G, H and I

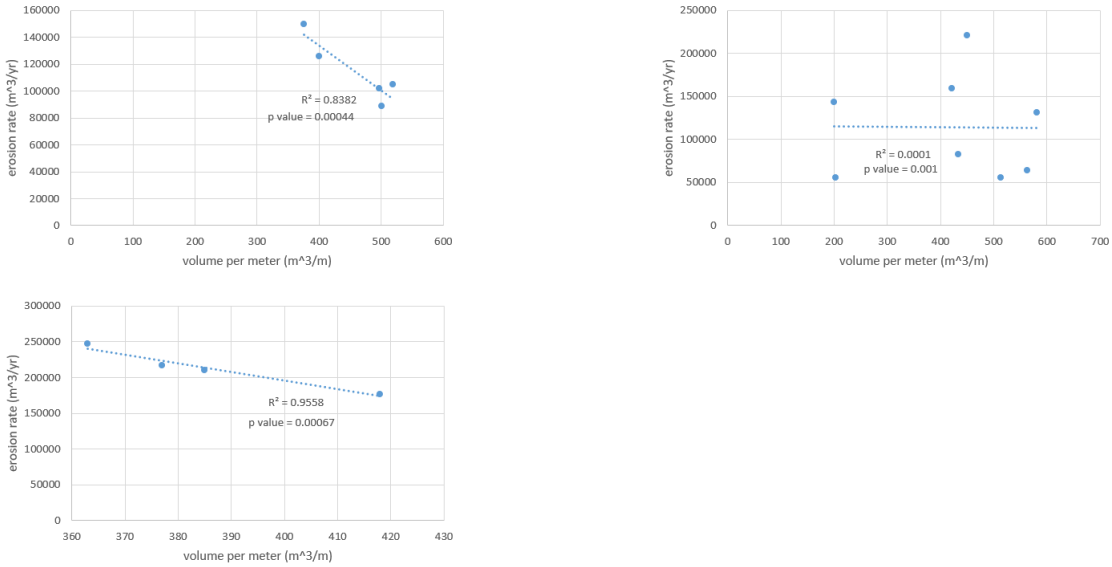

Figure D.15: the relation between volume per meter and erosion rate of subset G, H and I

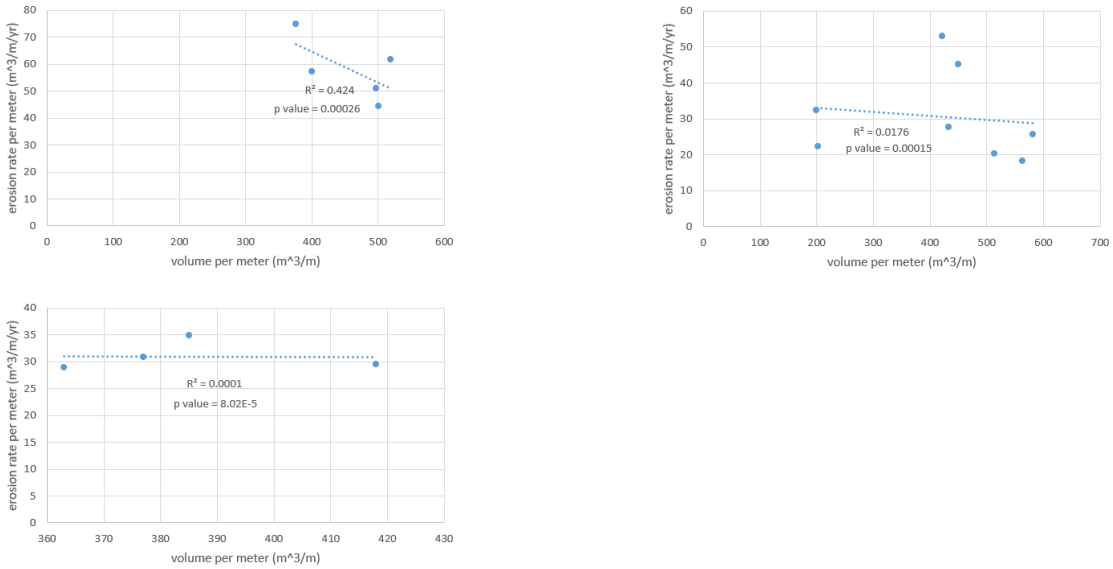

Figure D.16: the relation between volume per meter and erosion rate per meter of subset G, H and I

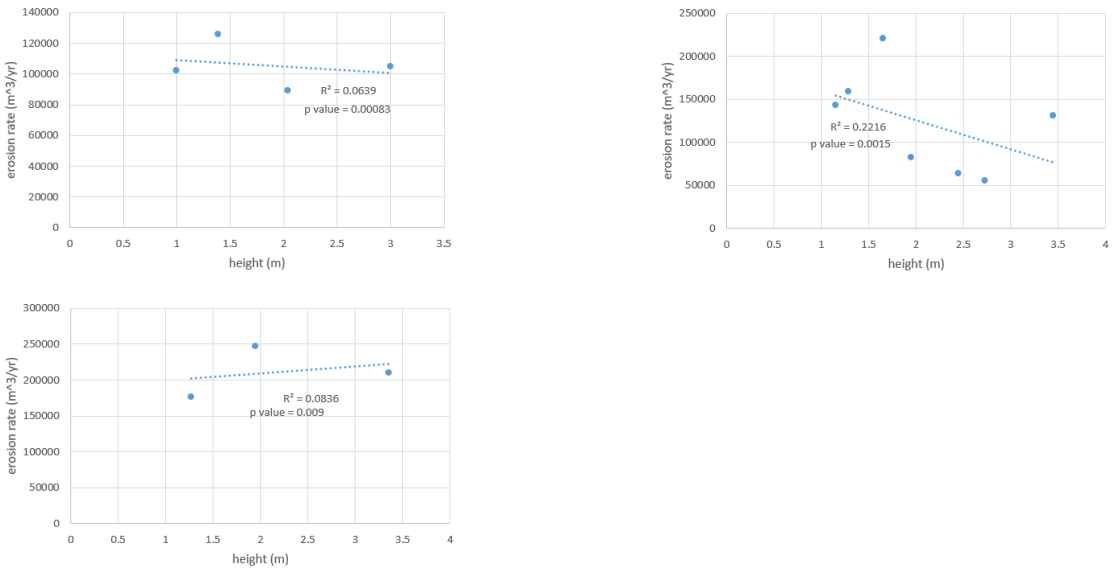

Figure D.17: the relation between height and erosion rate of subset G, H and I

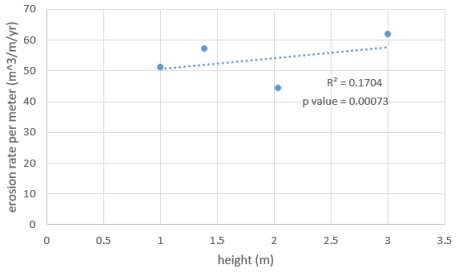

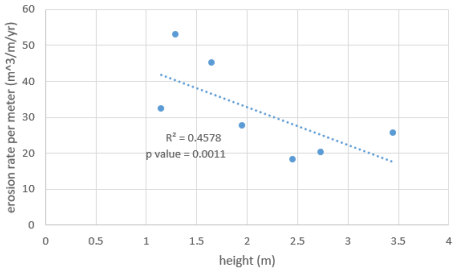

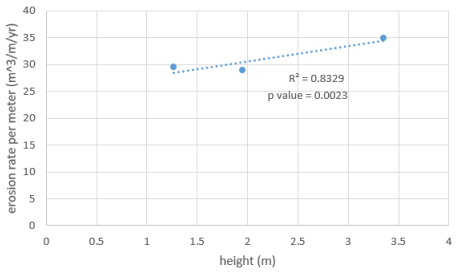

Figure D.18: the relation between height and erosion rate per meter of subset G, H and I

Appendix E

Outliers detection in linear regression

Table E.1: the Mahalanobis distance of each two related parameters of the Dutch shoreface nourishments

volume per meter/ erosion rate	volume per meter / erosion rate per meter	length/ erosion rate	length/ erosion rate per meter	volume/ erosion rate	volume/ erosion rate per meter	height/ erosion rate	height/ erosion rate per meter	water depth/ erosion rate	water depth/ erosion rate per meter	dimensionless wave height/ erosion rate	dimensionless wave height/ erosion rate per meter
0.71357	2.1039	2.41966	2.81776	2.45317	2.0444	-	-	3.90683	3.2374	3.99845	4.79925
0.79478	2.74295	1.46807	2.28463	0.76919	2.10854	1.48346	5.93946	1.03093	3.70801	0.48913	2.76675
2.19304	2.8943	1.16487	0.66359	4.68263	2.52734	2.88687	3.02468	0.06173	0.60472	0.32805	0.78928
4.37997	4.48297	0.08102	0.16928	1.49888	1.60599	1.17949	1.77026	0.07119	0.1877	2.3715	1.50853
0.19919	5.25672	3.2525	4.97526	2.3394	4.96599	-	-	2.86399	6.43963	1.34127	5.60409
0.00025	0.77688	1.53736	0.777	0.84799	0.77452	0.91188	1.57117	0.20679	0.97686	0.87073	1.13444
0.19092	0.39435	2.33674	2.37072	1.93743	1.46177	-	-	2.56808	1.72308	4.79998	5.32094
0.00285	0.35055	1.09962	1.05766	1.08989	1.10461	1.20937	1.788	1.50229	1.99652	1.28849	1.81458
0.06051	0.20458	2.84722	0.69939	1.95432	1.09696	2.10497	0.38043	2.10942	0.30488	1.99646	1.21283
4.26328	5.13869	2.13228	2.75855	2.14518	5.09648	2.28004	1.57678	2.41099	1.58741	1.90341	1.19319
0.52289	0.61193	0.89616	0.90304	0.71767	0.53902	0.65094	0.20445	0.93826	0.66275	0.63308	0.35045
0.00756	0.439	0.96891	1.14228	0.86271	1.0178	0.86273	0.6213	0.92155	0.57948	1.33995	0.44965
1.69817	3.44285	2.90902	2.3941	3.8453	1.64018	1.60551	2.05276	3.16264	3.76381	3.25103	1.89025
0.13112	0.17469	1.44236	1.12964	1.42702	0.69407	4.52244	2.54302	1.61716	0.484	2.58316	0.07519
0.04918	1.3379	1.31659	1.4015	1.01483	1.43055	0.70874	2.05134	0.08113	1.52378	0.39929	1.80299
0.47017	1.00223	0.95874	1.02239	0.57281	0.77201	2.15004	1.96624	1.84146	1.56164	0.75076	0.58312
0.32254	0.6455	5.16887	5.43321	3.84156	3.11979	3.44351	0.51013	6.70555	2.65833	3.65527	0.70444

Table E.2: the Mahalanobis distance of each two related parameters of subset A

ID	erosion rate / volume per meter	erosion rate per meter/ volume per meter	erosion rate/ length	erosion rate per meter/ length	erosion rate/ height	erosion rate per meter/ height	erosion rate/ water depth	erosion rate per meter/ water depth	erosion rate/ dimensionless wave height	erosion rate per meter/ dimensionless wave height
2	0.98365	0.98044	0.59416	0.70393	2.58148	2.52931	1.32355	3.82916	0.20098	2.2394
4	2.81606	1.85673	4.88974	4.91683	1.97212	2.18484	2.91911	1.34579	3.62011	1.45539
5	1.49382	3.66831	2.23393	2.31586	nan	nan	3.65463	3.61292	4.47975	4.13848
15	0.24957	0.24385	0.39159	0.19738	0.3891	1.2843	0.53953	0.53356	0.2483	0.19928
16	0.72892	0.94913	0.20762	0.22488	1.78401	1.27584	0.06769	0.09503	0.13433	0.33571
11	1.12507	1.82651	0.481	0.61513	1.27329	0.72572	0.43641	0.35069	0.42872	0.08835
10	4.6029	2.47503	3.20197	3.02598	nan	nan	3.05908	2.23284	2.88781	3.54338

Table E.3: the Mahalanobis distance of each two related parameters of subset B

ID	erosion rate/ volume per meter	erosion rate per meter/ volume per meter	erosion rate/ length	erosion rate per meter/ length	erosion rate/ height	erosion rate per meter/ height	erosion rate/ water depth	erosion rate per meter/ water depth	erosion rate/ dimensionless wave height	erosion rate per meter/ dimensionless wave height
1	0.55138	0.35841	1.67663	1.67279	1.02053	1.06352	0.9441	0.88745	0.9441	0.88745
6	2.17945	2.24197	2.12155	2.12455	2.1292	2.1642	2.13294	2.17828	2.13294	2.17828
12	1.62655	1.52858	2.12214	2.12133	2.21562	2.24516	2.1848	2.21006	2.1848	2.21006
13	1.64262	1.87104	0.07969	0.08133	0.63465	0.52713	0.73815	0.7242	0.73815	0.7242

Table E.4: the Mahalanobis distance of each two related parameters of subset C

ID	erosion rate/ volume per meter	erosion rate per meter/ volume per meter	erosion rate/ length	erosion rate per meter/ length	erosion rate/ height	erosion rate per meter/ height	erosion rate/ water depth	erosion rate per meter/ water depth	erosion rate/ dimensionless wave height	erosion rate per meter/ dimensionless wave height
3	3.56747	3.96058	2.98414	2.86267	2.48832	1.63437	3.19048	3.87487	3.38935	2.1578
7	0.50027	0.54058	0.31255	0.30805	-	-	0.37888	0.35686	2.46512	2.99072
8	1.90101	0.24143	0.38055	0.35381	2.09153	1.74797	1.34191	0.45733	0.86012	0.54402
9	2.1093	3.74898	3.21076	3.45798	0.53937	2.63781	3.29832	3.91515	0.27577	3.43604
14	0.51381	0.35975	0.24037	0.12602	1.63289	1.39467	0.46077	0.84252	0.32497	0.3917
17	1.40814	1.14868	2.87163	2.89146	1.24788	0.58518	1.32964	0.55328	2.68468	0.47972

Table E.5: the Mahalanobis distance of each two related parameters of subset D

ID	erosion rate/ volume	erosion rate per meter/ volume	erosion rate/ length	erosion rate per meter/ length	erosion rate/ height	erosion rate per meter/ height	erosion rate/ water depth	erosion rate per meter/ water depth	erosion rate/ dimensionless wave height	erosion rate per meter/ dimensionless per meter
1	1.66783	1.98573	1.69791	1.88685	1.93947	0.86455	3.26651	3.8078	4.10453	4.01230
2	1.29491	1.96192	1.41206	1.94702	0.56588	3.28692	0.78084	2.0969	0.27079	1.96105
11	0.4632	0.45016	0.44519	0.44138	0.22478	0.28979	0.01648	0.16309	0.16567	0.24497
16	0.86165	0.65066	0.7986	0.63373	3.38685	2.91936	0.32874	0.97276	0.15146	0.61220
3	4.01232	3.81372	4.01364	3.90756	2.89214	1.43496	2.05592	0.5697	2.10597	0.47331
13	1.73636	1.13782	1.6326	1.18346	0.99088	1.20442	3.55151	2.38974	3.31905	2.72126

Table E.6: the Mahalanobis distance of each two related parameters of subset E

ID	erosion rate/ volume	erosion rate per meter/ volume	erosion rate/ length	erosion rate per meter/ length	erosioin rate/ height	erosion rate per meter/ height	erosion rate/ water depth	erosion rate per meter/ water depth	erosion rate/ dimensionless wave height	erosion rate per meter/ dimensionless wave height
6	0.74538	0.63798	0.66959	0.63446	0.632	0.83651	0.06221	0.74651	2.02266	1.546
8	1.99341	1.74446	2.35165	1.99902	0.70527	3.00968	1.35502	3.09961	0.9834	1.15765
9	1.7072	1.29144	1.76197	0.9509	2.9709	0.44177	2.54943	0.10119	1.83957	2.21086
15	1.306	1.53087	1.12018	1.44614	0.75798	1.19083	1.32284	1.3443	0.69438	1.1881
12	2.24802	2.79525	2.09661	2.96948	2.93385	2.5212	2.7105	2.70838	2.45999	1.89739

Table E.7: the Mahalanobis distance of each two related parameters of subset F

ID	erosion rate/ volume	erosion rate per meter/ volume	erosion rate/ length	erosion rate per meter/ length	erosion rate/ height	erosion rate per meter/ height	erosion rate/ water depth	erosion rate per meter/ water depth	erosion rate/ dimensionless wave height	erosion rate per meter/ dimensionless wave height
4	1.02504	0.82022	0.18441	0.28209	1.33333	1.33333	0.91777	0.8809	1.78494	1.73406
10	4.0575	2.55611	3.47976	3.12886	-	-	2.99834	2.55677	2.75779	0.88493
17	1.59697	1.58615	1.82632	1.86697	1.33333	1.33333	1.50465	1.17482	1.84049	0.19321
14	0.33068	0.30372	0.39701	0.13252	1.33333	1.33333	0.33493	0.55228	0.40797	0.02104
5	2.20893	4.01332	3.54835	4.02748	-	-	3.77902	4.02721	0.79307	3.95264
7	0.78089	0.72047	0.56415	0.56209	-	-	0.46528	0.80802	2.41574	3.21412

Table E.8: the Mahalanobis distance of each two related parameters of subset G

ID	erosion rate/ volume	erosion rate per meter/ volume	erosion rate/ volume per meter	erosion rate per meter/ volume per meter	erosion rate/ height	erosion rate per meter/ height	erosion rate/ water depth	erosion rate per meter/ water depth	erosion rate/ dimensionless wave height	erosion rate per meter/ dimensionless wave height
2	2.46096	0.50269	2.10663	2.36668	1.80293	2.07404	3.07512	3.09874	0.80081	2.5448
5	2.26213	2.17874	2.2788	2.32535	-	-	2.31614	2.58671	2.98495	3.01809
11	1.12736	1.78259	1.78056	1.40158	1.1628	2.12	1.85007	1.4186	2.63328	2.03309
15	0.62252	1.35768	1.48859	1.49204	1.82962	0.83462	0.23646	0.54027	1.21578	0.00831
16	1.52703	2.17829	0.34542	0.41436	1.20464	0.97135	0.52222	0.35569	0.36517	0.39571

Table E.9: the Mahalanobis distance of each two related parameters of subset H

ID	erosion rate/ volume	erosion rate per meter/ volume	erosion rate/ volume per meter	erosion rate per meter/ volume per meter	erosion rate/ height	erosion rate per meter/ height	erosion rate/ water depth	erosion rate per meter/ water depth	erosion rate/ dimensionless wave height	erosion rate per meter/ dimensionless wave height
1	0.98594	0.74863	1.33825	1.00069	1.33614	0.86865	2.18102	2.27107	2.89376	2.91243
4	1.48429	0.77786	2.46356	2.25043	1.34651	2.27998	0.37019	0.30603	1.63161	0.91163
9	3.25975	1.99251	3.2731	1.47693	2.86424	1.09679	3.39937	1.37791	3.88465	2.77544
12	0.29997	0.15407	0.27928	0.04501	0.75407	0.3253	2.09132	2.10925	1.95893	1.19096
6	1.05306	3.43821	0.56885	3.32915	0.97778	2.74324	0.61902	3.27456	0.81693	3.86196
13	1.47181	1.30062	1.61961	1.73246	0.98048	1.26797	4.07933	3.52496	1.58426	1.76332
3	3.34678	3.35567	1.28304	1.24792	3.74078	3.41806	0.30509	0.60262	0.16976	0.13422
10	2.0984	2.23244	3.1743	2.91743	-	-	0.95466	0.5336	1.06009	0.45004

Table E.10: the Mahalanobis distance of each two related parameters of subset I

ID	erosion rate/ volume	erosion rate per meter/ volume	erosion rate/ volume per meter	erosion rate per meter/ volume per meter	erosion rate/ height	erosion rate per meter/ height	erosion rate/ water depth	erosion rate per meter/ water depth	erosion rate/ dimensionless wave height	erosion rate per meter/ dimensionless wave height
7	0.04688	0.00003	1.22218	0.14226	-	-	2.08081	1.81452	2.19024	1.83014
8	2.16126	2.00478	2.16542	2.21903	1.33333	1.33333	1.57323	0.50806	1.61142	0.5061
14	1.84052	2	0.36697	2.01581	1.33333	1.33333	0.75457	2.20161	0.52438	2.20335
17	1.95134	1.99518	2.24543	1.6229	1.33333	1.33333	1.59139	1.47581	1.67396	1.46041

Table E.11: the Mahalanobis distance between mobility parameter and erosion rate/ erosion rate per meter of combined Dutch and international case

location	erosion rate/ mobility parameter	erosion rate per meter/ mobility parameter
Silver Strand State Park, CA	3.51291	0.04937
Perdido Key, FL	1.42135	0.71112
Ocean beach	5.04289	4.97095
Rijnland-Noordwijk	1.23642	0.49891
Noord-Holland-Egmond	0.10035	0.30271
Noord-Holland-Bergen	0.19363	0.36014
New River Inet	0.49245	5.10682

Table E.12: the Mahalanobis distance between dimensionless wave height and erosion rate/ erosion rate per meter of combined Dutch and international case

location	erosion rate/ dimensionless wave height	erosion rate per/ dimensionless wave height
Delfland-Scheveningen	2.70897	2.64686
Delfland-Terheijde	0.4753	0.44185
Delfland-Terheijde	0.04525	0.33445
Delfland-Monster	0.44197	0.67548
Rijnland-Katwijk	0.35524	0.35891
Rijnland-Noordwijk	0.19589	0.12134
Rijnland-Noordwijkerhout	2.64058	2.01027
Rijnland-Wassenaar	0.54844	0.49536
Rijnland-Zandvoort	1.57702	0.40307
Rijnland-ZandvoortZuid	1.4067	0.3776
Rijnland-Bloemendaal	0.491	0.17724
Noord-Holland-camperduin	1.13902	0.42374
Noord-Holland-callantsoog	1.13958	0.18514
Noord-Holland-Egmond	0.05605	0.10135
Noord-Holland-Bergen	0.50603	0.50799
Noord-Holland-Bergen&Egmond	2.62682	0.23313
Noord-Holland-julianadorp	0.79333	0.24178
South Padre Island, Texas	9.60309	6.92171
Silver Strand State Park, CA	3.2466	2.0102
Perdido Key, FL	3.27217	3.25506
Brunswick, GA (Mound "C")	6.86415	3.6413
Ocean beach	3.57797	3.68453
New River Inlet, NC	0.28881	14.75163

Appendix F

Detailed calculation method

F.1. Wave period

The wave period for different wave scenarios in the modelling test is calculated in the following steps (Equation F.1, Equation F.2). The wave length at deep water is calculated by keeping the wave steepness is approximately to 2.5 % Equation F.1:

$$\frac{H}{L} = 2.5\% \tag{F.1}$$

Then wave period can be calculated through the formulation of the wave length in deep water (Equation F.2):

$$L = \frac{gT^2}{2\pi} \tag{F.2}$$

F.2. Depth of closure

The depth of closure along the Dutch coast is calculated to associate with the numerical data. The yearly-significant wave height between 1987 and 2002 at Euro platform is used for calculation (Table 3.3). The corresponding peak wave period is presented in Table F.1.

Table F.1: the peak wave period at Euro platform

year	peak wave period (s)
1987	3.98
1988	4.1
1989	4.33
1990	4.55
1991	4.38
1992	4.41
1993	4.46
1994	4.44
1995	4.47
1996	4.43
1997	4.31
1998	4.55
1999	4.46
2000	4.28
2001	4.35
2002	4.28

The average value of significant wave heights at Euro platform between 1987 and 2002 is equal to 1.26m and the associated standard deviation is equal to 0.073m. The average value of the mean significant wave period between 1987 and 2002 is equal to 4.36s and the sediment diameter is equal to 0.0002m. According to Equation 2.1 and Equation 2.2, the inner and outer depth of closure is equal to 3.32 m and 16.9 m, respectively.

Appendix G

Detailed explanation of model results

Figure 5.3 shows that an abrupt change of the wave heights is observed at the tips of the nourishment. This is mainly due to the wave refraction. Waves tend to refract to the 'finite-length' nourishment over the side slope.

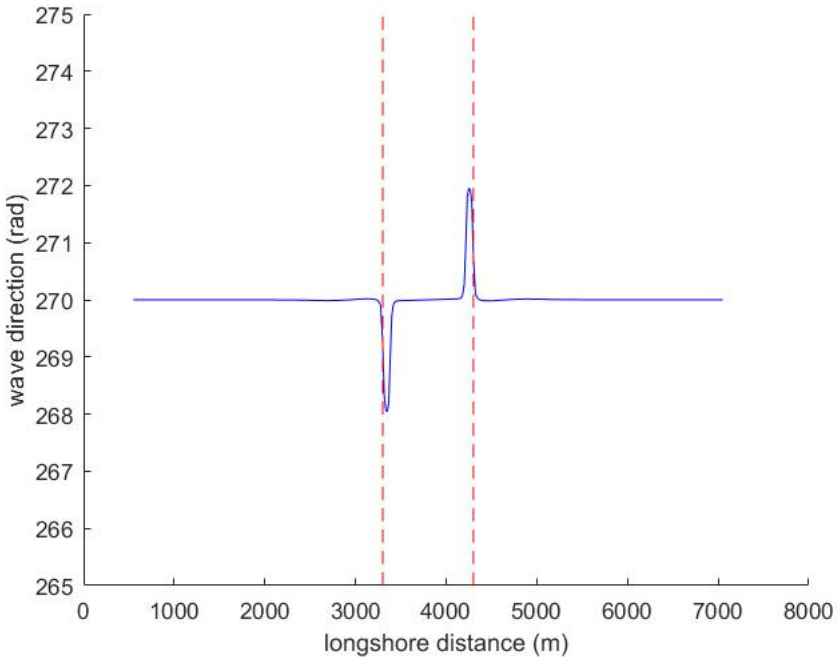

Figure G.1: wave angle at the location of x=2766.7 m, red dotted line is the location of the nourishment in the longshore direction

Figure G.1 shows that the wave angle is varying around the edge area of the nourishment. Waves are refracting to the nourishment over the side slope. It indicates that waves are concentrated at the tip of the nourishment crest. Consequently, wave heights are getting higher as well.

Figure 5.8 shows that the water level around the nourishment area is smaller than the deeper area just next to the nourishment at x= 2600m (at the offshore side of the nourishment crest). It is not the same as the expected result. Due to the horizontal circulation, currents in the ripple channel return back to the nourishment at the offshore side of the

nourishment. Then onshore currents are generated at the seaward area of the nourishment (Figure G.2). Figure G.3 shows that the cross shore velocity and longshore velocity is increasing at the extended seaward area of the nourishment (at x= 2375m). According to Bernoulli's equation ($\frac{u^2}{2g} + h = constant$), an increasing current velocity results in a lower elevation head. As a result, the water level has already decreased at the offshore side of the nourishment. That could be the reason why the water level around the nourishment area is lower than the deeper area just next to the nourishment at x= 2600m (at the offshore side of the nourishment crest).

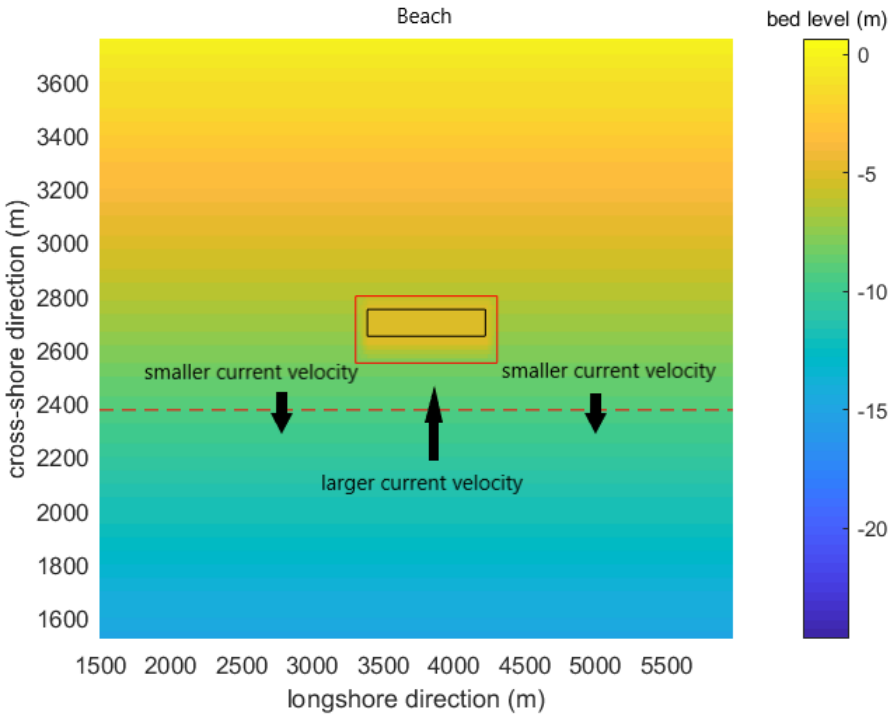

Figure G.2: schematization of currents flow at x= 2375m (red dotted line is the location of x= 2375m, black arrow represents the current direction, red box is the location of the nourishment, black box is the location of the nourishment crest, black arrow represents the current direction)

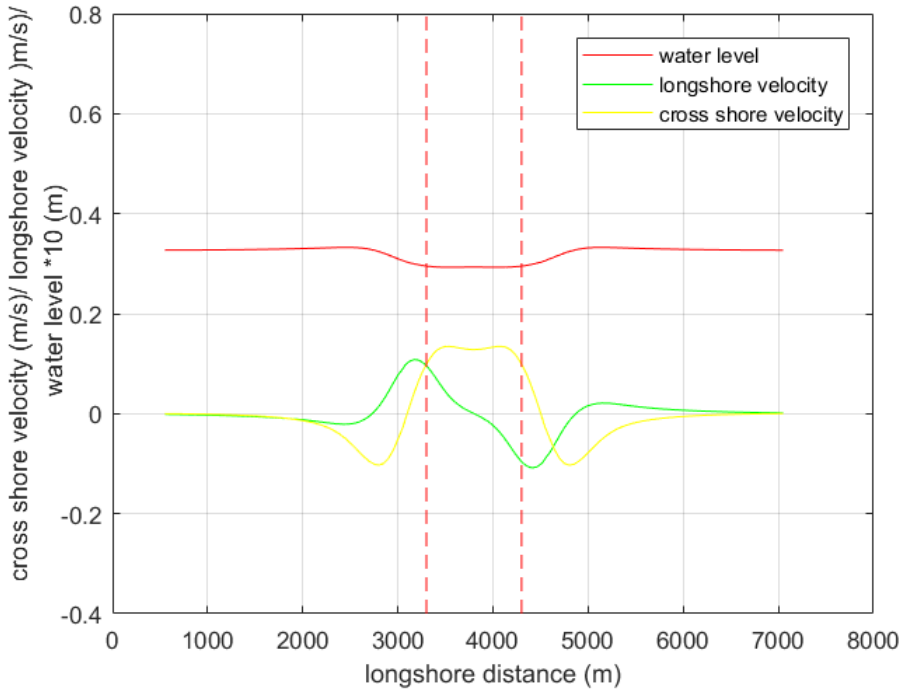

Figure G.3: combined results of water level and current velocity at x= 2375m (red dotted line is the extended seaward area of the nourishment in the longshore direction, water level is amplified by a factor of 10)

Figure 5.11 shows that an abrupt change of the longshore sediment transport at x= 2766.7m is observed at the tip of the nourishment. The longshore velocity induces the associated longshore sediment transports, consequently the longshore sediment transport has a nearly same patter as the longshore velocity. However, there is an abrupt change at x= 2766.7 which is not the case for the longshore velocity. According to Equation G.1, the longshore sediment transport is also depended on the sediment concentration. Waves could influence the sediment concentration. The wave heights also have an abrupt change at the tip of the nourishment which could lead to a lower sediment concentration and the associated longshore sediment transport.

$$q_y = \frac{\partial hCv^E}{\partial y} + \frac{\partial D_h h \frac{\partial C}{\partial y}}{\partial y} \tag{G.1}$$

Bibliography

John P Ahrens and Edward B Hands. Parameterizing beach erosion/accretion conditions. In *Coastal Engineering 1998*, pages 2382–2394. 1999.

James A Aidala, Cheryl E Burke, and T Neil McLellan. Hydrodynamic forces and evolution of a nearshore berm at south padre island, texas. *US Army Research*, page 76, 1992.

Patrick L Barnard, Li H Erikson, Jeff E Hansen, and Edwin Elias. The performance of nearshore dredge disposal at ocean beach, san francisco, california, 2005-2007. Technical report, US Geological Survey, 2009.

Tanya M Beck, Julie D Rosati, and James Rosati. An update on nearshore berms in the corps of engineers: Recent projects and future needs. Technical report, ARMY CORPS OF ENGINEERS VICKSBURG MS ENGINEER RESEARCH AND DEVELOPMENT CENTER, 2012.

Boers. Overview of historical pits, trenches and dump sites on the ncs. *SANDPIT: Sand Transport and Morphology of Offshore Sand Mining Pits. Process knowledge and guidelines for coastal management. End document May*, 2005.

M Bougdanou. Analysis of the shoreface nourishments, in the areas of ter heijde, katwijk and noordwijk. 2007.

RJ Bruins. Morphological behaviour of shoreface nourishments along the dutch coast: Data analysis of historical shoreface nourishments for a better understanding and design. 2016.

Ben de Sonneville and Ad Van der Spek. Sediment-and morphodynamics of shoreface nourishments along the north-holland coast. *Coastal Engineering Proceedings*, 1(33):44, 2012.

Nils Drønen, Harshinie Karunarathna, Jørgen Fredsøe, B Mutlu Sumer, and Rolf Deigaard. An experimental study of rip channel flow. *Coastal Engineering*, 45(3-4):223–238, 2002.

BS Everitt. The cambridge dictionary of statistics cambridge university press. *Cambridge, UK Google Scholar*, 1998.

AD Fockert and A Luijendijk. Wave look-up table building with nature. *Delft, The Netherlands: Deltares, Technical Note, Ref*, pages 1002337–002, 2011.

Joseph Z Gailani, Tahirih C Lackey, and J Smith. Application of the particle tracking model to predict far-field fate of sediment suspended by nearshore dredging and placement at brunswick, georgia. In *Proceedings XVIII World Dredging Congress 2007*, 2007.

KA Haas, IA Svendsen, and MC Haller. Numerical modeling of nearshore circulation on a barred beach with rip channels. In *Coastal Engineering 1998*, pages 801–814. 1999.

L Hamm, Michele Capobianco, HH Dette, A Lechuga, R Spanhoff, and MJF Stive. A summary of european experience with shore nourishment. *Coastal engineering*, 47(2):237–264, 2002.

P Hoekstra, KT Houwman, Aart Kroon, BG Ruessink, JA Roelvink, and R Spanhoff. Morphological development of the terschelling shoreface nourishment in response to hydrodynamic and sediment transport processes. In *Coastal Engineering 1996*, pages 2897–2910. 1997.

Klaas T Houwman and Gerben Ruessink. Cross-shore sediment transport mechanisms in the surfzone on a timescale of months to years. In *Coastal Engineering 1996*, pages 4793–4806. 1997.

Huisman et al. Observations and modelling of shoreface nourishment behaviour. *Journal of Marine Science and Engineering*, 7(3):59, 2019.

Charley R Johnson. *Migration of dredged material mounds: predictions based on field measurements of waves, currents, and suspended sediments, Brunswick, GA*. PhD thesis, Georgia Institute of Technology, 2005.

Leonard Juhnke, Thomas Mitchell, and Michael J Piszker. Construction and monitoring of nearshore placement of dredged material at silver strand state park, san diego, california. Technical report, ARMY ENGINEER WATERWAYS EXPERIMENT STATION VICKSBURG MS, 1990.

L Koster. *Humplike nourishing of the shoreface. A study on more efficient nourishing of the shoreface*. PhD thesis, M. Sc. thesis Delft University of Technology, 2006.

Magnus Larson and Nicholas C Kraus. Analysis of cross-shore movement of natural longshore bars and material placed to create longshore bars. Technical report, COASTAL ENGINEERING RESEARCH CENTER VICKSBURG MS, 1992.

Robert K Schwartz and Frank R Musialowski. Nearshore disposal: onshore sediment transport. Technical report, COASTAL ENGINEERING RESEARCH CENTER FORT BELVOIR VA, 1978.

Ruud Spanhoff and Jan van de Graaff. Towards a better understanding and design of shoreface nourishments. In *Coastal Engineering 2006: (In 5 Volumes)*, pages 4141–4153. World Scientific, 2007.

CWT Van Bemmelen. Long term process-based morphological modelling of pocket beaches. 2017.

MJP Van Duin, NR Wiersma, DJR Walstra, LC Van Rijn, and MJF Stive. Nourishing the shoreface: observations and hindcasting of the egmond case, the netherlands. *Coastal Engineering*, 51(8-9):813–837, 2004.

LC Van Rijn and DJR Walstra. Analysis and modelling of shoreface nourishments. *Z3748*, 2004.

Leo C Van Rijn. Unified view of sediment transport by currents and waves. i: Initiation of motion, bed roughness, and bed-load transport. *Journal of hydraulic engineering*, 133(6): 649–667, 2007.

Dirk Jan Roelof Walstra. On the anatomy of nearshore sandbars: a systematic exposition of inter-annual sandbar dynamics. 2016.

Ronald L Wasserstein, Nicole A Lazar, et al. The asa's statement on p-values: context, process, and purpose. *The American Statistician*, 70(2):129–133, 2016.

Kathelijne M Wijnberg. Environmental controls on decadal morphologic behaviour of the holland coast. *Marine Geology*, 189(3-4):227–247, 2002.

Paul A Work and Emre N Otay. Influence of nearshore berm on beach nourishment. *Coastal Engineering Proceedings*, 1(25), 1996.